LUND UNIVERSITY

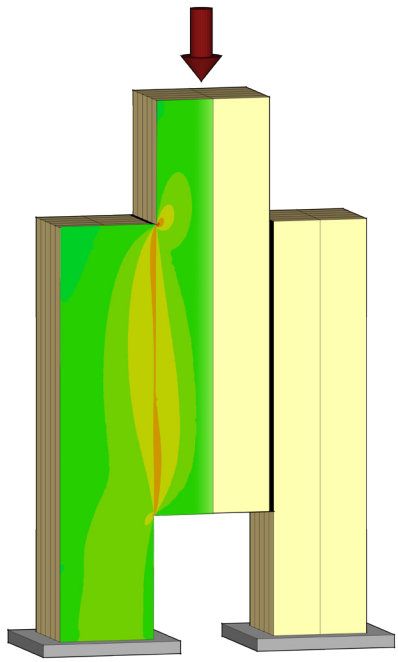

HIGH CAPACITY TIMBER JOINTS

Proposal of the Shear plate dowel joint

GUSTAF LARSSON

Structural Mechanics

Licentiate Dissertation

DEPARTMENT OF CONSTRUCTION SCIENCES

DIVISION OF STRUCTURAL MECHANICS

ISRN LUTVDG/TVSM--17/3078--SE (1-114) | ISSN 0281-6679

ISBN 978-91-7753-106-7 (Print) | 978-91-7753-107-4 (Pdf)

LICENTIATE DISSERTATION

HIGH CAPACITY TIMBER JOINTS

Proposal of the Shear plate dowel joint

GUSTAF LARSSON

Printed by Media-Tryck LU, Lund, Sweden, January 2017 *(Pl)*.

For information, address:
Div. of Structural Mechanics,
Faculty of Engineering LTH, Lund University, Box 118, SE-221 00 Lund, Sweden.

Homepage: www.byggmek.lth.se

Acknowledgements

The work presented in this thesis has been carried out as a joint venture between the divisions of Structural Mechanics and Structural Engineering at the Faculty of Engineering of Lund University. The financial support provided by Formas through grant 2012-879 for the project *Innovative connections for timber construction* is gratefully acknowledged.

Professor Per-Johan Gustafsson and Professor Roberto Crocetti impressed me during my master studies by their knowledge and passion for the subject. As my studies were coming to an end, the two of them had together recently started a project regarding innovative timber connections and were looking for a PhD student. This intriguing combination persuade me to pursue a PhD and for that I am thankful. Many of the ideas being central to the work presented in this thesis originates from these men, and I am very grateful for their inspiring and skilful guidance.

I would also like to thank my assistant supervisors Assistant Professor Henrik Danielsson and Assistant Professor Johan Jönsson, but also Professor Erik Serrano for valuable comments during my research. It has been a privilege to be able to work with and visit Associate Professor Huifeng Yang at College of Civil Engineering at Nanjing Tech University, as well as having the external addition to my reference group of Arne Emilsson from Limträteknik AB and Thomas Johansson from Moelven Töreboda AB. An inspiring work climate has been ensured by the nice staff at Structural Mechanics and Structural Engineering at Lund University.

And finally, to my foremost friend and loving life companion Evelina, thank you for being you.

Lund, January 2017

Gustaf Larsson

Abstract

An increased use of wood can reduce the environmental footprint of the building sector by being a renewable and ecological material. In order to improve the competitiveness of heavy timber structures, this thesis presents a novel type of timber connection with a high degree of prefabrication, which utilizes a resilient bond line.

It has previously been shown that a large conventional stiff adhesive bond line acting in shear can be made stronger by using a less stiff bond line, by e.g. introducing an intermediate rubber foil. The scientific contribution of this thesis starts by comparing such resilient bond lines to conventional non-resilient bond lines. It is numerically shown that the strength of the bond line is increased from 40% to 80% of the local shear strength by introducing a resilient bond line in large lap joints. Unlike other types of connections, a resilient bond line enables design of the stiffness depending on the application by varying the hardness and thickness of the intermediate bond layer.

Using the concept of the resilient bond line in a heavy timber connection design aiming for a high degree of prefabrication, the novel Shear Plate Dowel Joint (SPDJ) is proposed. Initially designed for truss nodes, the connection shows promising results in full scale tensile tests with an average shear stress at failure of 3.3 MPa. A bond line model to be used in FE analysis of the SPDJ is proposed and used in parameter studies of the connection. It is found that a softer bond line will increase the slip, but also the strength which asymptotically aligns with theory of perfect plasticity.

The strengths of the SPDJ design are high load carrying capacity and simplicity in design, but duration of load effects and fire resistance are, among other things, in need of further research prior to structural application.

Contents

Part I

Introduction and overview

1
Introduction

Gazing at a large forest, it is easy to be impressed by the sheer size of the trees. The stem is rising high, supporting all the branches which in turn supports the leaves or needles. For millions of years, trees have ever so slowly adapted their characteristics in order to survive in a large variety of habitats.

It is seemingly recent people have begun using timber as an engineered wood product. The once so optimised structure of branches in the tree and their efficient joint to the stem is now merely an imperfection in the engineered board as a knot; just one example of many. How to best use wood as a construction material has been studied extensively, and will continue to be studied as production methods develop. This work will look at the structural details, namely how timber connections can uphold heavy timber structures while minimizing the effects of these engineered imperfections.

1.1 BACKGROUND

Climate change is a fact, and every responsible person should be looking into their possibility to contribute to a more environmentally friendly society. Although the operation stage dominates the life cycle of buildings, the production stage becomes increasingly important in terms of emissions of greenhouse gases [1]. For the construction sector, a rather simple act is to reduce the use of steel and concrete in favor for timber.

Wood has indeed higher strength to weight ratio than common mild steel, but changing the naturally intended canopy to yet another engineered building floor introduces a set of chal-

lenges. Not only is wood highly anisotropic, i.e. strength and stiffness vary with the orientation of the grain, but it also needs to be manufactured into timber in order to be used efficiently. The effect of duration of load (DOL), the influence of moisture content and understanding in how timber degrades during fire are just some characteristics different for timber in comparison to other building materials.

By aligning and simply gluing the naturally limited cross sections of timber together, cross laminated timber (CLT) and glued laminated timber (GLT) have significantly increased the possibilities of high-rise timber buildings, some even believes in timber skyscrapers [2]. In comparison to the classic timber frame buildings, massive CLT panels in combination with GLT can withstand the large forces that arises in tall buildings. However, the key is combination as no single construction element can be designed to fit all requirements needed in a modern building, and the combination of elements is made possible by timber connections. New production methods and design approaches are needed in order to possibly build timber skyscrapers, including timber connections.

1.2 AIM AND RESEARCH METHODOLOGY

In order to facilitate an increased occurrence and efficiency of timber structures, the aim of this research project is to

> *Develop a good connection design for heavy timber structures suited for industrialized building processes with a high degree of prefabrication.*

This applied science project is well suited for an engineering design process rather than the standard scientific method. Functional requirements are thus identified accordingly and presented in Chapter 2. Contemporary timber connections are presented and discussed based upon the functional requirements, from which a new design concept is proposed. The proposed connector design is named the Shear plate dowel joint (SPDJ), and is based upon the use of a resilient bond line. The technique and design are studied to investigate its characteristics and potential use.

Empirical, analytical and numerical modelling are typical types of modelling in timber engineering. Empirical models are based upon observations or experience used to approximate a formula with a predictive power using some chosen input variables. In contrast, analytical formulas are derived to obtain exact solutions by being based upon fundamental theories of physics. Numerical modelling is based upon analytical relations, but typically using approximated solutions to differential equations to produce a result with high accuracy. The finite element (FE) method is the type of numerical modelling exclusively used in this thesis.

Empirical and numerical modelling are in themselves prone to inductive reasoning, which are subjected to criticism within philosophy of science. Among the critique and of special concern

in engineering is the problem of formulating generalized conclusions based upon a too small number of observations, typically relevant in empirical modelling but also in numerical. By establishing a hypothesis in accordance with hypothetico-deductive reasoning, more general conclusions can be obtained. Although analytical modelling is in general well regarded due to physical interpretations, it does necessarily not lend itself better to the favoured hypothetico-deductive reasoning.

In order to obtain a credible result, the work presented in this thesis typically includes analytical and numerical modelling, both compared to empirical data (though no empirical models are suggested). Although the engineering method is used in general, Paper A investigates the rubber foil adhesive joint technique by the following hypothesis:

Decreasing stiffness of the bond line will increase the strength of long lap joints.

The fallibility of the hypothesis lends itself well to the hypothetico-deductive model. The problem of demarcation is minimized by the use of the basics of the scientific method in combination with a Socratic approach. The methodology of inference of the best explanation was used for questions raised during the experimental study, but with limited possibility of further testing.

1.3 ORIGINAL FEATURES AND LIMITATIONS

The original features presented in this research comprises:

- Comparison of resilient and non-resilient bond lines as presented in Paper A.
- Experimental comparison of different single large diameter dowel joints, including the Shear plate dowel joint (SPDJ) design, presented in Paper B and in the introductory chapters.
- Detailed description of the SPDJ, including discussion regarding the functional requirements, is presented in the introductory chapters.
- Numerical bond line model for the SPDJ is presented in Paper C.
- Various design considerations of the SPDJ are investigated in Paper D.

In this thesis, a resilient bond line is considered a bond line with a lower stiffness than conventional adhesive bond lines. A resilient bond line can for example be made up by introducing a rubber foil between the adherends, but also by the use of an adhesive layer with very low stiffness.

The presented work has the following general limitations:

- Only short term quasi-static loading is considered in all theoretical and experimental analyses.
- The influence of moisture is not considered.
- Wood is modelled as a homogeneous orthotropic material with homogeneous material orientation. If not else specified, a rectilinear model with deterministic parameters are used.
- Glue lines in GLT are not explicitly considered.

1.4 THESIS STRUCTURE

The thesis is divided into two parts, of which the research is presented in a wider perspective in Part I while Part II compiles the appended research papers. Some results and conclusions from the papers are included in Part I to cover the conducted research as whole, while further reading is found in Part II.

Part I

Subsequent the introductory chapter you are now reading, this thesis starts by discussing different contemporary timber connections in Chapter 2. The connections are discussed regarding functional requirements and possible improvements. The thesis is to a great extent based upon numerical analysis, thus Chapter 3 attends the methodology used to model timber and the bond lines including results from Paper C. Chapter 4 presents the state of the art of resilient bond lines as intended use in civil engineering, including the research conducted in Paper A. The Shear plate dowel joint is finally presented in Chapter 5, which is the novel connection design mainly studied in this thesis. The presentation will include results from Paper B, C and D but will also be discussed in a broader perspective including comparison to existing solutions. Concluding remarks are found in Chapter 7.

Part II

Part II of this thesis compiles the appended papers. Paper A compares the length-to-strength ratio for adhesive lap joints using resilient and non-resilient bond lines. A variety of single large diameter dowel connections are tested in Paper B, of which the SPDJ clearly stands out as the strongest, thus merits further investigation. By such, a numerical model for the SPDJ is presented in Paper C and parameter studies of the connection are carried out in Paper D. A more extensive summary of the appended papers is found in Chapter 6.

2
Timber connections

Structures commonly consist of a vast number of elements lumped together by connections. The fundamental purpose of a connection is to allow forces to be transferred from one member to the next. This chapter will further break down the functional requirements and highlight some design difficulties in contemporary timber connections before presenting connections commonly used in heavy timber structures.

2.1 FUNCTIONAL REQUIREMENTS

It is not far-fetched to consider strength as the primary functional requirement of a connection. However, strong timber connections can be achieved in numerous ways, and the diverse types of contemporary connections suggest that different functional requirements not only exist, but also vary in importance between different projects. Strength and stiffness are usually prioritized in large span structures, while the appearance can be more important in residential housing. Different functional requirements are listed below without any order of importance, and it is based upon a list originally presented by Borg Madsen [3].

Strength

A connection should ideally be able to transmit the internal forces from one structural member to the next, with the same reliability as adopted for the members. For many connection types used today, this is however not possible and it is common that the strength of the connection is only 60-70% compared to the strength of the member. This occurs due to local member

weakening by cutting or drilling, or due to occurrences of stress concentrations. Stress concentrations in wood are particularly difficult as they always have to be put in relation to its corresponding orthotropic strength, discussed further in Section 3.3. The low tensile strength perpendicular to grain is often the limiting factor in timber connections, thus the mode should be minimized in the design phase of any strong connection.

Strength may also be discussed in terms of time. Short term strength is typically higher than long term, and duration of load (DOL) studies are thus important. Strength can also be dependent of the time history of the load, regarding cyclic or impact loading.

Stiffness and deformations

The safety level can be increased using statically indeterminate structures. The redundancy of such systems enable different load paths in case of member weakening or failure, and can thus ensure structural integrity. However, the structural design will become more complicated by introducing several possible load paths, as the load then will choose the stiffest path possible. The stiffness of such a path depends greatly on the stiffness of the connections, making it an important functional requirement. In order to minimize unwanted deformations in the structure, it is important to be able to estimate the stiffness and creep behaviour of the connections.

Ductility

Wood is in general a brittle material and can thus fail without the warning sign of excessive deformations. This behaviour is undesirable for structures as loads cannot be redistributed in the structure in case of excessive deformations, nor does it leave much time for occupants to recognise and avoid danger. A ductile failure allows large deformations prior to system collapse, and is therefore favourable. The ductility of a timber structure must be achieved in the connections which is made possible by a sound connection design. This is of special importance in seismic regions.

Simplicity of design

Simplicity of design have the potential of minimizing the risk of human error in two aspects. Firstly, it is preferable that the design of a connection is done so that a clear understanding of how forces are transferred in the connection is made possible. Similarly but secondly, the design method of a connection should be straight forward and easy to understand.

Production friendly

The production of a timber joint includes the manufacturing and assembly. A high degree of pre-fabrication and a simple assembly are desirable features, although different connection designs fulfil such requirements to varying degree. Assembly can also be difficult if the connection designs are sensitive to moisture movements and general construction tolerances. Over-sized holes for bolts could simplify the assembly, but would significantly decrease the connection stiffness.

Appearance

In comparison to steel and concrete, wood is often considered a beautiful material and thus also timber structures. To combine aesthetics with functionality is however not an easy task, especially not for connections. An intimate collaboration between architect and structural designer is thus vital.

Durability

The service life of a connection should not fall short of the service life of the remaining structure in the present environment. Possible degradation due to e.g. corrosion of metallic components and/or moisture of timber members should always be considered.

Fire

As a timber connection usually consists of a combination of timber and steel components, a good connection design should also use the material characteristics to ensure good performance in the case of fire. Charring will occur on the timber surface, temporarily insulating the material within from degradation while steel requires external insulation in order to avert a sudden collapse. A sound connection design should thus have a minimum of exposed steel, or enable a simple application of insulation, e.g. intumescent paint.

Costs

As for every project and product, the cost can be critical. About 20-30% of the total cost of a GLT structure is normally spent on the connections [3], a percentage that possibly can be reduced. However, it should be kept in mind that the size of the structural members can be reduced if the strength of the connection matches the strength of the members, as discussed above. The total cost of some projects can thus be reduced by increasing the cost of the connection.

Environmental sustainability

Timber engineering has in recent years obtained considerable interest due to a growing environmental awareness. Although considerably better than steel or concrete structures, timber engineering can still improve its ecological footprint by e.g. life cycle assessment. Applied to connections, the possibility of reutilization or recycling is beneficial.

2.2 DIFFICULTIES IN TIMBER CONNECTION DESIGN

Although numerous different types of timber connections exist, some general difficulties can be identified. Looking at the material level, which will be further discussed in Chapter 3, the material properties of wood varies greatly with the orientation of the grain. The most extreme example of this is that the tensile strength of wood perpendicular to grain is only approximately 5% of the parallel to grain tensile strength [4]. This fact is very important to consider in connection design, as fracture perpendicular to grain will occur at a low load if the design triggers such failure mode.

Not only do the material properties differ in different orientations, a great variability is always found for each such property. In terms of strength, the variability is often considered by differentiating mean strength from characteristic strength, which is typically the 5^{th} percentile. Furthermore, the properties also vary with moisture content and duration of load effects, which also need to be considered.

Wood is in general a brittle material, which together with the variability to some extent limits all types of timber connections, but tension and bending resistant connections are typically identified by practitioners of timber engineering as cumbersome to design. In terms of brittle failure in nailed timber connections loaded in tension, Helena Johnsson [5] shows how an increasing amount of nails can actually decrease the strength of the joint. This counter-intuitive results is due to the brittle behaviour of wood, as the increased number of nails weakens the timber to such an extent that the nails do not have the opportunity to yield as needed to utilize the full potential of nails according to Johansen's yield theory [6], taking into consideration the reduced capacity of dowels placed in a row [7].

The difficulty of assembling many similar fasteners is however seldom solved by introducing another type of fastener due to different load-slip behaviours. As seen in Figure 2.1, glue is very stiff and typically fails at a deformation which only would allow a bolt to reclaim 10% of its maximum capacity [8]. Even though glue typically can be used to strengthen different type of connections, it then has to be modified in order to match the load-slip behaviour of the joint type (see further Chapter 4).

Although the stiffness of connections are essential in the determination of load paths throughout a structure, it is hard to identify a good estimate by analytical means. The difficulty spans several types of connections, but being of higher importance in bending resistant connections.

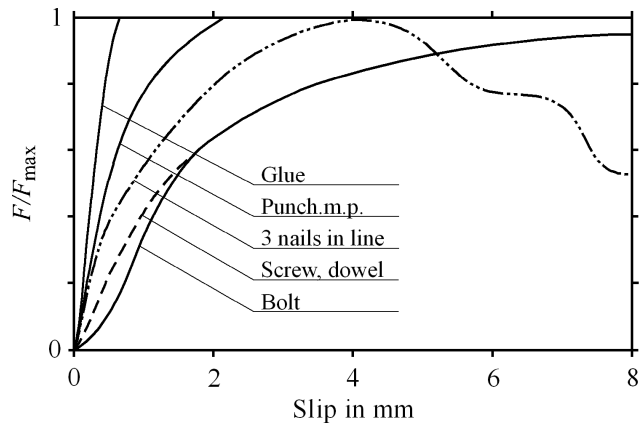

Figure 2.1: Typical normalized load-slip behaviours of different types of fasteners in a single lap joint design. [8]

2.3 CONTEMPORARY CONNECTIONS

In order to be able to present an novel connection for heavy timber structures, a review of contemporary connections are of special interest in this thesis. How loads are transferred in the connections will be presented along with the prominent features influencing design and performance. The discussion will be based upon the functional requirements presented in Section 2.1.

2.3.1 Punched metal plates

Even though typically designed for light structures such as single family houses, the punched metal plate (PMP), or truss plate in America, is used extensively throughout the world and thus worth mentioning. As shown in Figure 2.2, the PMP are an integration of nail plates and nails produced by punching edges in galvanized steel plates and bending the formed teeth into position perpendicular to the plate. Due to limitations in the punching process, the steel plate thickness usually does not exceed 2 mm and the PMP is thus bound to be considered a surface connection having a relatively low strength capacity.

Trusses are formed by pressing the PMP into the wood members using a hydraulic clamp or pushing the whole truss through a large roller press. By such, it is usually not practical to apply PMP on the building site. Common spans for PMP trusses are 9-15 m, but can reach up to 40 m.

The popularity of the PMP is in part due to the simple manufacturing and low production cost. From a design engineer perspective, the connection is however more complex. In the European design code, Eurocode, 11 strength parameters are needed for full connection characterisation [9]. Poutanen [10] highlighted this complexity in 1989 by comparing seven different design

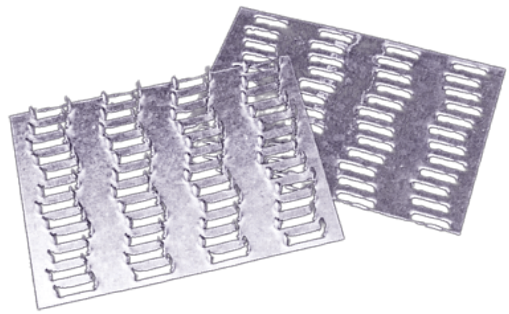

Figure 2.2: Punched metal plates, typically used for light timber trusses.

codes, in which an unreasonably large variety of truss sizes was found depending on what type of structural behaviour selected. More detailed analysis of the PMP is numerically enabled by the use of the Foschi model [11].

It is seldom that a truss span its entire length completely unsupported in residential housing due to interior walls. Many of the design assumptions are also very conservative and as a result, failures are generally rare in the field. However, when using PMP trusses in industrial buildings with clear and long spans, the boundary conditions are not as forgiving and creep deformations significantly higher than the short term elastic deformation have been found [12].

The popularity of the PMP is due to the simple manufacturing process and ease of use. However, the size limitations, creep, complex load path and fire characteristics makes it unsuitable in heavy timber structures.

2.3.2 Glulam rivets

In comparison to the PMP, the load carrying capacity can be increased by using thicker steel plates and replacing the punched nails by longer regular nails. This nail plate design has been further improved by B. Madsen in his Canadian Glulam rivets [3]. The system is shown in Figure 2.3 which illustrates two key features which distinguishes it from typical nail plates.

The first of the two key features is the shape of the cross section. Instead of round or close to square, the rivets are made rectangular with rounded corners. This allows the rivet to have increased bending stiffness with, if inserted correctly with its longest side parallel to grain, a minimal impact on the wood grain. As pre-drilling is not required, all fibres are left intact and only slightly bend when the rivet is inserted. The second key feature is the tapered head of the rivet, which causes significant hoop tension in the plate as the rivet is driven in ensuring a tight fit. The result is a strong cantilevering component with a similar effect to cold-riveting, and hence the name. [3]

Among the benefits of glulam rivets is the well-established manufacturing process. By small

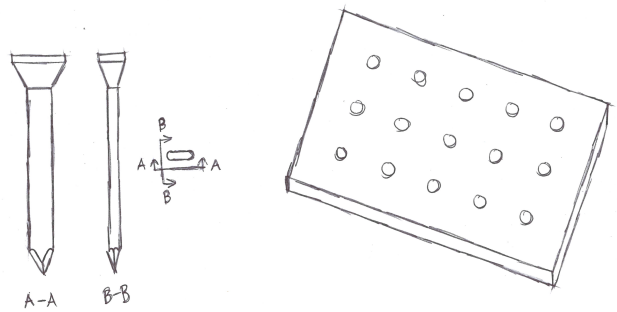

Figure 2.3: The glulam rivet has a rectangular cross section with rounded corners to maximize bending resistance and minimize grain impact. The tapered head causes hoop tension in the nail plate.

design alterations a strong and stiff connection is derived from existing solutions for light timber frame buildings. However, the installation of the glulam rivet connection is labour-intensive if used on heavy timber structures as a large quantity of rivets must be inserted. Even though the large quantity of rivets may prove useful in earthquake design, it is probably not favourable in environments prone to moisture content variations.

2.3.3 Screws and rods

Screws are extensively used in timber engineering and building construction in general. Traditionally, fasteners are placed perpendicular to the connection of two adjacent members and typically carry load by axial or shear forces. However, as screws typically have a considerable withdrawal strength if inserted at an angle to the grain, this is often a preferable mode of action. By inclining the screws typically 45°, it is possible to minimize shear action in favour for axial thus increasing the load carrying capacity and the stiffness of the connection, see Figure 2.4.

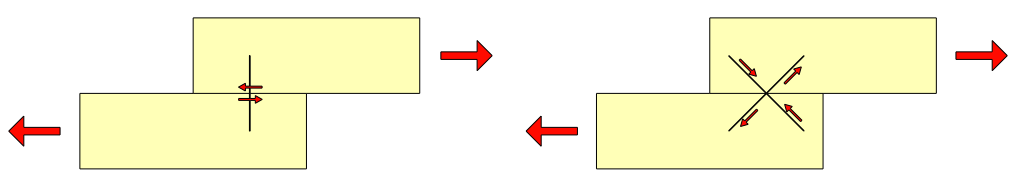

Figure 2.4: Schematic comparison between traditional and inclined screws in lap joints.

To enable easy on site assemblage, inclined screws can be used in combination with tenon joints. The load-carrying capacity of inclined screws shows an increase of 50% while the slip modulus increases by a factor of up to 12 compared to traditional screws [13].

The inclined screws can be included in the on-site production using well-known techniques. Furthermore, the very limited aesthetic impact of the joint is also a positive feature of the design. However, the strength is in general smaller than in e.g. connections made of slotted-in steel plates and dowels, making the inclined screws less ideal for heavy structures. Nevertheless, the strength and stiffness can be increased by using threaded bars in combination with adhesive, resulting in so-called bonded-in rods [14]. Such a system can typically be used as a connection or as a reinforcement in a similar manner as screws [15]. An advantage for bonded-in rods over screws is the increased strength when inserted parallel to grain.

2.3.4 Slotted-in steel plates

Dowel type connections are common in timber engineering, and an elegant way of using them in heavy timber structures is in combination with one or more slotted-in steel plates. The steel plates are used to transfer load between members, while the dowels transfer loads to and from the steel plates to the timber member, see Figure 2.5. The capacity of a single dowel is increased by the number of inserted plates, which in turn is limited by the GLT member width.

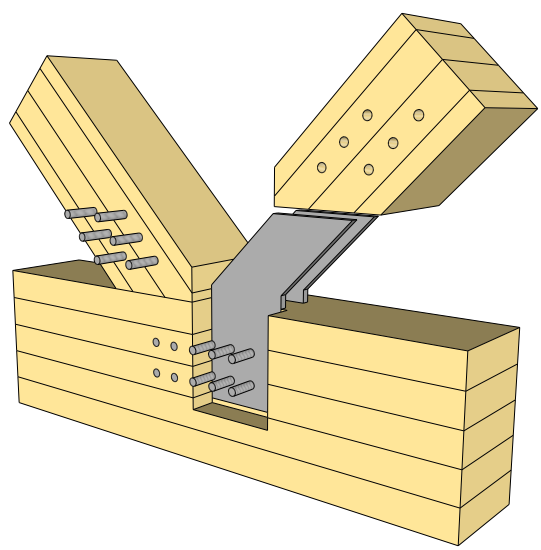

Figure 2.5: Slotted-in steel plates used in a truss node.

As the steel is embedded in timber, slotted-in steel plates are not only protected from fire, but also usually considered as an aesthetic connection. Slotted-in steel plates do not eliminate the possibility of brittle failure, but the risk is reduced by using small diameter dowels as well as adequate plate spacing and end distances.

The dimensions and number of the steel plates and dowels are proportional to the loads, primarily axial forces parallel to grain. Thinner slotted-in plates can be pierced by self-perforating dowels, which reduces the number of operations needed for installation. This method is also

very efficient when considering the connection stiffness as the slip is minimized. However, thicker steel plates or larger dowel diameters requires pre-drilling, which has to be done with a high degree of precision in order to prevent connection slip. The large number of dowels also requires long assembly times and all cuts made to insert the steel plates weakens the timber.

2.3.5 Wood adhesive joints

The use of timber in structural systems is sometimes in question due to its large variation of mechanical properties, further discussed in Chapter 3. Similar arguments are often also true for structural adhesive joints, as they possess a number of favourable characteristics but their reliability is often in question. To utilize these favourable characteristics, adhesive joints must be recognized by skilled design and craftsmanship.

One of the favourable characteristics of adhesive joints is the strength, for which a comparison is shown in Figure 2.6. Four different types of double lap joints are presented, all with a design load of approximately 150 kN but obtained at different lap lengths. The comparison is presented in [16], but the adhesive lap joint is here added with an average shear stress at failure of 1.8 MPa, according to EC5 and well below recorded values in Paper A. Similar comparison was also conducted by Adams and Wake in [17]. The adhesive joint is the smallest and thus most material efficient. In addition to high strength, Adams and Wake also argue that adhesive joints have better durability than corresponding mechanical fasteners.

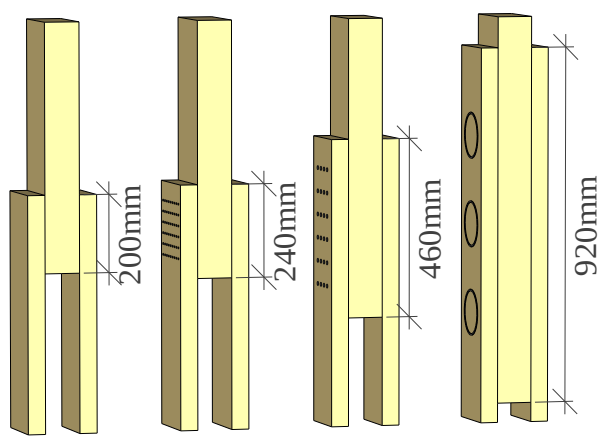

Figure 2.6: Four different double lap joints with similar design tensile load capacity using (from left): PUR adhesive; $2x6x9$ nails d=5; $4x6$ screws d=10; and $2x3$ split rings d=120 mm [16]. The illustration is drawn to scale.

There are however disadvantages using adhesive fasteners. The adhesive bond requires a controlled environment during gluing and curing, which is difficult to obtain on site. Curing pressure and a curing time is needed at a specific temperature and relative humidity range to obtain the desired results. It is furthermore difficult to inspect an adhesive joint since it

would then be necessary to dismantle the entire connection. The effects of several of these disadvantages can be minimized using a resilient lap joint as further discussed in Chapter 4.

2.4 ROOM FOR IMPROVEMENTS

A reasonable design basis for any type of connector is to match the member characteristics. A connection design is too weak if it requires an increase in member dimensions, and it is not designed properly against fire if it loses load carrying capacity prior to the members, just to mention two examples. This type of reasoning limits the level of optimisation of some functional requirements, while others can be improved endlessly such as production cost. A third category of functional requirements will always be subjected to subjective assessment, which of course is a typically difficult basis for optimisation.

The orthotropical nature of wood in combination with complex structures requires a surprisingly large number of different types of connections used in different situations. The aim of this thesis regards connections in heavy timber structures with a high degree of prefabrication, a distinction which enables a ranking among the functional requirements and limits the amount of possible design solutions.

One of the most typical connection types used for heavy timber structures today is slotted-in steel plates. The design suggested in this thesis should thus exceed the performance of slotted-in steel plates in one or more aspects, of which cost is the one indirectly highlighted in the project aim (c.f. Section 1.2). As often is the case in this kind of studies, new design difficulties and possible weaknesses are introduced with new solutions. Some will be discussed in this thesis, while further analysis will be presented in future research.

Some possible improvements as compared to slotted-in steel plates can be identified as:

- Higher load carrying capacity at long term loads, limited by ductile failure
- A designable stiffness with high prediction accuracy
- Lower the production cost by minimizing material usage and production time (especially on site)
- A connection design suitable for tension and bending loads

The novel connection design presented and studied in Chapter 5 has shown to improve some of these aspects.

3

Numerical modelling of timber and bond lines

Wood is the material created by trees which is optimised for the conditions trees are exposed to. Timber, however, is the engineered wood product used for structural applications. This distinction is important as "timber is as different from wood as concrete is different from cement", as nicely put by Borg Madsen [18]. In this chapter, the modelling choices from wood to timber will be discussed along with material properties of Norway spruce, the most commonly used wood species in northern Europe. The structure of wood is only discussed briefly, for more reading see e.g. Bodig and Jayne [19] and Dinwoodie [20]. All modelling in this thesis is conducted using the finite element (FE) method in the general purpose FE software Abaqus.

3.1 STRUCTURAL LEVELS OF TIMBER

Wood is an organic composite built up mainly of cellulose, hemicellulose and lignin which together forms fibres. Most of the fibres are aligned almost parallel to the stem and depending on what time of year the cells are formed, the characteristic lighter and darker rings in a wood cross section grow in number. The material properties vary greatly with respect to the direction of these annual growth rings, making wood a close to orthotropic material. As the round stem is of limited use in timber construction, the trees are commonly sawn into rectangular cross sections and if heavier cross sections are needed, several timber laminations are glued together forming glued laminated timber (GLT).

Depending on the type of problem investigated, timber needs to be modelled at different structural levels. Cellulose, hemicellulose and lignin are found at the ultrastructural level whereas fibres are represented at the microstructural level. Clear wood is normally regarded as the macroscopic level [21], which Mother Nature has then spent millions of years devising an arrangement that allows perpendicular branches to grow without impairing the strength of neither the branch nor stem. However, when timber is produced by sawing through this intricate handiwork these knots will become severe weaknesses which can initiate crack growth. Thus, clear wood is rare in timber engineering and consideration must be paid to knots and other defects. How these defects are taken into account differs for different engineering problems. Commonly used, also in this thesis, is that they are treated implicitly on the material properties rather on the geometry itself as seen in Figure 3.1. Not only is it common to ignore geometrical defects (b), but for some problems the effects of the growth ring curvature is also negligible, and a rectilinear material model can be used (d). This assumption typically introduces larger errors for cuts taken near the pith than if taken in the periphery, while the error is minimized if the cut is kept small in relation to the distance from the pith.

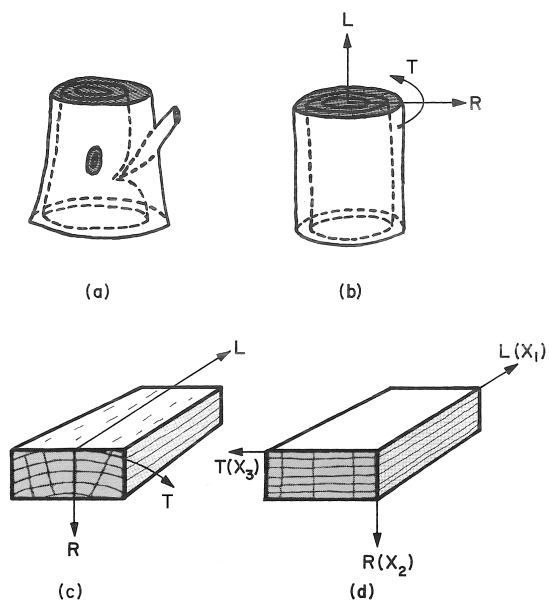

Figure 3.1: Reduction of a tree stem to an orthotropic model [19].

The macroscopic level is characterised by a distinction between the three orthogonal directions in relation to the growth rings and fibre direction: longitudinal (L), radial (R) and tangential (T), see Figure 3.1. Due to possible log taper and spiral growth, the longitudinal direction might not be fully aligned with the longitudinal direction of the tree stem.

Compared to other building materials such as steel or reinforced concrete, wood shows a higher degree of variation in terms of properties. Not only is it orthotropic, but also hygroscopic with properties varying with air humidity. While steel and concrete are manufactured according

to well-established procedures with controlled variability, timber is simply a sorted existing material. The sawn timber is produced from a very large variety of logs cut from many different trees grown in varying conditions. The timber is then sorted using non-destructive tests and statistical relationships. The variability of timber properties is the cost of wood being a natural material, which must be considered using sound engineering judgement.

3.2 WOOD ELASTICITY

A convenient way to represent wood at macro scale as a 3D continuum, is to use Hooke's generalized law as given in Equation 3.1 in Voigt matrix form. The constitutional law assumes small strains and has been adapted to the principal directions of wood. Robert Hooke stated the law in 1660 as the anagram *ut tensio, sic vis* — "As the extension, so the force" [22] which relates material stresses σ to the elastic strains ε according to Equation 3.1.

$$\bar{\boldsymbol{\varepsilon}} = \bar{\boldsymbol{C}}\bar{\boldsymbol{\sigma}} \tag{3.1}$$

where

$$\bar{\boldsymbol{\varepsilon}} = \begin{bmatrix} \varepsilon_{LL} & \varepsilon_{RR} & \varepsilon_{TT} & \gamma_{LR} & \gamma_{LT} & \gamma_{RT} \end{bmatrix}^T \tag{3.2}$$

$$\bar{\boldsymbol{\sigma}} = \begin{bmatrix} \sigma_{LL} & \sigma_{RR} & \sigma_{TT} & \tau_{LR} & \tau_{LT} & \tau_{RT} \end{bmatrix}^T \tag{3.3}$$

The elastic flexibility tensor $\boldsymbol{C}$ in Equation 3.4 is valid for orthotropic materials and organizes the moduli of elasticity E_i and shear G_{ij} along with Poisson's ratio ν_{ij}, where $i, j = L, R, T$ [19].

$$\boldsymbol{C} = \begin{bmatrix} \frac{1}{E_L} & -\frac{\nu_{LR}}{E_R} & -\frac{\nu_{TL}}{E_T} & 0 & 0 & 0 \\ & \frac{1}{E_R} & -\frac{\nu_{TR}}{E_T} & 0 & 0 & 0 \\ & & \frac{1}{E_T} & 0 & 0 & 0 \\ & & & \frac{1}{G_{LR}} & 0 & 0 \\ & sym. & & & \frac{1}{G_{LT}} & 0 \\ & & & & & \frac{1}{G_{RT}} \end{bmatrix} \tag{3.4}$$

The elastic parameters found in Equation 3.4 are material dependent and determined by tests. Comprehensive compilations for various wood species can be found in e.g. [20] and [23]. Dahl [4] presents in a recent study a comprehensive test program in order to identify the properties of Norway Spruce (*Picea Abies*), a species commonly used as timber in Sweden. His findings are presented in Table 3.1 along with mean stiffness values of some strength classes of timber as defined in EN 338:2016 [24] and GLT in EN 14080:2013 [25]. It can be seen that the European standards does not distinguish radial from tangential direction, thus taking one further step of simplifying the structure of wood to only parallel and perpendicular to grain, i.e. transverse isotropy. This simplification is implicitly included in *LR*- and *LT*-plane

Table 3.1: Elastic parameters for softwood from literature. Stiffness [MPa], density [kg/m^3] and Poisson's ratio

Species/Class	ref	E_L	E_R	E_T	G_{LR}	G_{LT}	G_{RT}	ρ
Norway spruce	[4]	9 040	790	340	640	580	30	400
Timber, C24	[24]	11 000	370	370	690	690		420
GLT, GL24h	[25]	11 500	300	300	650	650	65	420
Timber, C30	[24]	12 000	400	400	750	750		460
GLT, GL30h	[25]	13 600	300	300	650	650	65	480
		ν_{LR}	ν_{RL}	ν_{LT}	ν_{TL}	ν_{RT}	ν_{TR}	
Norway spruce	[4]	0.50	0.11	0.66	0.06	0.84	0.34	

stress analysis in 2D. Neither Poisson's ratio is considered of interest in the standards. Dahl argues that some of the discrepancies between his results and the standard possibly is due to the fact that the material sample was partly ungraded, but the differences between clear wood and structural timber also affect the results.

Considering the height of a tree and wind action upon it, it is reasonable to expect a high stiffness parallel to grain. The elastic property which stands out is the very low rolling shear stiffness G_{RT}. This difference in stiffness causes some interesting phenomena, e.g. how a uniform load causes a non-uniform stress distribution within the cross section as seen in Figure 3.2 [26, 27]. The practical influence of the low rolling shear stiffness has previously been limited, but to a large extent affects the behaviour of the increasingly popular CLT panels subjected to bending.

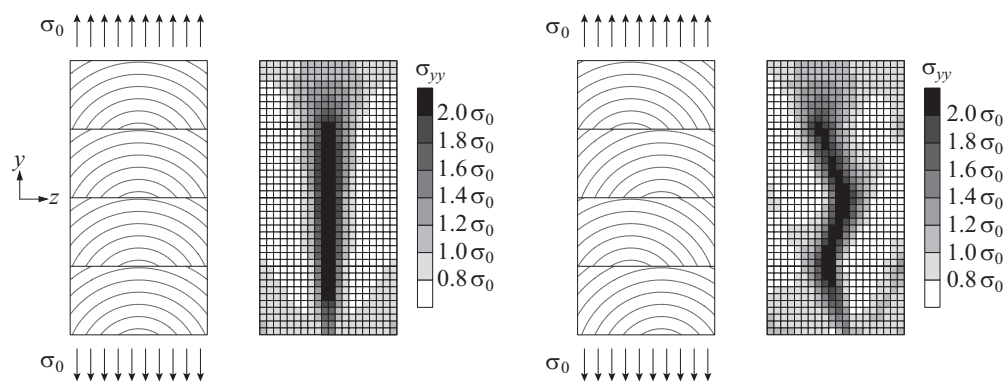

Figure 3.2: A non-uniform stress distribution σ_{yy} is found for a GLT cross section although subjected to uniformly applied stress σ_0 due to differences in stiffness [28].

The linear elastic parameters presented above are only valid up to the limit of proportionality after which non-linear behaviour is typically found prior to failure as shown in Figure 3.3. However, the non-linearities of wood are often of limited influence in timber engineering, and

thus often disregarded. Elasto-plastic material models can be suitable in compression parallel and perpendicular to grain, but the mechanisms are profoundly different from those in metal where many of elasto-plastic models are used.

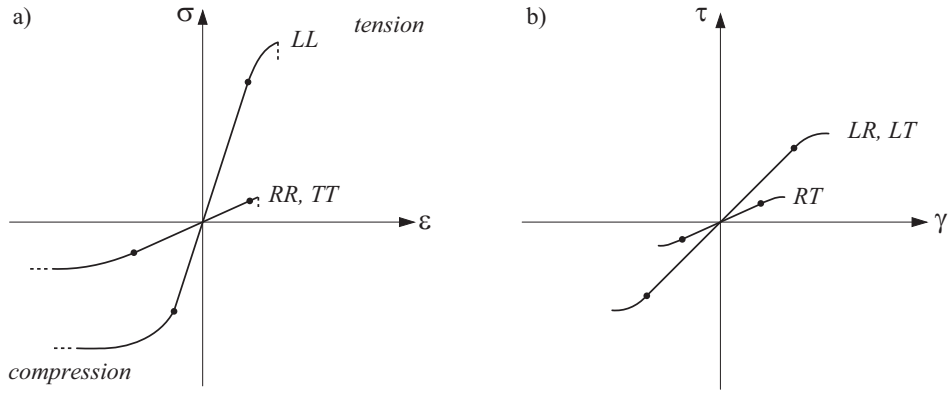

Figure 3.3: Schematic illustration of wood behaviour in normal (a) and shear (b) direction. The limits of proportionality are shown as dots.

3.3 WOOD FAILURE

As all structural materials, wood will eventually fail if subjected to increasing stress. Similarly to the elastic properties, also the strength properties of wood are of orthotropic nature but distinction must now also be made for compressive and tensile normal stresses. As seen in Figure 3.3, failure typically occurs close to the limit of proportionality making wood a brittle material, in which excessive deformations seldom are experienced prior to failure. Strength properties are experimentally determined but must be incorporated into a failure criterion in order to evaluate combined stress state of a material point. Failure can be defined in various ways, but focus will here be put on stress based failure criteria and fracture mechanics.

3.3.1 Strength properties

Handbooks and standards in timber engineering commonly refer strength values as the lower 5^{th} percentile of the distribution of graded and tested structural timber. The test specimen size is large enough to include defects in order to represent actual structural elements. The resulting strengths should therefore be considered defined on element level rather than at a single material point level [29].

Tests of clear wood specimens are however conducted for research purposes. Comprehensive experimental studies have been conducted on clear wood by e.g. Dahl [4] and Eberhardsteiner [30], whose results are compiled in Table 3.2 along with the properties of structural timber and GLT according to EN 338:2016 [24] and EN 14080:2013 [25]. The strengths f_{ij} are

Table 3.2: Wood and timber strength properties [MPa] for spruce.

Species/Class	ref	f_{Lt}	f_{Lc}	f_{Rt}	f_{Rc}	f_{Tt}	f_{Tc}	f_{LR}	f_{LT}	f_{RT}
Norway spruce	[4]	63	29	4.9	3.6	2.8	3.8	6.1	4.4	1.6
Norway spruce	[30]	75	50	4.9	7.0			8.6		
Timber, C24	[24]	14.5	21	0.4	2.5	0.4	2.5	4.0	4.0	
GLT, GL24h	[25]	19.2	24	0.5	2.5	0.5	2.5	3.5	3.5	1.2
Timber, C30	[24]	19	24	0.4	2.7	0.4	2.7	4.0	4.0	
GLT, GL30h	[25]	24	30	0.5	2.5	0.5	2.5	3.5	3.5	1.2

defined in the principal directions $i = L, R, T$ in compression and tension $j = c, t$. Shear strengths are direction independent and all strengths are defined as positive numbers.

Among the parameters influencing the strength of wood, size effects can be somewhat counter-intuitive as larger specimens fail at lower average tension levels than smaller specimens [31]. It can however be explained using Weibull weakest link theory [32] due to the presence of defects, as the probability of a large weakness occurring in the most loaded section is higher for a large specimen than for a small. The theory assumes that the weaknesses are of random size and position within the element, and that the material is brittle [33]. These effects are typically included in building codes specifying timber characteristics, such as Eurocode [24, 25]. These effects are however disregarded in clear wood specimens, such as tested by Dahl [4] (c.f. Table 3.1 and 3.2).

3.3.2 Failure criteria

In practical timber engineering, failure is commonly assessed by linear elastic stress analysis with a stress based criterion. It is a convenient approach which enables assessment of the strength of a member also by analytical hand calculations. However, the method is typically used on a single point assuming that no stress redistribution occurs. Even though wood is brittle, the single point evaluation can result in a low strength prediction if large stress gradients occur within the member. This can be improved using several different techniques, such as using a non-linear material model, stress averaging over a certain area or analysing crack propagation.

Regardless of what method used, the combined state of stress has to be evaluated by a failure criterion in each material point in order to asses a reasonable failure. Failure criteria typically look different for different materials, and three commonly used for timber are the maximum stress criterion, the Norris criteria [34] and the Tsai-Wu criterion [35].

Maximum stress criterion

The maximum stress criterion is a common and simple failure criterion used for both uniaxial and multiaxial stress states. The criterion assumes that a material can always withstand a certain stress level in one direction regardless of the stress levels in other directions, i.e. does not consider stress interaction. As a single stress component reaches its strength, failure occurs according to Equation 3.5 as given for 3D analysis.

$$\max\left\{\frac{|\sigma_{LL}|}{f_{Li}}, \frac{|\sigma_{RR}|}{f_{Ri}}, \frac{|\sigma_{TT}|}{f_{Ti}}, \frac{|\tau_{LR}|}{f_{LR}}, \frac{|\tau_{LT}|}{f_{LT}}, \frac{|\tau_{RT}|}{f_{RT}}\right\} - 1 = 0 \tag{3.5}$$

The strengths with respect to normal stresses may have different values regarding compression or tension ($i = c, t$). If a material point experiences stresses in several directions, the maximum stress criterion is seldom an accurate description of material failure.

Norris criteria

Stress interaction can be achieved by means of the Norris criteria [34]. Instead of looking at a single stress ratio individually, a sum of several is used as shown in Equation 3.6 for the 3D case.

$$\max\left\{\begin{array}{l}\left(\frac{\sigma_{LL}}{f_{Li}}\right)^2 + \left(\frac{\sigma_{RR}}{f_{Ri}}\right)^2 + \left(\frac{\tau_{LR}}{f_{LR}}\right)^2 - \frac{\sigma_{LL}}{f_{Li}}\frac{\sigma_{RR}}{f_{Ri}} \\ \left(\frac{\sigma_{LL}}{f_{Li}}\right)^2 + \left(\frac{\sigma_{TT}}{f_{Ti}}\right)^2 + \left(\frac{\tau_{LT}}{f_{LT}}\right)^2 - \frac{\sigma_{LL}}{f_{Li}}\frac{\sigma_{TT}}{f_{Ti}} \\ \left(\frac{\sigma_{RR}}{f_{Ri}}\right)^2 + \left(\frac{\sigma_{TT}}{f_{Ti}}\right)^2 + \left(\frac{\tau_{RT}}{f_{RT}}\right)^2 - \frac{\sigma_{RR}}{f_{Ri}}\frac{\sigma_{TT}}{f_{Ti}}\end{array}\right\} - 1 = 0 \tag{3.6}$$

The Norris criteria are commonly used for timber. However, as tensile and compressive strengths differ, the criteria must be applied in a piece wise manner. Each of the equations represents a closed surface in the respective stress spaces.

Tsai-Wu criterion

The stress interaction of the Norris criteria are often considered sufficient, but the piece wise application of the criteria are sometimes undesirable. The Tsai-Wu criterion [35] uses matrix notation to form a more efficient failure criterion according to 3.7, which also allows for different tensile and compressive strengths.

$$\bar{\boldsymbol{\sigma}}^T \bar{\boldsymbol{q}} + \bar{\boldsymbol{\sigma}}^T \bar{\boldsymbol{P}} \bar{\boldsymbol{\sigma}} - 1 = 0 \tag{3.7}$$

where $\bar{\boldsymbol{\sigma}}^T$ is defined in Equation 3.3. The stress interaction is obtained using the Tsai-Wu matrices $\bar{\boldsymbol{q}}$ and $\bar{\boldsymbol{P}}$ given by [4]

$$\bar{\boldsymbol{q}} = \begin{bmatrix} F_{LL} \\ F_{RR} \\ F_{TT} \\ 0 \\ 0 \\ 0 \end{bmatrix} \quad \text{and} \quad \bar{\boldsymbol{P}} = \begin{bmatrix} F_{LLLL} & F_{LLRR} & F_{LLTT} & 0 & 0 & 0 \\ & F_{RRRR} & F_{RRTT} & 0 & 0 & 0 \\ & & F_{TTTT} & 0 & 0 & 0 \\ & & & F_{LRLR} & 0 & 0 \\ & sym. & & & F_{LTLT} & 0 \\ & & & & & F_{RTRT} \end{bmatrix} \tag{3.8}$$

Uniaxial tensile and compression strengths along with shear strengths are used to define the parameters F_{ii}, F_{iiii} and F_{ijij} according to

$$\begin{aligned} F_{ii} &= 1/f_{it} - 1/f_{ic} && i = L, R, T \\ F_{iiii} &= 1/\left(f_{it} f_{ic}\right) && i = L, R, T \\ F_{ijij} &= 1/f_{ij}^2 && i, j = L, R, T \ (i \neq j) \end{aligned} \tag{3.9}$$

The remaining strength interaction coefficients F_{iijj} must be determined by uniaxial off-axis or biaxial tests. The coefficients must satisfy Equation 3.10 in order to produce a closed and convex failure surface. The inequality is for example satisfied for $F_{iijj} = 0$ as F_{iiii} and F_{jjjj} are defined as positive, which is a simplification often used. However, of special interest in this thesis is the shear strength of wood, which can be increased if a compressive stress interacts as suggested in Section 4.2.7 of SIA 265 [36]. This is not considered if F_{iijj} are disregarded.

$$F_{iiii} F_{jjjj} - F_{iijj}^2 \geq 0 \qquad i, j = L, R, T \ (i \neq j) \tag{3.10}$$

The Tsai-Wu criterion presents an effective method to evaluate the combined state of stress in an orthotropic material. However, the main difficulty is to determine the strength interaction coefficients [37].

3.3.3 Fracture mechanics

Fracture mechanics is the branch of solid mechanics which studies structural failure due to separation of material. The microscopic mechanisms which govern the separation and predictions from a macroscopic point of view are both topics of interest in order to predict the load-carrying capacity of structural members. [38]

The type of relative displacement in the vicinity of a crack is governed by the load acting on the structural element. However, there are only three basic displacement modes as shown in

Figure 3.4: the opening mode I, the in-plane shear mode II, and the out-of-plane mode III. As the stress state in the crack tip often is multiaxial, a mixed mode fracture often occur in which a combination of mode I and II is most common, also for the problems studied in this thesis. The orthotropic nature of wood further enables six possible orientations of plane cracks in the principle planes, resulting in a total of 18 basic fracture situations.

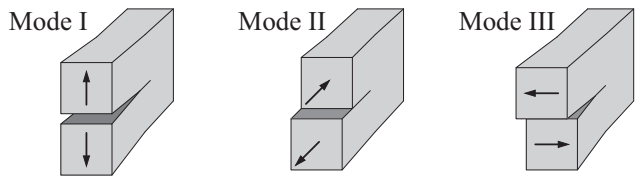

Figure 3.4: The three fundamental modes of fracture deformation.

Traditional fracture mechanics considers the effect of existing cracks, often under the assumption that cracks of limited size are always present in materials due to e.g. manufacturing methods or natural variation. Intense research in the traditional linear elastic fracture mechanics (LEFM) was conducted during mid-20^{th} century due to its application on vehicles, ships and aircrafts. Later developments also includes the creation of cracks as well as material non-linearity outside the crack tip, often referred to as non-linear fracture mechanics (NLFM).

Linear elastic fracture mechanics

LEFM deals with pre-existing cracks in a continuous linear elastic material with infinite strength [39]. Although linear elastic materials can have arbitrary high strains without failure, small strain and displacement theory is commonly adopted in stress analysis. The combination of an existing crack tip and the linear elastic material model implies singular stresses at the crack tip, making the stress based failure criteria as discussed in Section 3.3.2 useless. Instead, energy release rate at crack propagation or stress intensity are commonly used quantities.

LEFM can be very useful although no real material possesses ideal elastic properties. The main requirement for good applicability is that the size of the fracture process region around the crack tip is small compared to typical dimensions of the structure, including the crack length.

Non-linear fracture mechanics

NLFM is distinguished from LEFM by the possibility to regard the material non-linearity outside the crack tip, the limited stress capacity and/or the non-linear stress-deformation performance of the material at the crack tip. This can be achieved using various approaches, of which a more direct one is done by characterisation of fracture properties of the material by a stress-deformation relation which includes material softening, commonly denoted a σ-w curve.

The σ-ε curve shows the properties of the material outside the fracture region while the σ-w curve shows the properties within. By finite element analysis including this model, it is possible to calculate how the fracture process region initiates and moves as the external action is increased. A schematic σ-w curve of wood is shown in Figure 3.5, plotted alongside a typical bilinear approximation.

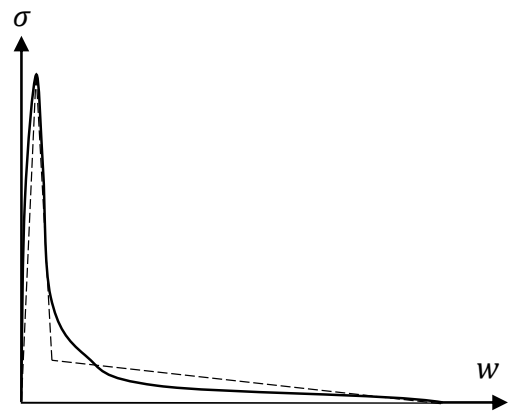

Figure 3.5: A schematic σ-w curve of wood in tension perpendicular to grain with a typical bilinear approximation. The curve is obtained by a displacement-controlled tensile test.

Perpendicular to grain fracture properties

The orthotropic nature of wood complicates the discussion of crack orientations, as six possible orientations of plane cracks are thus possible as shown in Figure 3.6. The nomenclature is such that the first index indicates the direction normal to the crack plane, while the second indicates the straightforward direction of the crack length extension. Combined with the fracture modes in Figure 3.4, this will sum up to 18 different basic fracture situations with, in general, different fracture resistances [39]. The high tensile strength in the longitudinal direction will, for example, result in high resistance to mode I crack growth for LR and LT orientations.

Fracture resistance can be defined by material stiffness and the fracture energy G_f. G_f is defined as the energy required to bring one unit area of the material from unloaded state to complete fracture. In the case of pure shear, the mathematical definition is thus found being:

$$G_f = \int_0^\infty \tau \ d\delta \tag{3.11}$$

It should be noted that the fracture energy G_f in general differs from the critical energy release rate G_c used in LEFM. While G_f is looking at a single material point during fracture, G_c

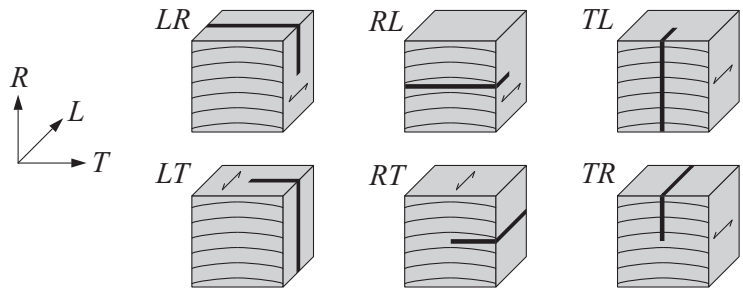

Figure 3.6: Crack plane orientation relative to the LRT directions.

Table 3.3: Fracture properties for spruce and pine found in literature. Density ρ in kg/m^3, moisture content u in %, fracture energy G_f in J/m^2 and material strength f in MPa.

Mode I				Orientation R		Orientation T	
Species	ref.	ρ	u	$G_{f,RR}$	f_{Rt}	$G_{f,TT}$	f_{Tt}
Scots pine	[40]	450	8	450	5.3	550	4.1
Scots pine	[40]	470	10	445	5.0	500	4.2
Scots pine	[40]	470	13	535	4.5	460	4.0
Scots pine	[40]	460	26	515	4.1		
Norway spruce	[41]	463	13			298	3.3
Mode II				Orientation R		Orientation T	
Species	ref.	ρ	u	$G_{f,RL}$	f_{LR}	$G_{f,TL}$	f_{LT}
Scots pine	[40]	460	13	815	11		
Norway spruce	[41]	463	13			965	8.4
Norway spruce	[42]		14			1240	9.8

represents the energy dissipated at the distinct tip of a progressing sharp crack. However, in the case of a material with a small fracture process region in relation to other dimensions, G_f and G_c are the same.

Various test setups can be used to determine the fracture energy of wood, also dependent on what crack mode is of interest. Commonly used for mode I is the single edge notched beam design (SENB), whereas small-scale notched specimen can be used for both mode I and II. A compilation of results found in literature is shown in Table 3.3 for spruce and pine. Of special interest in this thesis is mode II in tangential direction for Norway spruce as it is the dominating orientation in GLT lap joints.

3.4 BOND LINES

As will be discussed in more detail in Chapter 4, the strength of lap joints is greatly dependent on the properties of the bond line joining the adherends. In this section, the conventional non-resilient bond line will be distinguished from a resilient bond line, and methods of numerical modelling of the two are presented, based upon Paper C.

3.4.1 Non-resilient bond lines

Conventional bond lines used in the timber industry are made using stiff structural adhesives. The high stiffness causes stress concentrations in which fracture initiates, and the importance of the material softening behaviour has been shown in several studies [43, 44] and Paper C. NLFM is thus needed, and a bilinear softening behaviour is typically used in this thesis as presented in Section 3.3.3 in combination with a linear elastic material response for which a stress based failure criterion is to be fulfilled. A continuum-based modelling of the adhesive can be obtained using cohesive elements in which the adhesive has a finite thickness.

3.4.2 Resilient bond line

The resilient bond line, as defined in this thesis, is made of elastomeric materials, typically rubber. The main specific property of those materials is the ability to sustain large straining without permanent deformation [45]. From a modelling point of view, rubber is a hyperelastic material characterised by low non-linear elastic stiffness and a high Poisson's ratio, see Figure 3.7.

In order to numerically model rubber, hyperelastic models are typically based upon the assumption of isotropic behaviour throughout deformation history and thus being able to describe the material model in terms of strain energy potentials [46]. Typical forms of strain energy potentials used for rubber are the polynomials Yeoh and neo-Hookean forms, for which the specific coefficients for a resilient bond line is presented by Danielsson and Björnsson [47]. Non-linear geometry and special elements must be used in order to obtain reasonable results. More comprehensive reading on the mechanical properties of rubber can be found in e.g. [48].

As seen in Figure 3.7, rubber can be modelled as linear elastic in shear with only a small deviation from the real behaviour. This is often desirable in order to minimize the computational cost of an analysis. Paper C shows that this is indeed possible for the Shear plate dowel joint with reasonable accuracy, if special consideration is made to the high normal stiffness rubber obtains under plane strain conditions. The simulation procedure presented therein is used throughout this thesis.

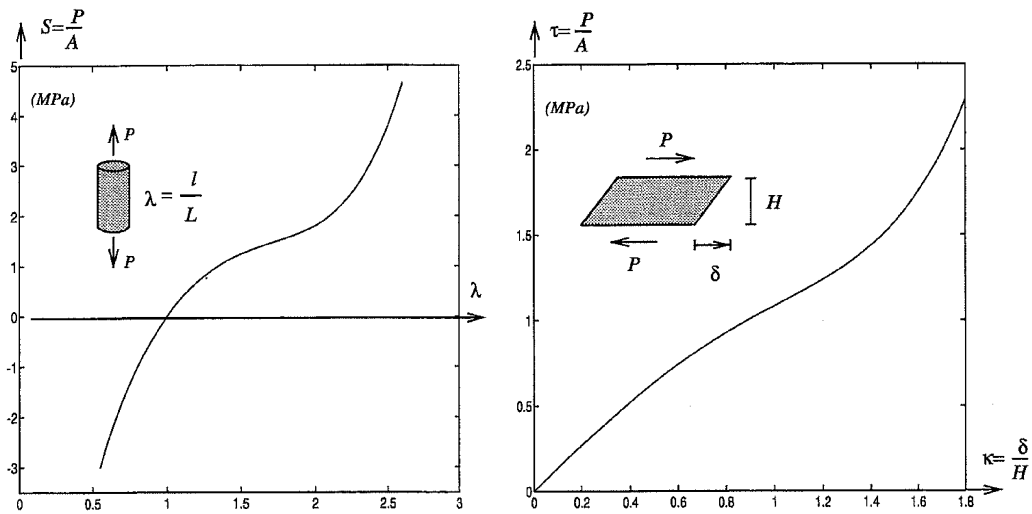

Figure 3.7: Typical non-linear elastic behaviour of rubber in tension (left) and in shear (right) [45]. l is the deformed length while L is the undeformed, together defining the stretch λ.

4

The resilient bond line

The scientific contribution of this thesis is to a large extent presented in the following two chapters. In this chapter, resilient bond lines in lap joints are investigated in comparison to more conventional non-resilient bond lines. This chapter is based upon the findings in Paper A, in which numerical, experimental and analytical analyses have been conducted.

4.1 BACKGROUND

While studying the Volkersen theory [49] regarding shear stress distribution of lap joints, Gustafsson [50] found that the fracture energy rather than shear strength in terms of maximum stress is decisive for the load carrying capacity of a lap joint. He also found that the relevant measure of fracture energy of the bond line included the elastic part of the stress vs. deformation response. As common adhesives are very stiff, this elastic part is usually of very limited size. However, the elastic part can be made considerably larger by introducing a resilient bond which thus increases the load carrying capacity of lap joints. A resilient bond line can be made up by introducing a rubber layer as shown schematically in Figure 4.1, or by using a resilient adhesive.

The effect of a resilient bond line can also be discussed in terms of shear stress distribution over the lap length. Common adhesives typically have a high stiffness which do not allow the different axial strains of the adherends. This causes shear stress concentrations at the ends of the joint as shown in blue in Figure 4.2. The failure strength is reached early and fracture is thus initiated prematurely at low external load. By having a low stiffness, the resilient bond

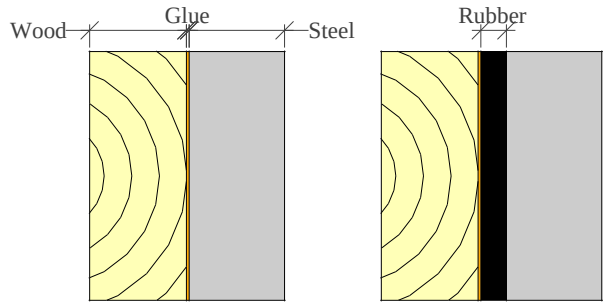

Figure 4.1: The schematics of non-resilient (left) and resilient bond line (right). Note that resilient bond lines can consist of other components than rubber as discussed in Paper A, and that the bond line can be used for different adherend materials.

line enables different axial strains of the adherends, resulting in a close to uniform shear stress distribution across the joint area.

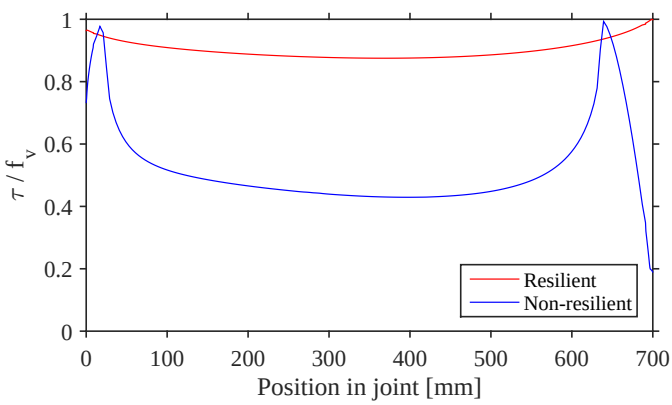

Figure 4.2: A comparison of the shear stress distribution in a common non-resilient bond line and in a resilient bond line at failure. Bilinear softening is used in the FE model. Geometry and loading is shown in Figure 4.3, using a lap length of 700 mm.

The concept has been studied in several publications [51–53], typically using a 1 mm thick rubber foil to promote the flexibility. The stiffness of the lap joint with resilient bond line is similar to a conventional nailed joint, although the resilient bond line shows an elastic behaviour up to large loads unlike the plastic behaviour of nailed joints due to yielding. In the comprehensive test series conducted by Gustafsson [51] it is shown that, among other things, the resilient bond line can be used to create interaction between dowel type fasteners and adhesive. Preliminary long duration load tests and creep tests have been performed using small lab-size specimens, see Björnsson and Danielsson [47].

4.2 DOUBLE LAP JOINTS

Shear stress concentrations are typical for long lap joints, suggesting that a positive influence of a resilient bond line is higher in such cases. In order to study this possible strength increase in a simple geometry with a dominant shear action, an experimental study of double lap joints was conducted for increasing lap length, see Figure 4.3. The lap width was 225 mm, while the width of the GLT elements were 230 mm and 280 mm for the outer and centre members respectively. Three different lap lengths of 200, 400 and 700 mm were used in a comparative study between resilient and non-resilient bond lines. Independent numerical and analytical analyses were conducted using material properties found in literature, with strength and stiffness as the main characteristics investigated.

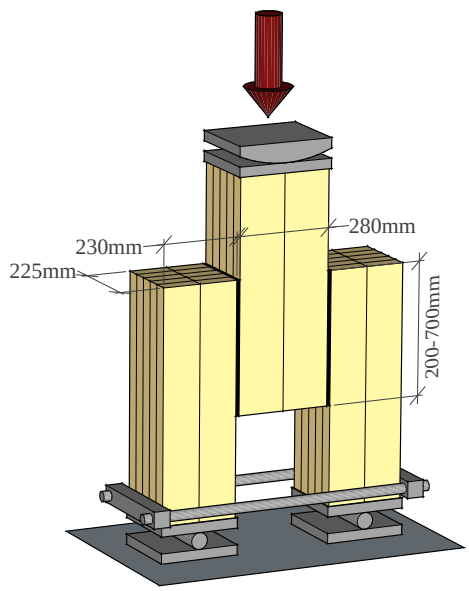

Figure 4.3: Double lap joint design used in the experimentally and numerically comparative study between resilient and non-resilient bond lines, c.f. Paper A.

4.3 CHARACTERISTICS

In terms of structural performance, strength and stiffness are of high interest. Strength is the fundamental property of a connection as to be able to withstand the forces occurring in a structure. However, the forces occurring are typically dependent on the stiffness of the connections, as the load is transferred by the stiffest load path possible. Thus, in order to have control over the actual load path, the stiffness of the connections must be known. An even greater control is obtained if the stiffness of the connections can actively be designed. The

results indicate that a resilient bond line can indeed increase the strength of long lap joints in comparison to non-resilient bond lines, as well as allowing the joint stiffness to be actively designed.

The strength of the lap joints are evaluated by means of the analytical Volkersen theory, numerical FE simulations as well as full scale tests as shown in Figure 4.5. The Volkersen theory [49, 54] presented in Paper A considers a linear elastic shear action without bending. The effects of both these limitations are visible in Figure 4.5, as bending decreases the load carrying capacity of the short resilient joints while the large influence of the softening behaviour increases the strength of non-resilient joints in comparison to the numerical analysis according to Chapter 3.

In addition to Figure 4.2, a shear stress comparison of the timber adherends is found in Figure 4.4. The non-resilient bond line (b) is loaded until failure at 720 kN using a shear strength of 4.4 MPa, and the same load is applied to the resilient specimen (a). The more uniform stress distribution is found for the resilient bond line, with lower maximum values. The propagating crack is visible in b) as it moves from the top and downwards.

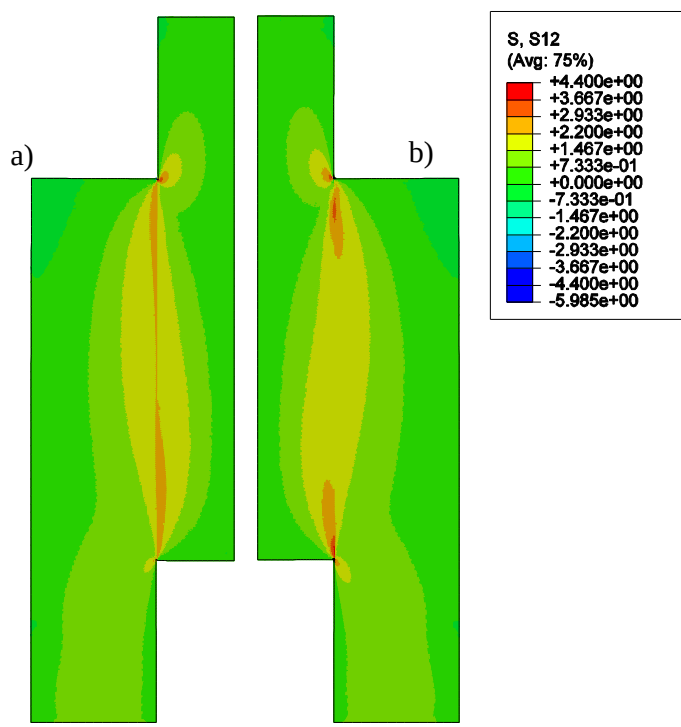

Figure 4.4: A comparison between the resilient (a) and non-resilient bond line (b) in terms of shear stress distribution in a 700 mm lap length. The non-resilient bond line is loaded to failure at 720 kN and corresponding load is applied to the non-resilient specimen.

A reasonable resemblance between the numerical, analytical and experimental results are found for the resilient bond line. Although considering the softening behaviour with material data presented in literature, little resemblance is found between the numerical model of the non-resilient bond line and the test results. The experimental study indicates similar load carrying capacities for resilient and non-resilient bond lines, which is not in agreement with numerical findings nor previously presented results [51] and Paper B. It is reasonable to assume that several influencing factors have led to the strength increase, among which the influence of boundary conditions is deemed most influential. Other factors comprise a possible underestimation of the fracture energy and influence of the softening behaviour. This is further discussed in Paper A.

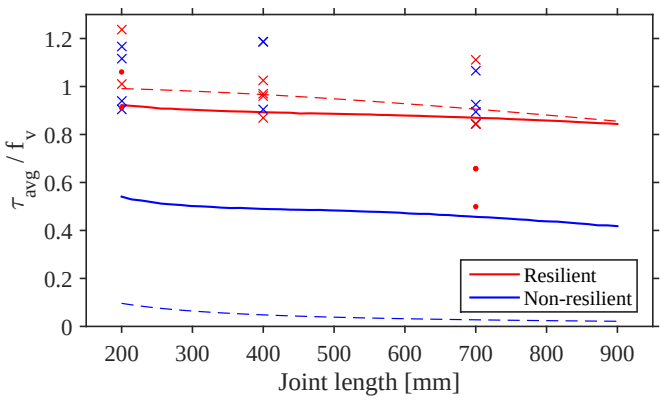

Figure 4.5: Numerical results of experimental setup compared to experimental data. Wood failure close to the bond line is marked with x while dots mark premature failures. The solid lines are numerical FE results while the dashed lines are analytical results according to Volkersen theory, using shear strength $f_v = 4.4$ MPa.

A great variability in rubber properties can be obtained using different fillers during the production, and also several different types of rubbers are produced. In terms of properties relevant in structural applications, the different products vary in e.g. durability, creep, usable temperature ranges, strength and stiffness. Not only can the elastic properties of the material be varied using fillers, but the thickness of the bond line can be chosen in a lap joint design. This combination enables a vast range of possible effective stiffnesses, which possibly enables strength interaction between a resilient bond line and e.g. dowel type connections.

Four types of resilient bond lines are tested in Paper A of which the result is summarized in Table 4.1. Two rubbers were tested: A mixture of natural rubber (NR) and styrene-butadiene rubber (SBR) as well as chloroprene rubber (CR). In addition, two elastomeric adhesives were also tested: SikaTack Move IT (IT) and Collano RESA HLP-H (CO). Although CR was found unsuitable for the application due to low strength, the bond lines combined well illustrate the possibilities of strength interaction as shown in Figure 4.6. Slip curves of different types of connectors will typically never be identical, but a strength interaction can theoretically be

Table 4.1: Mean strength [kN], mean average shear stress at failure [MPa] and mean stiffness [kN/mm] of 700 mm double lap joints of the four resilient bond lines tested in Paper A, as well as common adhesive PUR. Individual test results in parenthesis, while t is the bond line thickness [mm].

Type	t	Strength	Stress	Stiffness
SBR/NR	3.5	1290[a,b]	4.1	190
CR	0.5	360[c]	1.2	720
IT	2.0	760[c]	2.4	270
CO	1.5	730[c]	2.3	260
PUR	-	1290[b]	4.1	5470

a) Premature failure specimens excluded.
b) Failure in wood close to bond line.
c) Bond line failure in the adhesive/wood interface.

obtained as long as the different types are active in the same slip region.

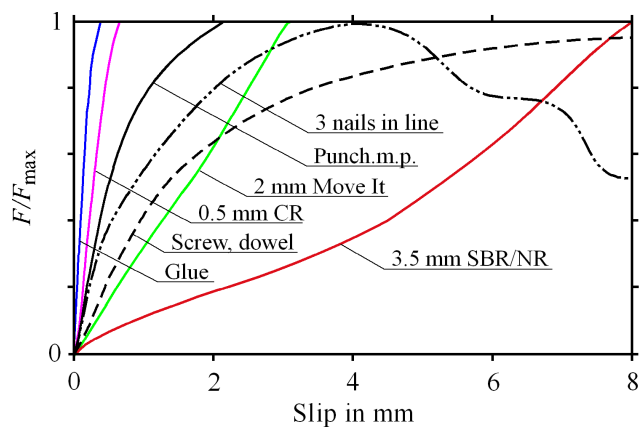

Figure 4.6: Slip comparison between common connectors and the resilient bond line.

In addition to strength and stiffness, there are several interesting and challenging characteristics of resilient lap joints not discussed here, but in future research.

4.4 APPLICATIONS

Resilient bond lines can typically be used whenever a conventional non-resilient bond line can be used. However, a higher production cost and lower stiffness is not suitable for all applications. Continuous bond lines in structural elements such as GLT and CLT are best made by a non-resilient bond line for common uses. The resilient bond line is typically advantageous

in applications when large forces are to be transferred in relatively small areas, such as in connections. The bond line can also be used to increase damping in elements when resistance to dynamic loads and/or impact loads is needed.

The double lap joint is not common in modern timber engineering. It has previously been used to lengthen timber elements, but GLT can today be produced in sufficient lengths directly and thus minimizing material use and improving design aspects. However, the key concept of this study is not the double lap joint itself, but rather the resilient bond line which is further used in the Shear plate dowel joint presented in Chapter 5.

Paper A also discusses the importance of the correct rubber treatment if used in a flexible bond line. The study shows a strength increase of the rubber-adhesive interface by 60 times when comparing no treatment to the one used. In terms of load carrying capacity of a joint, correct rubber treatment is vital for the structural integrity. This sensitivity is a clear potential drawback of the technique, but can possibly be eliminated by developing a standard treatment procedure with simple inspection techniques as partly suggested in Paper A.

5

The Shear plate dowel joint

The aim of this project is to develop a novel timber connection design for heavy structures with a high degree of prefabrication. The design should exceed the performance of existing solutions regarding one or more functional requirements, as discussed in Chapter 2, in order to be of interest. The Shear Plate Dowel Joint (SPDJ) design is proposed in this chapter, and utilises a resilient bond line for increased strength and a single dowel to promote efficient production.

5.1 BACKGROUND

When considering a production efficient truss node, the simplicity of a single large diameter dowel design is very appealing. As indicated by Figure 5.1, the members can be aligned and joined together in a single operation. However, this design requires special attention to plug shear failure as shown in Figure 5.2. In order to avoid this failure mode, Eurocode stipulates that the dowel to member end distance should be exceed $7d$, were d is the dowel diameter. Using a single large diameter dowel, this end distance would result in bulky and unpractical nodes. To minimize the end distance, different reinforcement techniques have been tested using screws and dowels [55,56]. Although the load carrying capacity was significantly improved in comparison with no reinforcement at all, the shear plug failure remained and the strength was still typically lower than competing solutions using several smaller dowels.

Parallel to the work on single large diameter dowels, Gustafsson developed a new adhesive joint technique based upon resilient bond lines, and conducted a large test series previously discussed [51]. Included in this experimental study was also a single large dowel design, but

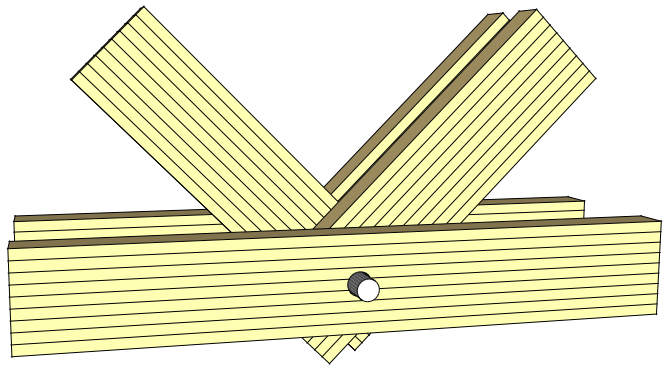

Figure 5.1: A single large diameter dowel enables fast erection of timber trusses, but is however prone to plug shear failure.

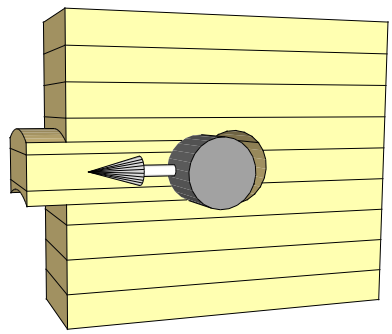

Figure 5.2: Typical plug shear failure when using a large dowel without reinforcement.

instead of internal screws as reinforcement he used externally bonded metal plates using a resilient bond line consisting of SBR rubber foil. This would distribute the stress over a larger area as shown in Chapter 4, thus preventing the formation of a shear plug resulting in increased strength. This combination of external plate and a single dowel is the basis for the Shear Plate Dowel Joint (SPDJ).

5.2 DESIGN AND APPLICATIONS

The SPDJ can be considered as a centrically loaded lap joint in a steel-wood configuration. Just like the previously discussed wood-wood lap joints, the resilient bond line can also here consist of rubber sheeting or a resilient adhesive. However, as rubber can be vulcanized to steel creating a very strong bond, the rubber is in this configuration preferred. An exploaded view of the SPDJ is shown in Figure 5.3, where a rubber sheeting is used.

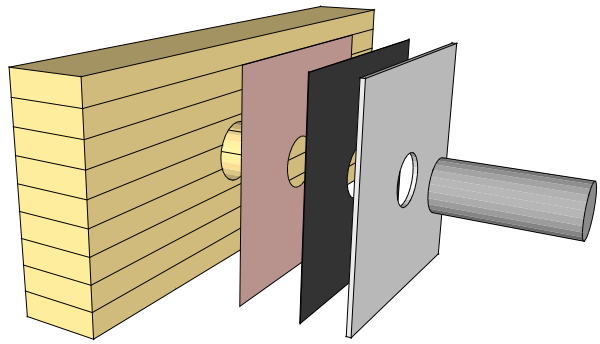

Figure 5.3: SPDJ components: GLT, adhesive, rubber, steel plate and dowel. Externally bonded on both sides of the GLT member.

The SPDJ was originally designed for truss nodes, thus being very similar to Figure 5.1. The main difference is the use of externally bonded metal plates which distribute the forces over a large area, see Figure 5.4. The resilient bond line technique is used to ensure that the entire plate area is active in load transfer. To ensure shear action rather than bearing stress in the timber, the hole is made somewhat larger in the GLT than in the steel plates. The dowel is thus not in direct contact with the timber, preventing it from splitting prematurely as a shear plug. The plates are bonded on both sides of each member in order to allow free rotation.

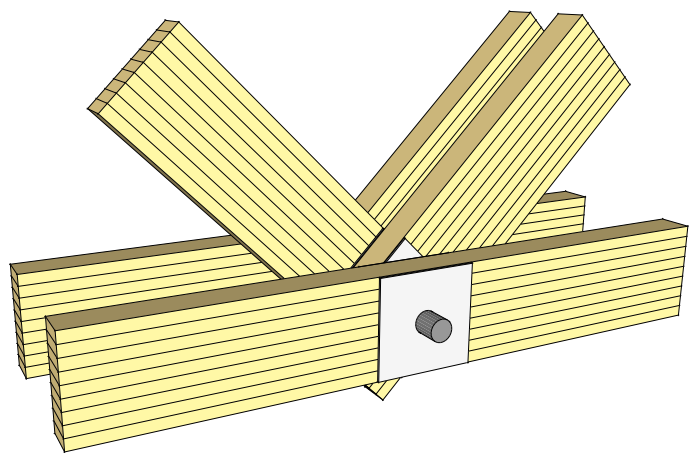

Figure 5.4: The Shear Plate Dowel Joint used in a truss node.

The strength of the SPDJ is strongly related to the steel plate size, which is determined by the design load. The dowel size is typically in the order of 15-30% of the member height and it is mainly limited by the bearing strength. The dowel can be made solid or hollow. Even though not yet tested, it should also be possible to create the entire connection using engineered wood

products at the expense of a decrease in load carrying capacity.

Even though primarily designed for truss nodes, the SPDJ can possibly also be used where a hinge is needed, e.g. in arch springings and beam-column connections as shown in Figure 5.5 and 5.6 respectively. A moment resisting connection could possibly be created by combining several dowels.

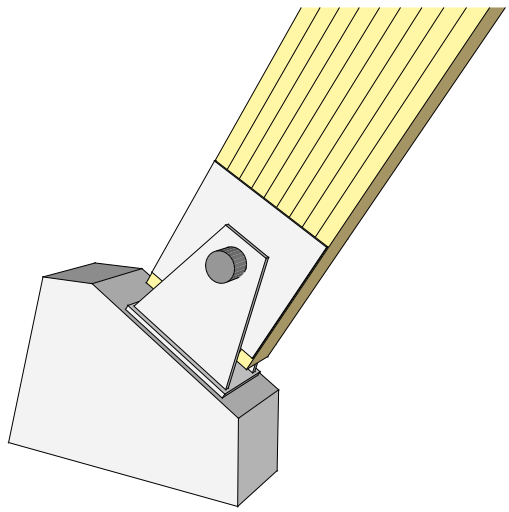

Figure 5.5: Arch springing with a SPDJ

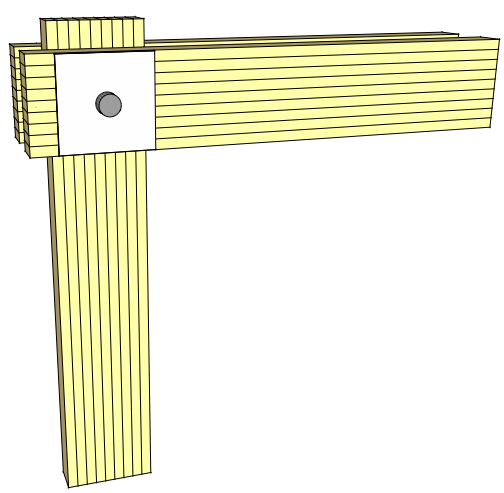

Figure 5.6: Beam-column connection using the SPDJ

5.3 EXPERIMENTAL STUDIES

A full scale test series comparing different singe dowel joint designs was carried in collaboration with associate professor Huifeng Yang at College of Civil Engineering at Nanjing Tech University, China. The study consisted of full sized single dowel joint designs and the findings are presented in Paper B. The study was designed to enable a simple comparison to a previous study conducted by Kobel [56], who also studied large dowel connections. Some of the tested joints from this combined effort are illustrated in Figure 5.7, were it should be noted that all uses different reinforcement techniques for the same dimensions of GLT and dowel. These tests also includes the SPDJ shown as f).

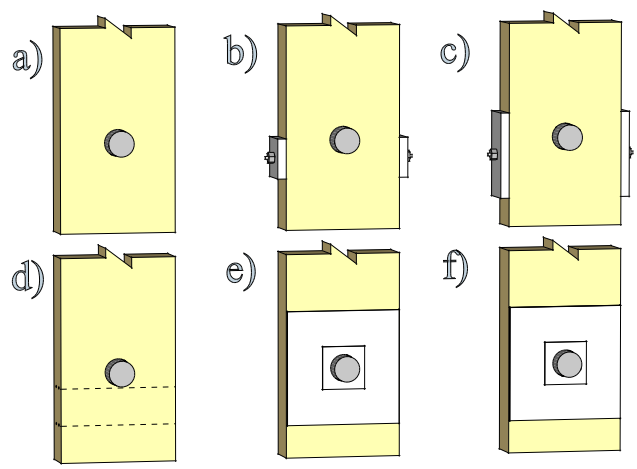

Figure 5.7: Different reinforcement techniques tested for single large dowel joints in Paper B and [56]. a) Non-reinforced reference, b) single rod, c) prestressed rod, d) 4 screws, e) glued steel plate and f) the SPDJ.

The results are compiled in Table 5.1 using a GLT cross section of 405x140 mm^2 and a dowel diameter of 90 mm. The reference case without any reinforcement is found having an average strength of 130 kN, at which point a shear plug failure occurred. An increased load carrying capacity was found using all reinforcement techniques, but often with questionable results in comparison to production time. While the steel plate joint without resilient bond line showed a premature failure at 220 kN in the steel-adhesive interface, the SPDJ outperformed all other designs by a vast margin. With a load carrying capacity of close to 1 000 kN, the design was worth investigating further.

Table 5.1: Average experimental strength and stiffness of the single dowel designs shown in Figure 5.7.

Specimen	Strength [kN]	Stiffness [kN/mm]
a) No reinforcement[1]	134	308
b) Rod	195	-
c) Rod, prestressed	298	-
d) Screws[1]	237	336
e) Glued steel plate joint [2]	220	-
f) SPDJ	990	484

1) From [56]
2) Premature failure

Table 5.2: Strength comparison between experimental and numerical results. [kN]

Specimen	Experimental	Numerical	Diff.
SPDJ without rubber	220[1]	560[2]	90%
SPDJ	990	1 050	6%

1) Premature failure
2) Assuming wood failure

5.4 NUMERICAL STUDY

The experimental results proved the design concept of the SPDJ and numerical models were developed to allow further analysis. The models are presented in Paper C and Section 3.4; one considering the glued steel plate with a non-resilient bond line, and one considering the SPDJ using a resilient bond line.

Of major interest during the development of the numerical models were the influence of peel stresses on the design. As the load is applied to the externally bonded steel plates, bending stresses develop due to the eccentricity. In order to fully capture this behaviour, a 3D model with a combined stress state failure criterion was required.

A premature failure was found in the experimental study for the glued steel plate joint by failure in the glue to steel interface. The numerical model was thus developed to reveal its full potential if the interface could be made sufficiently strong, admitting failure in the wood as limiting factor. Using a bilinear softening response, the load carrying capacity was found being 560 kN. A significant increase, but still not as strong as the SPDJ as shown in Table 5.2.

The SPDJ did however show wood failure close to bond line, thus showing considerably better agreement between the experimental and numerical analysis. The reasonable agreement between experiments and numerical analysis, but also with analytical analysis by the use of

Volkersen theory [49], allows the numerical model to be used for further parameter analysis of the SPDJ presented in Paper D.

Besides an increased joint slip, it was also found that an increasingly resilient bond line would increase the strength as the shear stress distribution approaches a uniform one. To minimize stress concentrations around the hole, two different types of steel plate designs shown in Figure 5.8, were compared to the original square design. Although a strength increase was found for the strip design, without any bond line along a strip at the height of the hole, the original design was found the most suitable as being most material efficient.

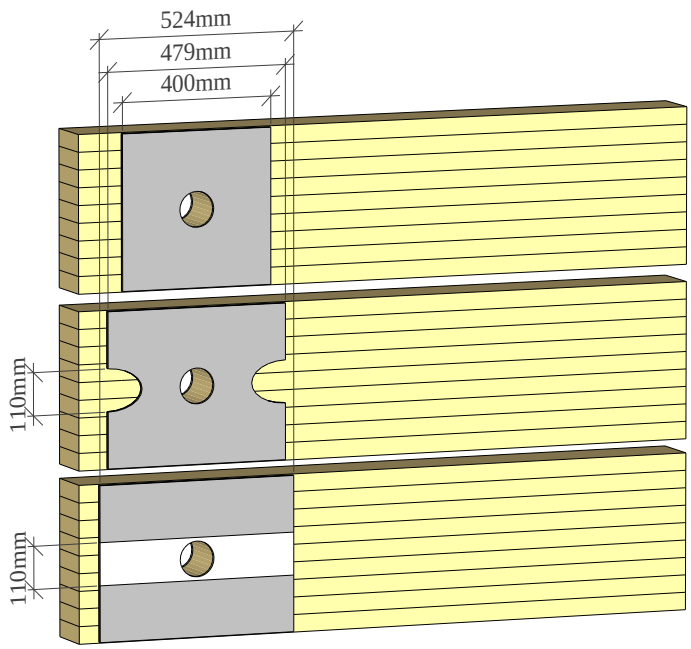

Figure 5.8: Alternative plate designs to the SPDJ studied in Paper D: The original square design (top), elliptical cut-outs (middle) and the strip design (bottom). All designs have the same bond area.

5.5 THE SPDJ AND THE FUNCTIONAL REQUIREMENTS

The presented results have yet only concluded that the SPDJ has a high load carrying capacity in terms of short term loading. The design is however expected to be useful also for dynamic loading, but the functional requirements of effective timber connections presented in Section 2.1 includes also other factors than strength. That is the topic of this section, and as the SPDJ is yet not existing in any real structure, the discussion is based upon available research results and sound engineering judgement. A short summary is found in Table 5.3.

Beside the load carrying capacity, the stiffness of the SPDJ is especially interesting as it can be designed to meet specific needs. Such a possibility is very uncommon in contemporary connections. The basic concept is explained and to some extent studied in Section 4.3 and Paper A, and numerically applied to the SPDJ in Figure 5.9. The stiffness of the joint can be designed varying the rubber hardness and thickness, with only a small influence on the load carrying capacity.

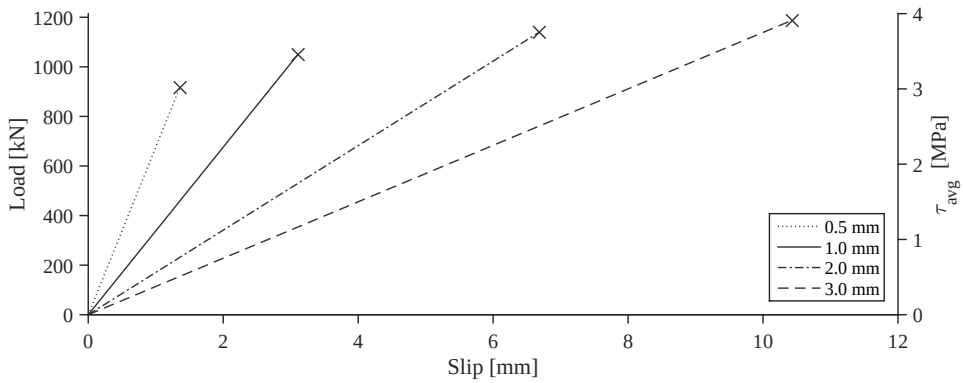

Figure 5.9: Linear slip curves using different rubber thicknesses with a shear modulus G= 1.1 MPa. Bond line failure marked with x.

The presented work has had the aim of finding the ultimate strength of the SPDJ design, which has resulted in the characteristic brittle wood failure. However, brittle behaviour is not a favourable characteristic regarding structural safety. A ductile joint performance can be achieved by careful design of the steel parts. Two possibilities exists: (1) the plate is made thin to obtain a deformation zone in the unbonded region of the hole, or (2) the steel dowel can be designed to deform in the contact zone, e.g. by choosing a hollow cross section. The latter has been studied in various designs in e.g. [57, 58] and is considered the best alternative. Further studies are necessary to fully implement this design concept for the SPDJ.

The SPDJ is a very simple design with a clear load path. Paper A and C also indicate the applicability of the Volkersen theory to the resilient bond line, making it possible to determine the load carrying capacity using a single analytical expression with reasonable agreement. The joint is also expected to be production friendly as the steel plates can be mounted onto the GLT member off-site, leaving only alignment and mounting of the single dowel on-site. A possible weakness in the manufacturing is the treatment sensitivity discussed in Paper A, and the practicality of the acid rinse.

Appearance is subjective, but the truss node in Figure 5.4 has the potential weakness of having to stack the members in the out-of-plane direction, creating wide nodes in comparison to e.g. slotted-in steel plates. Possible design alterations, e.g. using internally glued plates or locally reduced GLT thickness, can potentially improve this.

Of the resilient bond lines tested in Paper A, an SBR rubber foil was found most reliable in

Table 5.3: Summarized characteristics of the SPDJ based upon the functional requirements. Weak performance (-), average (~), good performance (+) and characteristics in need of further research (?) is indicated.

Strength	+	Stiffness and deformations	+	Ductility	?
Simplicity of design	+	Production friendly	+	Appearance	–
Durability	?	Fire	–	Costs	~
Sustainability	~				

terms of adhesion properties and strength. The idea of subjecting rubber to high permanent loads are often met with healthy scepticism regarding durability and also fire resistance, which both have to be studied further. Unpublished results following the study of Björnsson and Danielsson [47] show that small test specimens can be subjected to permanent load during a period of more than 6 years, and the tests were thereafter demounted as the lab facility was renovated.

The production cost of the joint is not known at this point. In comparison to slotted-in steel plates, the SPDJ is expected to be more labour intense off-site while less on-site, a combination often claimed being cost effective. Approximately the same amount of material is needed for both types of connections, but the easy dismantling of the SPDJ suggests that it can be reused. Recycling is although difficult due to the bonding of different materials.

Several suggestions for further research on the SPDJ have been presented here, which to some extent is needed prior to structural application. Fire and DOL performance are currently considered as possible crucial weaknesses.

6

Summary of appended papers

Four papers are appended to this thesis, of which the majority of scientific work have been conducted by the author in three. Summaries of the papers are presented below, differing from the respective abstracts in order to present a line of argument. For each paper, the contribution of the author is indicated. Some results and conclusions drawn in the appended papers are included in Part I.

Paper A

Use of a resilient bond line to increase strength of long adhesive lap joints
G. Larsson, P.J. Gustafsson, R. Crocetti
Submitted in January 2017.

Conventional non-resilient bond lines in long lap joints are compared to new resilient bond lines, which can increase the load carrying capacity by minimizing stress concentrations. A comprehensive comparative study is conducted numerically, analytically and experimentally, indicating differences between the methods used. The numerical and analytical results clearly shows the benefits of a resilient bond line, while the experimental results to some extent indicates the opposite. Difficulties in achieving a strong bond between adhesive and rubber are discussed as well as the influence of softening behaviour and boundary conditions. Despite the experimental results, the authors conclude that resilient bond lines typically increase the load carrying capacity of long lap joints.

The author planned and performed the research tasks including the experimental and numerical work, as well as writing the article. The co-authors contributed by a general supervision of the work, suggested experimental methods and test setup as well as reviewed the work.

Paper B

Experimental study on innovative connections for large span timber truss structures
H. Yang, R. Crocetti, G. Larsson, P.J. Gustafsson
Proceedings of IASS W.G. 12 + 18, 2015.

On-site assemblage can be made significantly more efficient by the use of a single large dowel. Reinforcements are however needed in order to prevent premature splitting failure, and several different reinforcing techniques are experimentally compared in this article. 15 full scale quasi-static tensile tests in 5 different designs were conducted on glulam members with identical connections at each end. It was found that all reinforcement techniques enhanced the performance of the connection, of which the Shear plate dowel joint clearly outperformed the others by using a resilient bond line in a wood-to-steel design.

The study was planned and conducted by assistant professor Huifeng Yang of the College of Civil Engineering, Nanjing Tech University, China. The author assisted in the experimental work conducted in China as well as in reviewing the paper.

Paper C

Bond line models of glued wood-to-steel plate joints
G. Larsson, P.J. Gustafsson, E. Serrano, R. Crocetti
Engineering Structures, 121: 160-169, 2016

As the experimental results of the Shear plate dowel joint were promising, developement of a representative and efficient numerical bond line model was of interest. Paper C presented such model which is in well agreement with the experimental results. The importance of fracture softening analysis of the non-resilient bond line is highlighted, and the analysis indicates a premature failure in the Paper B test series of the non-resilient specimens. Thus, the benefits of a resilient bond line is not as high as the experimental results indicate, but still increases the load carrying capacity by 150%. Comparison is also made to the analytical Volkersen theory describing the shear stress distribution of lap joints.

The analytical and numerical work was conducted by the author, as well as writing the majority of the paper. Remaining authors assisted in reviewing, writing shorter sections of the paper and general supervision of the work.

Paper D

Analysis of the shear plate dowel joint and parameter studies
G. Larsson, P.J. Gustafsson, E. Serrano, R. Crocetti
Proceedings of WCTE 2016.

This conference paper is a direct follow-up of Paper C, in which the previously presented bond line model is used to conduct parameter analysis of the Shear plate dowel joint. Alternative

designs are investigated along with a discussion of the applicability of the joint. Alternative joint designs are presented, for which it is concluded that the original square design is material efficient but not the strongest.

The author carried out all simulations as well as wrote the paper while the co-authors assisted in reviewing.

7
Concluding remarks

A summary of the research progress made within the Formas project *Innovative connections for timber construction* is presented in this chapter. Emphasis of the research has been put on resilient adhesive joints and the new connection design Shear plate dowel joint, but further research is needed prior to industrial use which is also discussed.

7.1 CONCLUSIONS

Despite to some degree conflicting results in Paper A, the general conclusion of this study is that a resilient bond line can increase the load carrying capacity of lap joints by reducing stress concentrations[1]. The technique is typically applicable whenever a conventional adhesive bond line is applicable, and special interest has been taken in the Shear plate dowel joint. The following conclusions are drawn:

Resilient bond lines

- Increase the load carrying capacity of long lap joints by minimizing stress concentrations.
- Enable the possibility to design joint stiffness.

[1] There is a saying that *Nobody believes the simulation results except the person doing them, whereas everybody believes the experimental results except the person doing them.* After this reading, would you agree or have I in this case convinced you otherwise?

- Analytical predictions regarding shear stress distribution and load carrying capacity can, in a simple manner, be made with reasonable high accuracy using the Volkersen theory.
- The resilient bond line can be made by either an intermediate rubber sheeting or a resilient adhesive.
- Show a high sensitivity to the manufacturing method, thus detailed instructions are needed.

The shear plate dowel joint

- A new connection for heavy timber structures is proposed.
  - High degree of prefabrication is possible
  - Fast installation
- Full scale short term tests shows promising results.
- Experimentally verified numerical model is developed.
- The square plate design is found most suitable.

7.2 FURTHER RESEARCH

Although the Shear plate dowel joint shows promising initial results, more research is needed before it can be used safely in heavy timber structures. Areas of interest are mainly related to the functional requirements discussed in Section 5.5, and are presented below.

Resilient bond lines

- Further investigations of the unexpected good performance of non-resilient bond lines in Paper A in order to determine causality.
- Development of production methodology with minimal variance in the achieved bond strength.

The shear plate dowel joint

- Influence of load direction to fibre orientation. Only load parallel to grain has yet been studied, but perpendicular to grain is important for some possible applications, e.g. beam-column connections.

- Duration of load effects must be investigated as rubber typically is prone to creep.
- Proposal of a design procedure should be developed, possibly based upon the Volkersen theory.
- Response to fire and possible solutions to counteract the temperature influence on rubber strength. Possible solutions include insulating materials, choice of rubber fillers and/or designing the curing pressure screws according to fire load.
- Investigate measures to increase joint ductility, possibly by the use of cylindrical dowels allowing deformations.
- Investigate possible vibration reduction by the use of SPDJ.

It should be noted that the resilient bond line possibly can be used wherever a common bond line is used. In some cases the strength can be increased, in other the stiffness can be lowered. Some of the presented items are planned for further research to the upcoming PhD thesis.

References

[1] Dodoo, A., Gustavsson, L., Sathre, R. (2016), *Climate impacts of wood vs. non-wood buildings*, Tech. rep., The Swedish Association of Local Authorities and Regions.

[2] Green, M.C., Karsh, J.E. (2012), *Tall Wood*, Canadian Wood Council.

[3] Madsen, B. (2000), *Behaviour of timber connections*, Timber Engineering Ltd.

[4] Dahl, K.B. (2009), *Mechanical properties of clear wood from Norway spruce*, Ph.D. thesis, NTNU Trondheim.

[5] Johnsson, H. (2004), *Plug shear failure in nailed timber connections. Avoiding brittle and promoting ductile failures*, Ph.D. thesis, Luleå University of Technology.

[6] Johansen, K. (1949), *Theory of timber connections*, in: *International Association of Bridge and Structural Engineering*, vol. 9, 249–262.

[7] Jorissen, A.J.M. (1998), *Double shear timber connections with dowel type fasteners*, Ph.D. thesis, Delft University.

[8] Larsen, H.J. (2003), *Introduction: Fasteners, Joints and Composite Structures. Ch.16 in: Timber Engineering ed. by Thelandersson,S., Larsen, H*, Chichester West Sussex.

[9] Eurocode 5, *SS-EN 1995-1-1*.

[10] Poutanen, T.T. (1989), *Analysis of trusses with connector plate joints*, in: *Proceedings of the Second Pacific Timber Engineering Conference, University of Auckland, New Zealand, 28-31 August 1989 Volume 1*, 155–159.

[11] Foschi, R.O. (1977), *Analysis of wood diaphragms and trusses. Part II: Truss-plate connections*, Canadian Journal of Civil Engineering 4(3), 353–362.

[12] Feldborg, T., Johansen, M. (1981), *Wood trussed rafter design: Strength and stiffness tests on joints. Long-term deflection of W-trussed rafters*, Statens Byggeforskningsinstitut, SBI.

[13] Blass, H.J. (2003), *Joints with Dowel-type Fasteners. Ch.17 in: Timber Engineering ed. by Thelandersson,S., Larsen, H*, Chichester West Sussex.

[14] Bengtsson, C., Johansson, C.J. (2002), *GIROD – Glued-in rods for timber structures*, Tech. Rep. 2002:26, SP Technical Research Institute of Sweden.

[15] Tlustochowicz, G., Serrano, E., Steiger, R. (2010), *State-of-the-art review on timber connections with glued-in steel rods*, Materials and Structures **44**(5), 997–1020.

[16] Natterer, J., Sandoz, J.L., Rey, M. (2004), *Construction en bois: matériau, technologie et dimensionnement*, Traité de génie civil de l'Ecole polytechnique fédérale de Lausanne, Presses Polytechniques et Universitaires Romandes.

[17] Adams, R.D., Wake, W.C. (1984), *Structural adhesive joints in engineering*, Elsevier Applied Science Publishers Ltd.

[18] Madsen, B. (1992), *Structural behaviour of timber*, Timber Engineering Ltd.

[19] Bodig, J., Jayne, B.A. (1982), *Mechanics of wood and wood composites*, Van Nostrand Reinholt Publishing.

[20] Dinwoodie, J. (2000), *Timber - Its nature and behaviour*, E&FN Spon, 2nd edition edn.

[21] Persson, K. (2000), *Micromechanical modelling of wood and fibre properties*, Ph.D. thesis, Lund University.

[22] Petroski, H. (1996), *Invention by Design: How Engineers Get from Thought to Thing*, Harvard University Press.

[23] Hearmon, R.F.S. (1948), *The elasticity of wood and plywood*, HM Stationery Office London.

[24] EN 338:2016, *Structural timber - Strength classes*.

[25] EN 14080:2013, *Timber structures - Glued laminated timber and glued solid timber - Requirements*.

[26] Astrup, T., Clorius, C.O., Damkilde, L., Hoffmeyer, P. (2007), *Size effect of glulam beams in tension perpendicular to grain*, Wood Science and Technology **41**(4), 361–372.

[27] Aicher, S., Dill-Langer, G. (2005), *Effect of lamination anisotropy and lay-up in glued-laminated timbers*, Journal of structural engineering **131**(7), 1095–1103.

[28] Danielsson, H. (2013), *Perpendicular to grain fracture analysis of wooden structural elements-Models and applications*, Ph.D. thesis, Lund University.

[29] Thelandersson, S. (2003), *Introduction: Wood as a construction material. Ch.2 in: Timber Engineering ed. by Thelandersson,S., Larsen, H*, Chichester West Sussex.

[30] Eberhardsteiner, J. (2013), *Mechanisches Verhalten von Fichtenholz: Experimentelle Bestimmung der biaxialen Festigkeitseigenschaften*, Springer-Verlag.

[31] Aicher, S., Dill-Langer, G., W, K. (2002), *Evaluation of different size effect models for tension perpendicular to grain*, in: *CIB-W18 Timber Structures, meeting 35*, 35-6-1.

[32] Weibull, W. (1939), *A statistical theory of the strength of materials*, 151, Generalstabens litografiska anstalts förlag.

[33] Johansson, M. (2015), *Structural properties of sawn timber and engineered wood products*, vol. 1, chap. 2, Swedish Forest Industries Federation, 2 edn.

[34] Norris, C.B. (1962), *Strength of orthotropic materials subjected to combined stresses*, FPL-1816. Madison, Wis. : U.S. Dept. of Agriculture, Forest Service, Forest Products Laboratory .

[35] Tsai, S.W., Wu, E.M. (1971), *A general theory of strength for anisotropic materials*, Journal of composite materials **5**(1), 58–80.

[36] Swiss Society of Engineers and Architects (2012), *Timber beams notched at the support*, SIA 265.

[37] Mascia, N.T., Nicolas, E.A., Todeschini, R. (2011), *Comparison between Tsai-Wu failure criterion and Hankinson's formula for tension in wood*, Wood Research **56**(4), 499–510.

[38] Hellan, K. (1985), *Introduction to fracture mechanics*, McGraw-Hill.

[39] Haller, P., Gustafsson, P.J. (2002), *An overview of fracture mechanics concepts*, Rep. No. RILEM TC **133**.

[40] Boström, L. (1994), *The stress-displacement relation of wood perpendicular to the grain*, Wood science and technology **28**(4), 309–317.

[41] Riberholt, H., Enquist, B., Gustafsson, P., Jensen, R. (1992), *Timber beams notched at the support*, Tech. Rep. TVSM-7071, Div. of Struct. Mech., Lund University.

[42] Stefansson, F. (2001), *Fracture analysis of orthotropic beams - Linear elastic and non-linear methods*, Licentiate thesis, Lund University.

[43] Serrano, E. (2000), *Adhesive joints in timber engineering. Modelling and testing of fracture properties*, Ph.D. thesis, Lund University.

[44] Wernersson, H. (1994), *Fracture characterization of wood adhesive joints*, Ph.D. thesis, Lund University.

[45] Austrell, P.E. (1997), *Modeling of elasticity and damping for filled elastomers*, Ph.D. thesis, Lund University.

[46] Dassault Systèmes (2012), *Abaqus Analysis User's manual*, Tech. rep.

[47] Björnsson, P., Danielsson, H. (2005), *Strength and creep analysis of glued rubber foil timber joints*, Master's thesis, Lund University.

[48] Freakley, P., Payne, A. (1978), *Theory and Practice of Engineering with Rubber*, Applied Science Publishers.

[49] Volkersen, O. (1938), *Die Nietkraftverteilung in zugbeanspruchten Nietverbindungen mit konstanten Laschenquerschnitten*, Luftfahrtforschung **15**(1/2), 41–47.

[50] Gustafsson, P. (1987), *Analysis of generalized Volkersen-joints in terms of non-linear fracture mechanics*.

[51] Gustafsson, P. (2007), *Tests of full size rubber foil adhesive joints*, Tech. Rep. TVSM-7149, Div. of Struct. Mech., Lund University.

[52] Gustafsson, P. (2008), *Stress equations for 2D lap joints with a flexible bond layer*, Tech. Rep. TVSM-7148, Div. of Struct. Mech., Lund University.

[53] Gustafsson, P. (2006), *A structural joint and support finite element*, Tech. Rep. TVSM-7143, Div. of Struct. Mech., Lund University.

[54] Gustafsson, P. (2008), *Tests of Wooden Cleats Oriented Along Fibre*, Tech. Rep. TVSM-7155, Div. of Struct. Mech., Lund University.

[55] Crocetti, R., Axelson, M., Sartori, T. (2010), *Strengthening of large diameter single dowel joints*, Tech. Rep. 2010:14, SP Technical Research Institute of Sweden.

[56] Kobel, P. (2011), *Modelling of strengthened connections for large span truss structures*, Master's thesis, Lund University.

[57] Pavković, K., Rajčić, V., Haiman, M. (2014), *Large diameter fastener in locally reinforced and non-reinforced timber loaded perpendicular to grain*, Engineering structures **74**, 256–265.

[58] Leijten, A. (2000), *The tube joint. Ch.10 in: Behaviour of timber connections by Madsen, B.*, Timber Engineering Ltd.

Part II

Appended publications

Paper A

Use of a resilient bond line to increase strength of long adhesive lap joints

G. Larsson[a], P.J. Gustafsson, R. Crocetti

[a]*Division of Structural Mechanics, Lund University, P.O. Box 118, SE-221 00 Lund, Sweden, gustaf.larsson@construction.lth.se*

Abstract

The strength of long adhesive lap joints are often limited by fracture energy rather than failure stress, suggesting that maximum load only is obtained after failure initiation due to stress concentrations at lap ends. This paper investigates a method to minimize these stress concentrations by introducing a resilient bond line, which increases the load carrying capacity of the lap joint while maintaining an elastic behaviour by allowing some shear deformation to occur. The study comprises analytical, numerical and full-sized experimental work on double lap joints comparing non-resilient to resilient bond lines.

The numerical analysis clearly indicates the strength increase made possible using resilient bond lines. A good agreement is also found between the numerical the analytical Volkersen theory for resilient bond lines, indicating that reasonable strength predictions can be obtained by hand calculations if peel stress interaction can be minimized.

The experimental results of the resilient bond line verifies the numerical findings, although production difficulties decreases the statistical significance of the result. On the contrary, the experimental results of non-resilient bond lines significantly exceed expectations, probably due to the specific boundary conditions used in the test setup.

Despite some contradictory experimental results, the conclusion of this study is that the efficiency of long lap joints can be increased by the use of resilient bond lines.

Keywords: timber, resilient bond line, lap joint, rubber foil, tests

1. Introduction

Lap joints have historically been used in engineering as a simple means of assembling structural members. Lap joints are today still used on a variety of materials, but the early examples are mainly for wood. Standing for well over a millennium, high-rise Japanese pagodas as well as the slightly younger Nordic stave churches are good examples of how timber can be assembled for durability, in which some joints are based upon a lap joint design [1, 2]. Today's efficient production and optimized material usage often rule out the old production methods and lap joints are hence rarely seen in modern timber structures. However, the resilient adhesive lap joints studied herein might prove to again increase the competitiveness of lap joints in heavy timber structures.

Consider an adhesive lap joint in a heavy modern timber structure. In such, large forces are typically transferred through the joint which requires large lap areas. For a given point along the lap length, the two adherends will typically experience different axial strains, particularly at the lap ends. This discrepancy causes severe shear stress concentrations in which fracture is initiated, thus limiting the total load bearing capacity of the joint.

While studying the Volkersen theory [3], it was realized that the stress concentrations of lap joints can be minimized if a bond line with low shear stiffness and high fracture energy, henceforth denoted a resilient bond line, is used. A test series based upon the idea using an intermediate rubber foil was conducted [4], without any comparisons to non-resilient bond lines. Further work has since been conducted on different types of applicable rubber [5], other full scale tests of innovative timber joints using the technique [6] and a numerical bond line model has been presented [7].

The present paper aims to determine the possible effect of using a resilient bond line in full scale wooden lap joints by a comparative study. The study comprises:

- Numerical and analytical analyses of an ideal lap joint comparing geometrically similar resilient and non-resilient bond lines. Sensitivity analysis according to the method of factorial design is also conducted, and

- a full scale experimental test series of double lap joints with lap lengths up to 700 mm. Non-resilient and resilient bond lines are compared,

but also different techniques to achieve a resilient bond line are tested. Additional numerical studies are conducted for the experimental setup.

2. Methods

Double adhesive lap joints were tested experimentally in full scale quasi-static compression tests, accompanied by numerical analyses using bond line models presented in [7]. Rational design equations can possibly be derived from analytical expressions based upon Volkersen theory [3]. The study is designed to investigate possible benefits of using a resilient bond line for large lap joints, in which a standard adhesive bond line is used as reference.

2.1. Tests

2.1.1. Test series

Double adhesive lap joints with increasing lap lengths according to Figure 1 were used, in which the bond line material varied according to Table 2. The height of the test specimens was 225 mm, and the width was 230 mm and 280 mm for the side members and centre member respectively.

In order to achieve a resilient bond line, a sheeting made from a mix of natural rubber (NR) and styrene-butadiene rubber sheeting (SBR) was primarily used. In order to possibly simplify the manufacturing process of resilient bond lines, three additional types were added to the test series. The use of chloroprene rubber sheeting (CR) could possibly decrease preparation work while rubber can also possibly be replaced entirely using resilient adhesives such as SikaTack Move IT (IT) and Collano RESA HLP-H (CO). The non-resilient reference PUR-series consisted of a 2-component polyurethane (PUR), the same as used for the rubber specimens.

The SBR/NR used was 3.5 mm thick with a shear modulus of 1.2 MPa and a tensile strength of $\geq$17.5 MPa and an elongation at failure of 400%. The CR was 0.5 mm thick with a density of 1.30 g/cm3 and a tensile strength of $\geq$13 MPa and an elongation at failure of $\geq$250% according to ISO standards. The hardness was the same as for the SBR/NR. The resilient adhesive SikaTack Move IT was slightly stiffer with a shear modulus of 1.4 MPa with a shear strength of 5 MPa and an elongation at failure of 300%. Collano RESA HLP-H is the softest material tested with a shear modulus of 0.4 MPa and an elongation at failure of approximately 260%.

Table 1: Bond line specifications

Specimen	L	Rubber	Adhesive	Qty
SBR-200	200	SBR/NR, 3.5 mm	SikaForce 7710 + hardener 7020	4
SBR-400	400	SBR/NR, 3.5 mm	SikaForce 7710 + hardener 7020	4
SBR-700	700	SBR/NR, 3.5 mm	SikaForce 7710 + hardener 7020	6
PUR-200	200	-	SikaForce 7710 + hardener 7020	4
PUR-400	400	-	SikaForce 7710 + hardener 7020	4
PUR-700	700	-	SikaForce 7710 + hardener 7020	4
CR-700	700	CR, 0.5 mm	SikaForce 7710 + hardener 7020	2
IT-700	700	-	SikaTack Move IT, 2 mm + SikaPrimer-3 N	2
CO-700	700	-	Collano RESA HLP-H, 1.5 mm	2

2.1.2. Manufacturing

Glued laminated timber (GLT) of strength class GL30c (Norway spruce) with a cross section depth of 225 mm was paired using SikaBond 545 in order to obtain the required dimensions. The lamella thickness was 45 mm. To reduce the risk of premature splitting, the upper member of the largest specimens was further reinforced by 2-3 6.5x220 mm screws inserted perpendicular to grain at the low end. The density was 440-460 kg/m3 at an average moisture content of 8.7% during testing.

The manufacturing method used for the bond line was dependent on the bond line material, and all methods were verified by tests. The method used for the SBR/NR is presented in detail in [4], which involves sulphuric acid treatment of the rubber prior to application of the adhesive. The acid treatment was conducted with 97% sulphuric acid at room temperature. The same gluing technique was used for the SBR/NR specimens as the PUR specimens. The GLT was planed within 2 hours prior to bond line gluing. All adhesive was applied to the GLT surfaces, one-sided for each bond, and cured in room temperature with manually applied curing pressure using 4-6 sash clamps. Dependent on used adhesive, the pressure was typically applied for 24 hours and the specimens stored at minimum one week prior to testing.

The manufacturer of the CR recommended the use of CR-based contact adhesive for application, but pre-testing indicated low strength. In order to obtain the best result, the CR was also treated with sulphuric acid according

to [4] and 2-component PUR adhesive was used.

The resilient adhesive in the IT specimens was applied using a motorized mobile caulking gun after application of the primer. A maze of adhesive strings was applied to the wood surface which were flattened out by applying compression between the two adherends. The thickness of the bond line was ensured by 2.0 mm rubber distances. Due to the manual string-wise application, the bond line was not entirely continuous making the nominal bond line area smaller than intended with typically 90-95% coverage. The low viscosity of Collano RESA HLP-H enabled pouring of the adhesive on to the substrate, ensuring 100% coverage if the 1.5 mm rubber distances are disregarded. The CO specimens was stored for one month prior testing to ensure proper hardening.

2.1.3. Setup and loading procedure

The experimental test setup is shown in Figure 1. The test is designed to primarily fail in shear, in which the horizontal shackle reduces the effect of leg splitting during the displacement controlled quasi-static loading. The shackle was made up of UPE 80 beams and 8.8 M16 rods. Steel plates were used in order to uniformly distribute the bearing stress between the points of load application and the end grain.

The loading procedure was conducted according to the European Standard EN 26891 for timber structures. The load is applied up to 40% of the estimated failure load F_{est}, then reduced to $0.1F_{est}$ before loaded to failure at an actuator speed of 1.1 and 1.5 mm/min for non-resilient and resilient bond lines respectively. The relative shear displacement over the bond line was measured centrically on both sides using four LVDTs with 140 mm length of stroke. The measurement points were located 25 mm from the bond line on either side. The load was measured using the hydraulic oil pressure, which was calibrated up to 500 kN with a maximum error less than approximately 2%.

Possible failure modes include bond line failure in the wood/adhesive interface, rubber/adhesive interface, rubber failure, wood failure close to bond line by shear/peel stress interaction and wood tensile crack perpendicular to grain along the centreline of the specimen due to leg splitting. Except rubber failure, all these failure modes were visible in the experimental study. However, only wood failure close to bond line by shear/peel stress interaction is studied in the numerical analyses as further discussed in the following section.

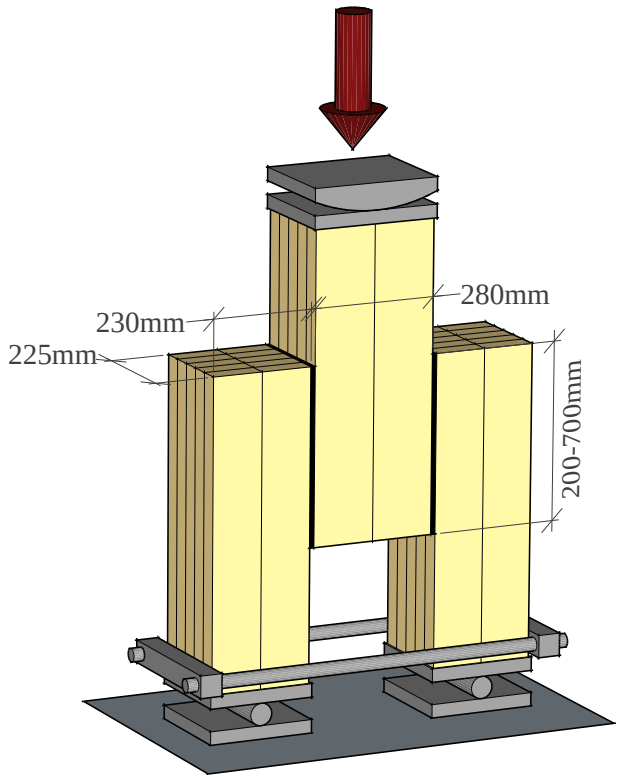

Figure 1: Double lap joint test setup

2.2. Numerical strength analysis

Numerical analyses with linear and non-linear fracture modelling were performed in order to determine a general length to strength behaviour for resilient and non-resilient bond lines respectively. The simulations were performed in plane stress 2D by means of finite element modelling using commercial general purpose FE software. The model consists of wood and a bond line. The bond line model is presented in [7], and represented by a cohesive layer with a single element in the thickness direction. The bond line thus represents either (1) the adhesive or (2) the adhesive and the rubber foil; including the material interfaces. As fracture softening is important for common adhesives while negligible for resilient bond lines, two separate approaches were used to

model the bond line. A bilinear softening model is used for the non-resilient specimens while the resilient bond line is represented by a linear elastic material, as shown in Figure 2. The specific bond line model includes a method to consider the normal stiffness variation of resilient bond lines due to Poisson's ratio $\nu \to 0.5$ in a linear fashion. The bond line strength is represented by wood failure while the shear modulus used was 1.2 and 1000 MPa for resilient and non-resilient bond lines respectively.

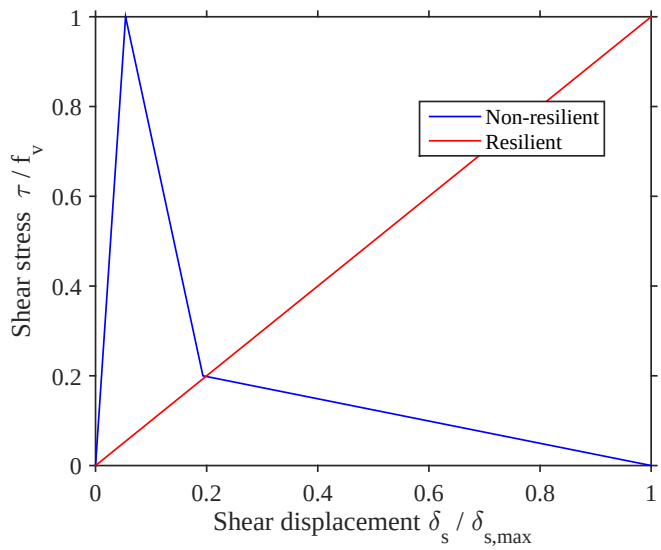

Figure 2: A linear shear stress-displacement behaviour was used for the resilient bond lines, while a bilinear model was used for the non-resilient.

The wood body is represented by a linear elastic rectilinear orthotropic material model, for which the 2D parameters are given in Table 2. Wood parameters were used in a stochastic fashion, where normal distribution was found for all parameters except for the stiffnesses, see Dahl [8]. Fracture softening of wood adhesive bonds has been studied by Wernesson [9], from whom fracture energies are found.

A load controlled analysis without artificial stabilization was used. Symmetry was regarded on the geometry built up by first order plane stress solid

Table 2: Adopted material parameters for wood [8, 9]. Parameters are given in MPa and [-] with corresponding coefficient of variation (CV). Fracture energies are given in Nm/m^2.

	Direction	Mean	CV
Young's modulus*	E_L	9040	0.38
	E_R	790	0.28
Shear modulus	G_{TL}	600	0.30
Poisson's ratio	ν_{TL}	0.06	0.07
Shear strength	f_v	4.4	0.38
Tensile strength	$f_{t,90}$	4.9	0.15
Fracture energy	$G_{f,I}$	230	0.14
	$G_{f,II}$	850	0.10

*) Lognormal distribution

elements with 4 nodes and full integration. Cohesive elements were used for the bond line with one element in the thickness direction. Failure was evaluated using a stressed based Norris failure criterion [10] for the resilient bond line while the maximum strength of the propagating fracture was adopted for the non-resilient bond line.

In order to obtain a reasonable strength comparison between resilient and non-resilient bond lines, boundary conditions in the numerical analysis were mainly set in order to achieve a dominant shear action in the lap joint, as well as using the same bond line thickness of 1 mm regardless of type (despite experimental test setup). The experimental geometry was otherwise emulated. In comparison to the boundary conditions illustrated in Figure 1, roller supports are in this section replaced by fixed and thus no shackle is needed. Comparison to test results are made with more realistic boundary conditions in Section 3.2.2.

A screening process for important factors was conducted using a two-level fractional factorial 2^{9-4}_{IV} design for the resilient and non-resilient model individually [11]. The analysis included 9 geometric and material parameters with a variation of $\pm 10\%$ including failure strengths, fracture energies and axial stiffness of the members. A full factorial 3^4 design was then conducted to discover possible non-linear responses and interactions between analysed factors, which is not possible in a common one-factor-at-the-time sensitivity analysis. The four most influential material parameters were then inserted

as stochastic variables in order to possibly verify a strength increase of the resilient bond line regardless the natural variability of wood.

2.3. Analytical

2.3.1. Shear stress distribution

The analytical expression used for determination of the shear stress distribution and bond line strength is based upon the Volkersen theory [3] as presented in [12]. For the compression-compression load configuration used in the test, but neglecting bending, the 1D shear stress distribution of the bond line τ_3 is found being

$$\tau_3(x) = C_1 \cosh(\omega x) + C_2 \sinh(\omega x) \tag{1}$$

$$C_1 = \frac{PG_3}{t_3\omega}\left(\frac{1}{E_1A_1\tanh(\omega L)} + \frac{1}{E_2A_2\sinh(\omega L)}\right) \tag{2}$$

$$C_2 = \frac{PG_3}{t_3\omega}\left(\frac{-1}{E_1A_1}\right) \tag{3}$$

$$\omega L = L\sqrt{\frac{G_3b_3(1+\alpha)}{t_3E_1A_1}} \tag{4}$$

$$\alpha = \frac{E_1A_1}{E_2A_2} \leq 1.0 \tag{5}$$

The shear stress distribution of the bond line (index 3) is thus governed by the properties of the two adherends (index 1 and 2) and the bond line properties: cross-sectional area A, longitudinal stiffness E, bond line length L, width b_3, thickness t_3 and shear stiffness G_3.

The shear stress distribution of the experimental geometry by means of Volkersen theory is presented in Figure 5. By identifying the maximum shear stress at $x = 0$ and introducing the material shear strength, the load carrying capacity P_f can be determined by

$$P_f = b_3Lf_v\frac{(1+\alpha)\sinh(\omega L)\tanh(\omega L)}{\omega L\left(\sinh(\omega L) + \alpha\tanh(\omega L)\right)} \tag{6}$$

As $\tanh(\omega L) \to 1.0$ for large ωL, Eq 6 can be reduced to

$$P_f \approx b_3 L f_v \frac{(1+\alpha)}{\omega L} \tag{7}$$

The approximation deviates less than 0.5% for $\omega L \geq 6$. The Volkersen theory does not include bending, which however does occur in the test setup.

2.3.2. Brittleness ratio in terms of long lap joints

This study argues for the benefits of a resilient bond line in long lap joints and the definition of a long lap joints must be put into perspective of the adherends, which properties influence the shear stress distribution. In order to obtain an estimate of the length needed for positive influence of a resilient bond line, the brittleness ratio of lap joints λ can be used. [13]

The normalized mean shear stress at failure is governed by the brittleness ratio λ of lap joints. In order to achieve a high utilization ratio of the bonded area, it is important to have a low brittleness ratio. Using the strength limits of ideal plasticity and linear elastic fracture mechanics (LEFM), it is possible to identify an approximation of the recommended maximum value of λ which allows for a high efficient lap joint as

$$\lambda = \frac{l^2 f_v^2}{t_1 E_1 G_f} \leq 2(1+\alpha) \tag{8}$$

where α is defined in Equation 5 and t_1 is the thickness of element 1. If a resilient bond line is used, then $G_f = f_v^2/2G_3$. The limitations of LEFM should be noted and the fact that bending is not included in Equation 8. In order to meet the recommended brittleness ratio, Equation 8 suggests that a resilient bond line should be used for lap lengths over 420 mm for the geometry used in the experimental study ($\alpha = 0.61$).

3. Results and Comparisons

The results of this study comprises numerical and experimental analyses comparing resilient to non-resilient bond lines, as well as influencing parameters. The numerical analyses will indicate an increasing strength difference in favour of the resilient bond line as the lap length increases, which however is in disagreement with the experimental results. It is the authors believe that the discrepancy between the results is due to the influence of boundary conditions and production difficulties.

3.1. Numerical results

The numerical analysis is based upon an ideal lap joint comparing geometrically similar resilient and non-resilient bond lines. Boundary conditions are set to promote shear action with minimal interference of tensile stresses in the bond line induced by leg splitting. Material parameters are found in Table 2.

3.1.1. Factorial design

Out of nine material and geometrical parameters analysed, the four most influential were further studied in a full 3^4 factorial design from which the results are presented in Figure 3. The analysis was conducted for a base bond line length of 500 mm, and all parameters were independently varied $\pm 10\%$ from the reference values discussed in Section 2.2.

The factorial design clearly highlights the fundamental differences between resilient and non-resilient bond lines. Due to high stress concentrations in non-resilient bond lines, a shear strength increase does not influence the load carrying capacity, which is more dependent on fracture energy. Although to some extent proportional, these material properties have been considered individually in this analysis for illustration purposes. Resilient bond lines have a strength advantage when used in long lap joints, as the average shear stress at failure does not drop at the same rate as for non-resilient bond lines for increased lap length as shown in Figure 3. Low stiffness, by either using a less stiff or thicker bond line, increases the load carrying capacity at the expense of a decreased joint stiffness. As the stiffness of the bond line approaches zero, the strength approaches the theory of perfect plasticity.

The factorial design analysis does not suggest any parameter interaction for the resilient bond line in the analysed parameter region in terms of average shear stress over the lap area. It does however suggest a slight interaction in case of non-resilient bond line between lap length and shear strength, as well as between fracture energy and shear strength.

3.1.2. Numerical comparison of strength to length performance

For the double lap joint geometry shown in Figure 1 using deterministically increasing length, independent stochastic material parameters were inserted in a numerical strength analysis. The stochastic material parameters were the shear strength f_v, shear fracture energy G_f, normal stiffness of wood E_L and tensile strength perpendicular to grain $f_{t,90}$. The result of 700 stochastic numerical simulations are shown in Figure 4 using a 2^{nd} order polynomial

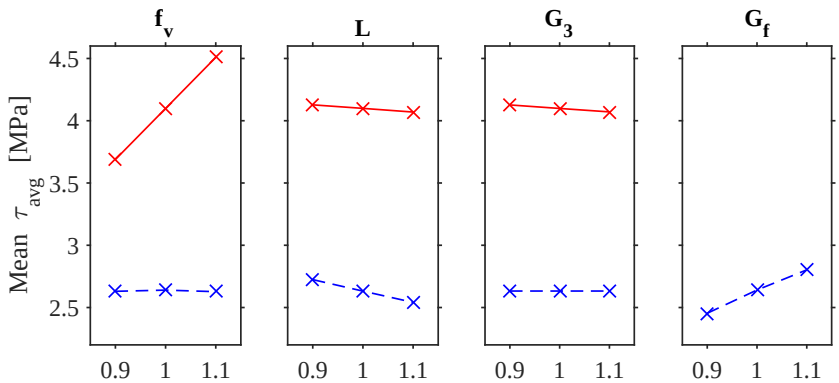

Figure 3: Parameters significantly influencing the average shear stress at failure according to full factorial 3^4 design using a $\pm 10\%$ variation of reference values: shear strength f_v, lap joint length L, stiffness of the bond line G_3 and shear fracture energy G_f. Resilient bond line as solid line while non-resilient in dashed. Reference values are found in Section 2.2.

fit with corresponding 95% confidence interval. A decreasing average shear stress at failure is visible for both non-resilient and resilient bond lines for increasing lap length, although the effect is less pronounced in case of a resilient bond line as also predicted by the factorial design.

To evaluate the applicability of the Volkersen theory on this specific design, a comparison is made to the numerical analysis in Figure 4. A good agreement is found between analytical and numerical results for a resilient bond line, while very poor agreement for non-resilient bond lines primarily due to the fact that fracture softening is not taken into account in the Volkersen theory.

The increased strength of resilient bond lines is due to the more uniform shear stress distribution as shown in Figure 5, which also illustrates a comparison to the analytical Volkersen shear stress distribution from Equation 1.

The numerical analysis indicates that damage is initiated in the non-resilient design at approximately 70% of maximum load, while no damage is modelled for the resilient bond lines.

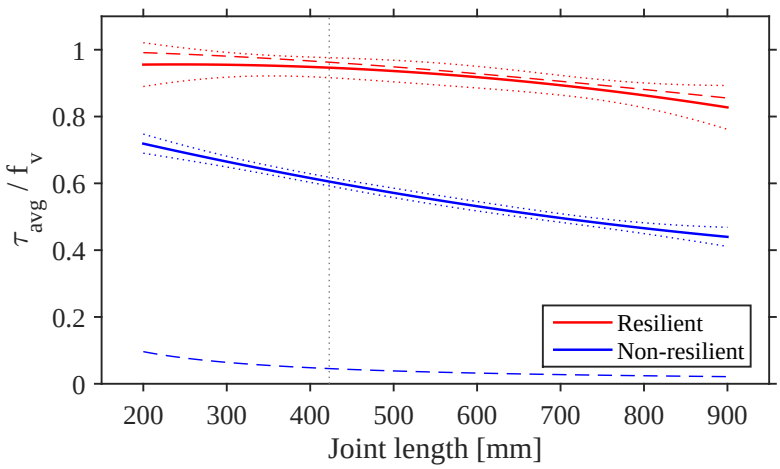

Figure 4: Normalized shear stress at failure for increasing joint length. Quadratic polynomial fit to numerical stochastic analysis is indicated by solid lines with corresponding 95% confidence dotted adjacent ($R^2_{flex} = 0.033$, $R^2_{n.flex} = 0.443$). Analytical results according to Volkersen theory in dashed lines where a good resemblance is found for the resilient bond line while very poor for the non-resilient. The vertical dotted line represents the suggested lap length limit according to Equation 8.

3.2. Test results

Experimental testing was conducted to relate to the numerical findings with a direct comparison between resilient and non-resilient bond line. A previously published production method for SBR/NR based resilient bond line [4] is also studied. Different means of achieving resilient bond lines are compared.

3.2.1. Adhesion between rubber and adhesive

The generally low surface energy of rubber is problematic in terms of adhesion as the adhesive used must have an even lower surface energy in order to achieve a strong bond [14]. However, this is seldom the case and poor adhesion, or no adhesion at all, follows.

It is a relative difference in surface energy that has to be obtained, which can be done by either modifying the rubber or the adhesive. In this study,

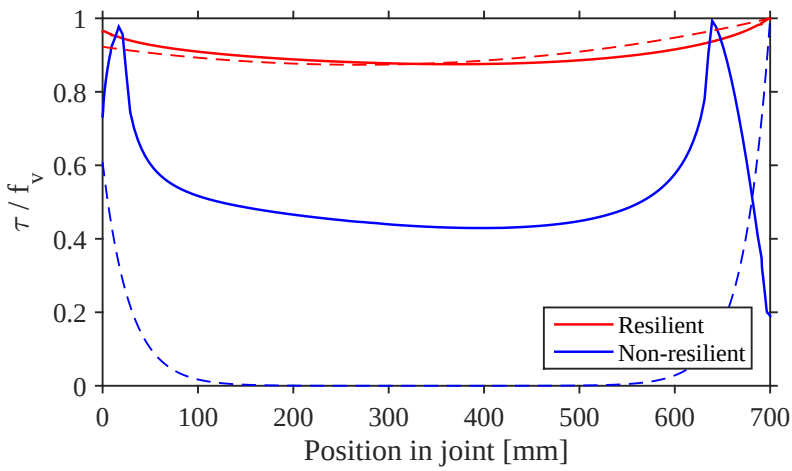

Figure 5: Normalized shear stress distribution at failure load of 700 mm double lap joints according to numerical analysis. Origo is placed at the low end of the lap joint in comparison to Figure 1. Stress distribution according to Volkersen theory as dashed line.

the surface energy of the rubber was increased by sanding and etching in concentrated sulphuric acid. Clean surfaces were obtained by rinsing the specimens in water and ethanol. In order to investigate the influence of the treatment, a small study was conducted on simple rubber-adhesive-rubber peel tests according to Figure 6 using 3.5 mm SBR/NR rubber and 2C PUR adhesive with a thickness less than 0.5 mm. Using two nominally equal test specimens, the effect of each process step was investigated according to Table 3 which also presents the corresponding load at failure. The importance of an adequate rubber treatment prior to bonding cannot be underestimated as this simple test suggests a strength increase of up to 60 times using a combination of 30 seconds of acid etching after rigorous sanding. In order to achieve a strong bond of the SBR/NR rubber, the initially shiny surface must be sanded until a matt surface is obtained.

3.2.2. Influence of lap length

The strengths of the non-resilient PUR- and the resilient SBR-series were compared for increasing lap lengths. In comparison to the numerical results

Table 3: The effect of rubber processing steps on tensile strength.

Category	Treatment				Avg force
	Water	**Ethanol**	**Sand paper[a]**	**Etched[b]**	**at failure [N]**
1	-	-	-	-	0
2	x	-	-	-	5
3	x	x	-	-	5
4	x	x	+	-	15
5	x	x	++	-	50
6	x	x	+	+	140
7	x	x	+	++	130
8	x	x	++	+	310
9	x	x	++	++	90
10	x	x	-	++	30

a) + corresponds to 5 seconds by belt sander while ++ is 30 seconds (results in a matt surface)

b) + corresponds to 30 seconds submerged in concentrated sulphuric acid while ++ is 3 minutes

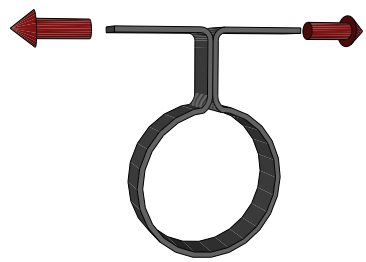

Figure 6: Rubber-adhesive adhesion tensile test. Bonded area was 50x50 mm^2.

shown in Figure 4, remarkably high strength of non-resilient specimens was found in the experimental results presented in Table 4 and Figure 8. The numerical analysis indicated a non-resilient failure load of 700 kN for the 700 mm specimen, while the experimental study averaged 1290 kN (c.f. Section 3.2.3).

All non-resilient specimens showed a brittle failure in wood close to the bond line, see b) in Figure 7. Two types of failure modes were visible in the resilient specimens. Some resilient specimens failed in similar wood bond line failure as the non-resilient, while other failed prematurely in the adhesive-rubber interface as indicated in Table 4. Visual inspection subsequent to failure indicates poor rubber treatment, in which some rubber areas were of type category 6 instead of the intended category 8 (Table 3) which is believed to initiate the premature failure. A reasonable agreement is found between experimental and numerical results of the resilient bond line if the specimens with premature failure are disregarded.

For a vast majority of the test specimens, a tensile crack perpendicular to grain was formed in the low end of the middle member prior to failure due to horizontal tensile stresses, see a) in Figure 7. The crack did not influence the global behaviour of the lap although an irregularity in the displacement plot was observed, i.e. at 700 kN for SBR-700-4 in Figure 9.

A comparison of the deformation of the resilient and non-resilient bond lines are found in Figure 9. By introducing the 3.5 mm thick SBR/NR sheet, the measured stiffness over the bond line was reduced by a factor of approximately 30.

Additional numerical simulations were also conducted with boundary con-

Table 4: Strength [kN] and average shear stress at failure [MPa] from experimental tests for non-resilient adhesive and the resilient SBR/NR with increasing lap length [mm]. Individual test results in parenthesis.

L	Non-resilient		Resilient	
	Strength	**Avg stress**	**Strength**	**Avg stress**
200	410 (359, 373, 461, 441)	4.5 (4.0, 4.2, 5.1, 4.9)	420 (490, 420*, 361*, 400)	4.6 (5.5, 4.7*, 4.0*, 4.4)
400	870 (941, 940, 716)	4.8 (5.2, 5.2, 4.0)	760 (687, 769, 759, 814)	4.2 (3.8, 4.3, 4.2, 4.5)
700	1290 (1168, 1285, 1242, 1480)	4.1 (3.7, 4.1, 3.9, 4.7)	1070 (911*, 692*, 912*, 1172, 1169, 1537)	3.4 (2.9*, 2.2*, 2.9*, 3.7, 3.7, 4.9)

*) Premature failure in glue-rubber interface

ditions according to the test setup. Roller supports were used, the shackle represented by a linear spring (k=35 kN/mm) and bond line thicknesses of 0.1 mm and 3.6 mm were used for non-resilient and resilient bond line respectively. It was found that the resilient SBR specimens were somewhat more sensitive to the shackle stiffness than the non-resilient PUR specimens, while shorter specimens were significantly more sensitive than longer. In comparison to the results shown in Figure 4, the use of the shackle stiffness causes a strength decrease of both types of bond lines as seen in see Figure 8. This is especially relevant for shorter lap lengths as these are more prone to bending. A general strength increase using a resilient bond line is found also in this analysis.

3.2.3. Influence of boundary conditions

In addition to the test setup described in Section 2.1.3, the influence of support conditions was experimentally investigated to possibly clarify the high strength observed for the non-resilient bond lines. The main study was conducted using steel plates covering the entire end area of the specimens as seen in Figure 1, which is restricting the formation and/or propagation of shear plugs on the side of the elements. One additional test specimen each of type SBR-700 and PUR-700 was made in order to experimentally evaluate this restriction by reducing the end grain area covered by the steel plate. The

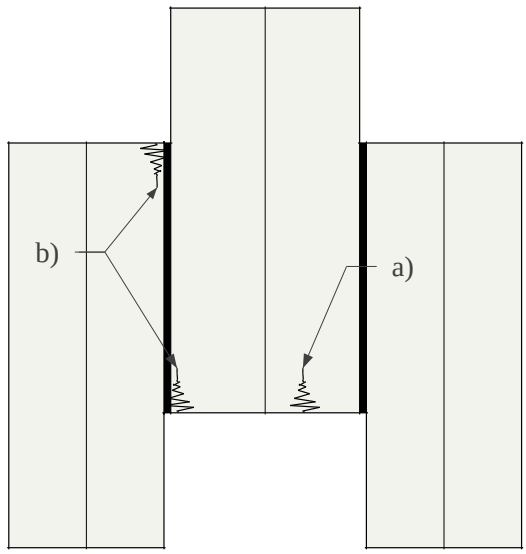

Figure 7: Typical failure initiation points seen during the tests: a) Horizontal thrust caused a tensile crack perpendicular to grain but not propagating to failure, and b) bond line failure in the wood close to the bond line. Failure typically occurred on one side followed by shear block failure.

steel plate covering the end grain of the top member was reduced in width, allowing 40 mm free end grain on each side. The test results shown in Table 5 and Figure 8 indicate a greater sensitivity in the non-resilient specimen than in the resilient. Using this setup, a better agreement for the non-resilient specimen with 13% deviation from the numerical findings was found.

3.3. Type of resilient bond line

To investigate the possibility of simplified manufacturing, the SBR/NR was experimentally compared to CR, Move IT and CO, in which the latter was supposedly more easily manufactured than the former.

Initial testing concluded that maximum bonding to the CR was achieved using the same acid-etching technique as the SBR/NR rubber, and thus its merits are diminished. Despite the same treatment, the CR was not as strong as the SBR/NR as shown in Table 6. Also for CR it was found that a matt rubber surface was bonded more strongly than a shiny, yet the very thin

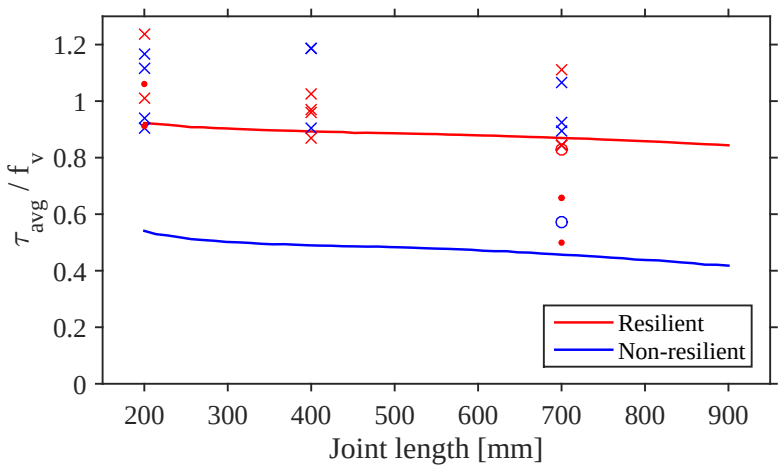

Figure 8: Numerical results of experimental setup compared to experimental data. Wood failure close to bondline is marked with x, dot marks premature failures and results of the test with smaller steel plates are marked with o.

sheet made production difficult. The resilient adhesives Move IT and RESA HLP-H enabled very simple production, although Move IT having difficulties in obtaining a uniform bond line. Both the CO and IT specimens also showed premature failure, now in the adhesive/wood interface.

The stiffness of the resilient bond lines is to a large extent dependent of the thickness of the layer, which is varied with the type of rubber. Figure 9 compares typical load-deformation curves of the different bond lines tested.

4. Discussion

It is very difficult to achieve a uniform shear stress distribution in a lap joint due to different axial strains in the adherends at a given point of the bonded area. The consequences of this difference can however be minimized by introducing a resilient bond line, which allows the adherends to deform more individually. This conclusion is drawn from the presented numerical analysis as well as previous studies [4, 6]. The experimental results are however not as

Table 5: The average shear stress [MPa] at failure using alternative support conditions of the ends of each test specimen.

BC	Non-resilient	Resilient
Restricted end	4.1	4.1*
Partially free end	2.5	3.6

*) Premature failure specimens excluded

Table 6: Mean strength [kN], mean average shear stress at failure [MPa] and mean stiffness [kN/mm] of 700 mm double lap joints of the four resilient bond lines as well as common adhesive. Individual test results in parenthesis and t is the bond line thickness.

Type	t	Strength	Stress	Stiffness
SBR/NR	3.5	1290[a,b]	4.1	190
CR	0.5	360[c] (439, 286)	1.2 (1.39, 0.91)	720
IT	2	760[c] (891, 619)	2.4 (2.83, 1.97)	270
CO	1.5	730[c] (682, 775)	2.3 (2.16, 2.46)	260
PUR	-	1290[b]	4.1	5470

a) Premature failure specimens excluded.

b) Failure in wood close to bond line.

c) Bond line failure in the adhesive/wood interface.

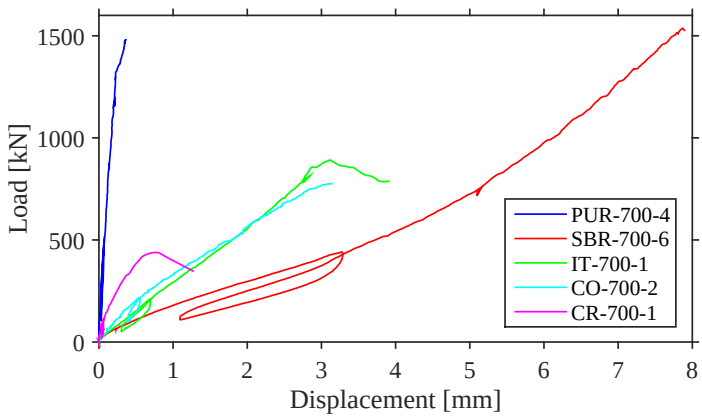

Figure 9: Load-deformation comparison between the different types of bond lines investigated.

simple to interpret due to different failure modes and unexpected influence of boundary conditions, but the data do not falsify the numerical results.

In comparison to previous experience and numerical analysis, the high strength of the non-resilient bond lines is interesting. All GLT specimens were manufactured and delivered at the same time. The test specimens were further produced similarly and also stored together, suggesting that the material parameters are similar for all. The parameters used in the numerical analysis are however based upon literature values rather than measured on the tests themselves. Hence it is possible that the material parameters do not necessarily consider the specific boundary conditions of this test. The load carrying capacity of non-resilient bond lines is also influenced by the fracture energy. The presented shear fracture energy of 0.85 kNm/m^2 was found at a shear failure of 3.56 MPa [9], which possibly should be higher if a higher shear strength is used. The normal distribution of the shear strength suggests a 95$^{\text{th}}$ percentile strength of up to 7.5 MPa, which would increase the numerical load carrying capacities. However, numerical analysis indicates that this effect alone cannot explain the high strength of the non-resilient bond lines.

A large variance in the experimental results of the resilient SBR/NR was found due to premature bond line failure in the rubber/adhesive interface.

The results highlight a sensitivity to rubber treatment, in which local differences are likely to initiate failure. However, this problem can be avoided by simple but detailed visual inspection and does thus not necessarily imply a large variance in the load carrying capacity in an established production method.

A similar double lap joint test setup using resilient bond lines was included in the large resilient bond line test series presented in [4]. Using close to identical production method, an average shear stress at failure of 4.6 MPa was recorded for a 600x223 mm^2 bond line failure, which is higher than measured in this study although higher bending stresses were induced by the thinner lower members. The higher strength is probably due to the influence of different boundary conditions.

Comparison between numerical and analytical findings suggests that the Volkersen theory is suitable for hand calculations of lap joints if (1) a resilient bond line is applied and (2) boundary conditions are such that they limit the influence of peel stress interaction. The numerical findings of the given geometry also suggest that a strength increase by introducing a resilient bond line can be achieved at shorter lap lengths than the analytical estimate suggests.

The additional testing of smaller steel plates at end grain suggests that the non-resilient bond line is more sensitive to boundary conditions than the resilient. The same shear stress in the bond line occur regardless of end plate boundary conditions at a given load, resulting in insignificant influence on the numerical model in which a stress based failure criterion is implemented in the bond line. The fundamental difference is found in the wood body, where the wood volume experiencing a shear stress level close to the shear strength is considerably larger than in the case of smaller end plate. This, in combination with the weakest link theory, is a plausible explanation for the decrease in average shear stress at failure from 4.1 to 2.5 MPa for non-resilient joints. The same reasoning is also valid for the insensitivity of the resilient bond line as no significant stress concentrations occur. When the shear stress approaches the strength of the material, nearly simultaneously for the whole lap joint, the weakest link theory predicts failure at some point regardless of end grain support.

Compared to the rubber based resilient bond lines, the manufacturing process of the IT and CO series was considerably more effective. If proper adhesion can be obtained to wood, a resilient adhesive is recommended in wood-wood lap joints. Similar to rubber based resilient bond lines, a low

shear stiffness and high shear strength are important parameters for the strength of the joint. Furthermore, manufacturing is more effective if the resilient adhesive also has a high viscosity and only need a low curing pressure.

As modern structural design often promotes redundancy, not only strength but also the stiffness of the connection is relevant to consider in a design phase in order to ensure the intended load path. The stiffness and slip are also decisive when several types of connectors are used in a single connection, in which simultaneous action requires similar behaviour. By using a resilient bond line, the stiffness can be designed specifically to match other connectors by varying the rubber stiffness and/or thickness, thus enabling the addition of strengths for the different connectors.

5. Conclusion

The presented research concludes the following findings:

- Numerical analysis shows that an increased load carrying capacity of lap joints can be achieved by introducing a resilient bond line due to a more uniform shear stress distribution.
- The experimental study indicates the difficulty of achieving a strong bond between rubber and adhesive, and thus a clear and reliable production method must be established.
- The experimental study shows that a long non-resilient bond line can be stronger than resilient bond line in certain conditions.
- The stiffness of lap joints with resilient bond lines can be designed with great variety.
- Resilient bond lines can be achieved by means of adhesives with low stiffness or rubber.
- Volkersen theory is applicable to lap joints with resilient bond lines.

Despite the experimental results, the authors conclude that resilient bond lines typically increase the load carrying capacity of long lap joints.

The use of resilient bond lines are not limited to wood-wood configurations nor to timber engineering at large. The study is conducted within a project regarding the Shear plate dowel joint (SPDJ), which uses the resilient bond line technique in a wood-steel configuration with intended use in heavy timber structures.

6. Acknowledgements

The financial support provided by *Formas* through grant 2012-879 is gratefully acknowledged. The authors would like to thank Thomas Johansson at Moelven Töreboda AB for delivering the GLT as well as Ante Salomonsson at Sika and Steffen Harling at Collano for adhesives and expertise. We would also like to thank Tommy Pettersson at Trelleborg AB for delivering the CR and to Maria Södergren for her expertise in handling strong chemicals. Special thanks also to Per-Olof Rosenkvist and Per-Erik Austrell, LTH.

7. References

[1] T. Sumiyoshi, G. Matsui, Wood joints in classical japanese architecture, Kajima Institute Publishing, 1991.

[2] Z. Klaus, Wood and wood joints, building traditions of Europe and Japan, Birkhuser, 2000.

[3] O. Volkersen, Die nietkraftverteilung in zugbeanspruchten nietverbindungen mit konstanten laschenquerschnitten, Luftfahrtforschung 15 (1/2) (1938) 41–47.

[4] P. Gustafsson, Tests of full size rubber foil adhesive joints, Tech. Rep. TVSM-7149, Div. of Struct. Mech., Lund University (2007).

[5] P. Björnsson, H. Danielsson, Strength and creep analysis of glued rubber foil timber joints, Master's thesis, Lund University (2005).

[6] H. Yang, R. Crocetti, G. Larsson, P.-J. Gustafsson, Experimental study on innovative connections for large span timber truss structures, in: Proceedings of the IASS WORKING GROUPS 12+ 18 International Colloquium 2015, International Association for Shell and Spatial Structures (IASS), 2015.

[7] G. Larsson, P. J. Gustafsson, E. Serrano, R. Crocetti, Bond line models of glued wood-to-steel plate joints, Engineering Structures 121 (2016) 160–169.

[8] K. B. Dahl, Mechanical properties of clear wood from norway spruce, Ph.D. thesis, NTNU Trondheim (2009).

[9] H. Wernersson, Fracture characterization of wood adhesive joints, Ph.D. thesis, Lund University (1994).

[10] C. B. Norris, Strength of orthotropic materials subjected to combined stresses, FPL-1816. Madison, Wis. : U.S. Dept. of Agriculture, Forest Service, Forest Products Laboratory.

[11] G. E. Box, W. G. Hunter, J. S. Hunter, et al., Statistics for experimenters.

[12] P. Gustafsson, Tests of wooden cleats oriented along fibre, Tech. Rep. TVSM-7155, Div. of Struct. Mech., Lund University (2008).

[13] P. Gustafsson, Analysis of generalized volkersen-joints in terms of non-linear fracture mechanics (1987).

[14] D. Dillard, A. Pocius, The mechanics of adhesion, 2002.

Paper B

Proceedings of the IASS WORKING GROUPS 12 + 18 International Colloquium 2015
"Bio-based and Bio-inspired Environmentally Compatible Structures"
10 to 13 April 2015, Tokyo Denki University, Tokyo, Japan
Andreas FALK, Petr VEGH and John CHILTON (eds.)

Experimental study on innovative connections for large span timber truss structures

Huifeng YANG *, Roberto CROCETTI [a], Gustaf LARSSON [a&b], Per Johan GUSTAFSSON [b]

* College of Civil Engineering, Nanjing Tech University
P.O. Box 80, NO. 30, South Puzhu Rd. Nanjing, China
yhfbloon@163.com

[a] Division of Structural Engineering, Lund University, roberto.crocetti@kstr.lth.se

[a&b] Division of Structural Engineering, and Division of Structural Mechanics, Lund University, gustaf.larsson@construction.lth.se

[b] Division of Structural Mechanics, Lund University, per-johan.gustafsson@construction.lth.se

Abstract

This paper summarizes an experimental investigation on several innovative reinforcing techniques for the "Single Large Diameter Dowel Connection", SLDDC in timber truss structures. Besides lateral reinforcing or prestressing also steel plates glued on two sides of the glulam specimens were used as reinforcing measure. To study the efficiency of these techniques, 15 full-scale quasi-static tensile tests on glulam members with a SLDDC on either ends of each member were performed. It was found that the reinforcing techniques produced significant increase in the bearing capacity of the SLDDCs. All of the reinforcing techniques showed a quite efficiency, in which the splitting of wood can be prevented. Moreover, the residual strength of most of the specimens remains at a high level.

Keywords: timber structure, truss, singe large-diameter dowel connection, reinforcement, improvement, experimental study

1. Introduction

Timber trusses are competitive for relatively large spans, typically larger than 30 m. For such span lengths, however, the magnitude of loads which have to be transferred between truss members becomes significant, often resulting in complex (and expensive) connections.

To find simpler large dowel connections for timber structures, several studies have been carried out. Haller et al. [1] produced and tested some textile reinforcements on the large dowel connections with different textile structures like biaxial weft knitted and stitch bonded. It showed significant increase on the strength, stiffness and also ductility of the connections. The plug shear and splitting failure of the wood are avoided. However, the ultimate fracture is the wood tensile failure because of the stress concentrations and the reduced net cross section. Also, multi inserted reinforcement layer will result in the relative complex and expensive production process.

Kobel [2] conducted an experimental study on the reinforcement of large dowel connections for timber truss structures, in which the dowel has a diameter of 90mm. The study presented several reinforcement methods including reinforcing with self-tapping screws of various configurations and lateral prestressing with threaded rod. It was found that reinforcing screws can effectively impede splitting of the timber and as a result of the remarkable increase of the bearing capacity. By applying lateral prestresses, no splitting occurred and the bearing capacity is even higher.

Pavkovic´ et al. [3] investigate the bearing capacity of reinforced large diameter dowel connections loaded perpendicular to grain of timber with experimental and FEM analytical work. For the glass fiber textile layers reinforcement glued between the timber lamellas, the result demonstrated remarkable enhancement of the strength and ductility of the connections.

In this research, several efficient and relatively inexpensive reinforcement methods of SLDDCs were presented. By means of experimental investigations, the aim of this paper is to study the efficiency of different types of innovative reinforcing techniques for the SLDDC.

2. Material and methods

2.1. Wood materials

Spruce glulam with the strength class of GL30c was used for all of the 15 glulam specimens in the test. The characteristic tensile strength parallel to the grain of $f_{t,0,k}$ = 20 MPa. The average density and the moisture content was 443 kg/m^3 and 11.1%, respectively. And they were measured after testing on samples taken from the part of the specimen where failure had occurred (i.e. from the shear plug). These values varied in the range of 324 ~ 551 kg/m^3 for density and 8.9 ~ 13.4 % for MC.

2.2. Steel

The steel plates and the large diameter dowel were all made of steel quality Q345B, with a nominal yield stress of 345 MPa. The threaded rods, with a diameter of 24 mm, had a nominal yield stress of higher than 800 MPa. The large diameter dowels had a hollow cross section with the outer diameter of 89 mm and the inner one of 38 mm. The yield strength was 320 MPa for the hexagon head wood screws with 6 mm in diameter and 70 mm in length.

2.3. Rubber

The rubber was mixed of natural rubber and SBR (styrene-butadien), of which the density is 1220 kg/m^3, the hardness is 62°, the shear modulus G≈1.2 MPa, the tensile strength is 22.4 MPa, the shear strength is 9.4MPa and the elongation at break is 595 %. The thickness of the rubber layer vulcanized to steel plates was 1.0-1.2 mm. The outer surface of the vulcanized rubber layer was treated by the sulfuric acid in order to get a satisfy bonding between the timber and rubber layer.

2.4. Glue

The glues used in vulcanized steel – glulam interface were Purbond CR 421 (glue+hardener). While the glues used in smooth steel – glulam interface were epoxy (glue+hardener).

2.5. Layout of the reinforcement

The test series were divided into five groups of three specimens each.

The specimens of the group "Non-Pre" and "Pre" had dowel holes with 92 mm diameter in both end of the glulam specimens, implying they were 3 mm larger than those of dowels. The area between the dowel and the loaded end was reinforced using a threaded rod (See Fig. 1(a) and Fig. 1(b)). Meanwhile for the load transmission from the threaded rods to the glulam, a 30 mm thick steel plate was also used. The prestress in the threaded rods of group "Pre" was about 3.8 MPa while applying at about three month before the test. As to group "Non-Pre", it had no prestress inside the threaded rods. The threaded rods acted as the reinforcement of the timber perpendicular to the grain.

The specimens of the group "S2" and "S2+R" presented reinforcement by bonding steel plates to the glulam surfaces around the large dowel holes. The hole diameter of glulam and steel plates was 102 mm and 91.5 mm respectively. It means a 6.5 mm gap between the dowels and the glulam specimens aimed to transfer the applied loads from dowel to timber by bond shear stress of the vulcanized steel – glulam interface. The major difference between these two groups was that the bonding surface of group "S2" was smooth steel, while group "S2+R" was vulcanized rubber layer onto the steel plates (See Fig. 1(c) and Fig. 1(d)).

The specimens in the group named "S1+R" were also reinforced by bonding steel plates but with a doubled glulam elements (See Fig. 1(e)). Furthermore, in all of the bonding steel plates reinforced specimens, each steel plate was anchored by 34 wood screws in order to bear the normal stress at the bonding interface as well as give the pressure while gluing.

The lamellae thickness was 45 mm for glulam specimens. The specimens in the group named "S1+R" (See Fig. 1(e)) had a doubled glulam elements with each had a cross section of 61 mm × 405 mm. And the other groups of specimens had a single cross section of 140 mm × 405 mm. All the glulam specimens were 2, 00 m in length.

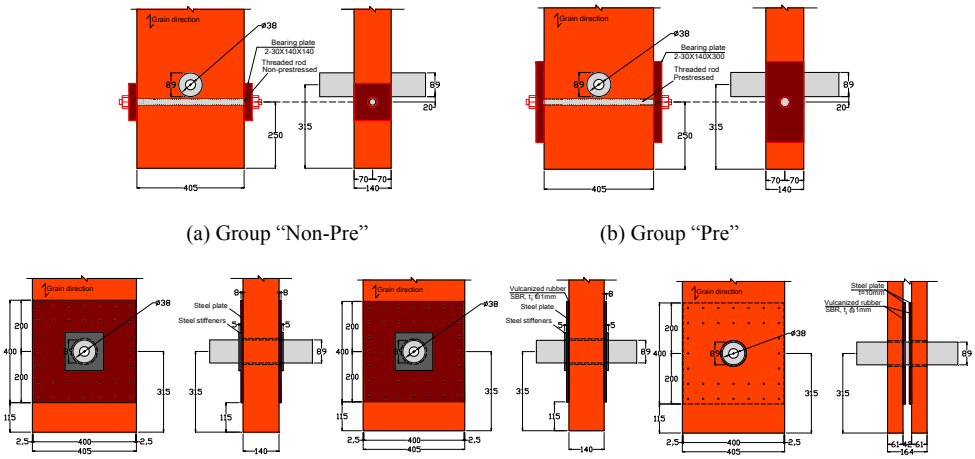

(a) Group "Non-Pre" (b) Group "Pre"

(c) Group "S2" (d) Group "S2+R" (e) Group "S1+R"

Figure 1: Configuration of test specimens. Units: [mm]

2.6. Test setup

All tests were conducted at the Jiangsu Key Laboratory of Civil Engineering, Disaster Prevention and Mitigation, Nanjing Tech University. The general setup for all of the specimens is illustrated in Fig. 2. The tests were quasi-static tensile tests under displacement control and the actuator speed was 0.5 mm/min. Each specimen was equipped with an identical design of reinforced SLDDC on both ends. The loads were applied by the loading rods or loading plates between the dowels and the hydraulic device.

The dowel slip as well as the lateral deformation was continuously measured in both end of the specimens for group "Non-Pre" and "Pre". As to the other three groups, only the steel plate slip was measured.

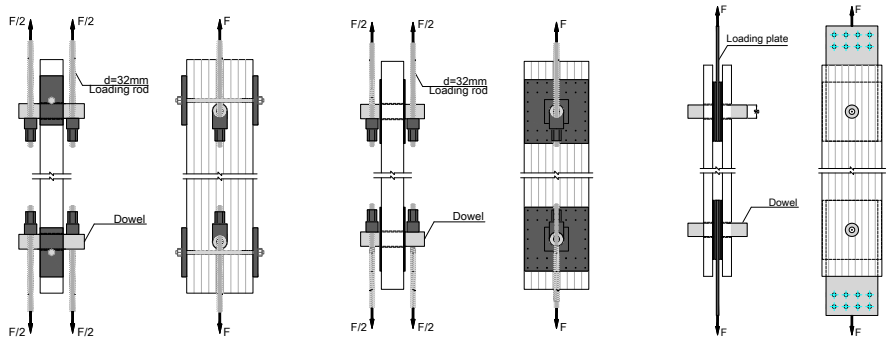

(a) Group "Non-Pre" and "Pre" (b) Group "S2" and "S2+R" (c) Group "S1+R"

Figure 2: General test setup.

3. Results and discussions

3.1. Bearing capacity

Table 1 displays average values of the test results for the specimens. And Fig. 3 gives a comparison on the bearing capacities and the residual strength of different groups. For a comparison, some of the test results of

Kobel [2] are also presented here. From Table 1 and Fig. 3 it can be seen that the bearing capacity of the SLDDCs were significantly increased due to the reinforcements. And the gains in bearing capacity range from 46% to 639%.

For the reinforcement by bonding steel plate with vulcanized rubber layer, e.g. for the specimens in group "S1+R" and "S2+R", the bearing capacities were most greatly improved. It is considered that the introduction of the rubber layer lead to a big decrease of the stress concentration at the bonding interfaces. As a comparison, the bearing capacity of group "S2", in which the reinforcement was by bonding smooth steel plate, the gains in bearing capacity was much less than those of group "S2+R", despite its gains reached to 64%.

Lateral non-prestressing or prestressing is also effective way to improve the load bearing capacities of the SLDDCs. The bearing capacities were 46% and 122% higher than those of non-reinforced "Basic" specimens. As compared to Group "Dywidag" in Kobel [2] (See Fig. 4) with a prestress of about 3.1 MPa, the bearing strength of group "Pre" had no obvious difference. In other words, it can not be seen the notable effects on the bearing capacity by the location of the prestressed rods and the magnitude of the prestress values.

Table 1: Summary statistics of the test results

Specimen group and no.	Bearing capacity F_{max} [kN] Mean (STDV[2])	Residual Strength F_{res} [kN]	$(\frac{F_{res}}{F_{max}})_{mean}$	Density ρ [kg/m^3]	Moisture content MC [%]
Basic[1]	134 (4.1)	0	0	523	12.1
Non-Pre	195 (3.7)	95	49	433	11.0
Pre	298 (7.9)	47	16	456	10.9
S2	220 (22.9)	112	51	423	11.5
S2+R	990 (11.6)	57	6	457	11.4
S1+R	755 (7.4)	347	46	443	10.9
Dywidag[1]	306 (9.4)	90	29	392	9.2

Note: 1. From Kobel [2]; 2. STDV refers to coefficient of variation. Hereby the bearing capacity of another end which stayed intact was conservatively taken as the same as that of failure end. So the sample size was six for each group.

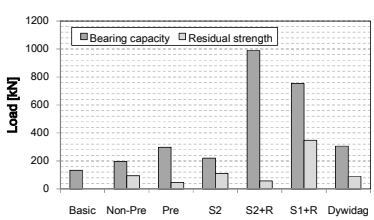

Figure 3: Bearing capacities and residual strength

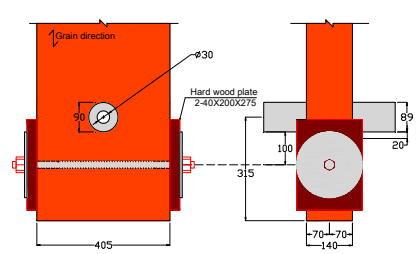

Figure 4: Configuration of "Dywidag" from Kobel [2]

The residual strength was defined here as the minimum load just after the first failure of the specimen. The values of the residual strength for group "Non-Pre", "S2" and "S1+R" were about 50% of the maximum load. For group "S2+R" and "Pre" the value was only 6% and 16%, respectively. The maximum residual strength of 347kN was recorded by group "S1+R" and it was due to the failure just occurred in one side of the specimen (It is considered of the effect of the loading eccentricity by the test arrangement). After this first failure, another side was also able to bear a high load. For group "S2+R", F_{res} to F_{max} ratio was only 6% because of the high load and the sudden failure. And the specimen would bear a big impact load from the fracture and thus result to a very small residual strength.

Another interesting phenomenon occurred in the load-displacement curves recorded by the test machine for group "S2". After the first failure and the recorded residual strength, the load increased to a higher level

compared to the F_{max}. And then the load dropped and again increased to a high level, so back and forth several times (See Fig. 5). This observation indicates that this kind of specimen failed gradually in the last load stage. This may due to the fracture of the bonding surface near the load end caused by the stress concentration, and then some load was transferred to the wood screws nearby. While the second bonding fracture occurred with the increasing load, growing number of wood screws participated in the work. As a result, the ultimate load was usually higher than that at the first failure.

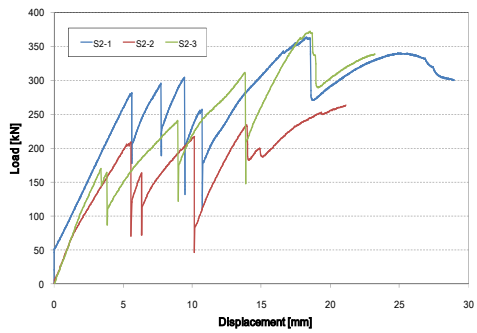

Figure 5: Load-displacement curves of group "S2"

3.2. Failure mode

For the SLDDCs with lateral reinforcement, the ultimate failure mode was a shear plug fracture (See Fig. 6). For a comparison, giving a prestress in the lateral reinforcement would generally lead to a larger shear plug and so as to reach a higher bearing capacity. It showed that even when there was no prestress in the rods, not any splitting appeared in the glulam specimen.

(a) Group "Non-Pre" (b) Group "Pre"

Figure 6: Failure modes of SLDDCs with lateral reinforcement

For the bonding smooth steel plate reinforced specimens, the failure caused by the first bonding shear fracture between the steel plate and glulam. And then the rest of the bonding layer combined with some of the wood screws worked together to bear the applied load, till to the failure of the whole bonding surfaces (See Fig. 7(a)). While for the group "S2+R", with a rubber layer, the ultimate failure showed a fully wood shear failure around the bonding area (See Fig. 7(b)). The average value of the shear stress at ultimate load reached to 3.1 MPa. As to group "S1+R", with a double glulam specimens, the failure mode was combined the wood shear failure and tensile failure (caused by the load eccentricity for the glulam), see Fig. 7(c).

Another observation was that there was also the shear plug failure for the SLDDCs reinforced with bonding steel plates. However, it did not mean that it is a failure mode of this kind of specimens. For the reason of that this shear plug was just caused by the large impact load while the wood shear failure, i.e. the shear plug occurred just after the failure.

(a) Group "S2" (b) Group "S2+R" (c) Group "S1+R"

Figure 7: Failure modes of SLDDCs reinforced with bonding steel plates

3.3. Stiffness

The Load-slip stiffness is steel plate slip for the group "S2", "S2+R" and "S1+R". While it is dowel slip for the other groups, groups in Kobel [2] is also included. And it was determined as the rate of dowel or steel plate slip in load direction between 0.4 F_{max} and 0.7 F_{max}.

Due to the test arrangement error, the dowel slip values were unfortunately not valid. But it can be seen from the test result of Kobel [2] that the lateral reinforcement has no contribution to the stiffness. For group "S2", there was quite little slip before the first failure, implying quite high slip stiffness. And due to the load eccentricity of the glulam in group "S1+R", the slip value was also invalid. So only the slip value of group "S2+R" was recorded. According to the sip value of this group, the stiffness (484 kN/mm) was obtained and gave a comparison with group "Basic" (308 kN/mm) and "Dywidag" (311 kN/mm) from Kobel [2]. So the gains of the stiffness was about 57% for group "S2+R" to group "Basic" and "Dywidag".

The load-slip behaviour of group "S2+R" was given in Fig. 8. There was a quite small variation in the stiffness and the bearing capacity. The relative smaller bearing capacity of S2+R-1 was due to the eccentricity caused by the big load to the test equipment. And then an update was provided to the other two specimens in this group. It could also be observed from Fig. 8 that there was an increasing stiffness during the late loading stage due to the strain hardening of the rubber layer.

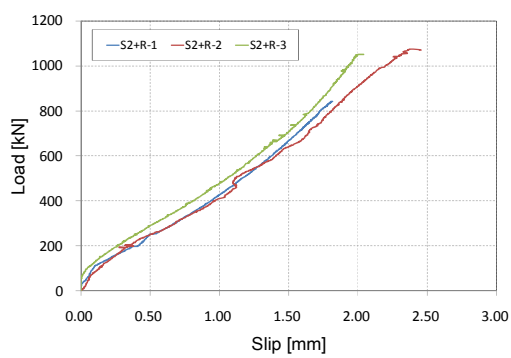

Figure 8: Load-slip behaviour in group "S2+R"

4. Conclusions and future work

From the results of the full-scale test series for SLDDCs the following conclusions can be drawn:

- Lateral reinforcing or prestressing are both able to prevent the splitting, but lateral prestressing will lead to a larger bearing capacity.
- The location of the prestressed rods around the dowel hole in glulam specimen appears to has little effect on the bearing capacity.

- The prestress may be reduced to some level since it is so close in the bearing strength between the groups "Dywidag" (prestress was about 3.1 MPa) and "Pre" (prestress was about 3.8 MPa).
- The reinforcement with bonding steel plates to the glulam is a quiet efficient way to the SLDDCs, especially while a rubber layer is vulcanized to the steel plates. The gains in bearing capacity reached to 639%. The main reason is the considerably reduced stress concentration and therefore come into a quite uniform shear stress distribution on the bonding surfaces.
- The slip stiffness of the group with a rubber layer on the steel plate can also be increased into a high level compared to the control "Basic" group.
- For a bonding smooth steel plate reinforcing, the gains in bearing capacity was much less than that had a rubber layer. But even so, its gains reached to 64%.

From the test and the observation, further studies should be carried out including:

- The lateral prestressing with a lower level should be taken into consideration.
- In order to further improve the efficiency of the bonding steel plate reinforcement, different kinds of shapes and placement of steel plate need to be studied.
- Since the wood screws can prevent the sudden fracture of the bonding smooth steel plate reinforcement, it is noteworthy that the arrangement of the wood screws should also an important factor on the bearing capacity as well as the slip stiffness.
- For the group with bonding steel plate vulcanized a rubber layer, some measures should be taken so as to endure the sudden impact load on the glulam specimen caused by the fracture at a very high load level.
- Numerical model is a more efficient and economical way to carry out some parametric analysis and also the stress distribution study.

Acknowledgement

The cooperation received from Moelven Töreboda AB (http://www.moelven.com) for the supply of glulam and Henkel for the Purbond CR 421 glue. Also we would like to thank master students Wenxiang Zhu and Wei Xu from Nanjing Tech University for the hard and valuable test work.

References

[1] Haller P., Birk T., Offermann P. and Cebulla H., Fully fashioned biaxial weft knitted and stitch bonded textile reinforcements for wood connection. *Composites: Part B*, 2006; 37; 278-285.

[2] Kobel P., Modelling of strengthened connections for large span truss structures. *Master's Thesis*, Department of Structural Engineering, Lund Institute of Technology, Sweden; 2011.

[3] Pavkovic´ K., Rajčić V. and Haiman M., Large diameter fastener in locally reinforced and non-reinforced timber loaded perpendicular to grain. *Engineering Structures*, 2014; 74; 256–265.

Paper C

Engineering Structures 121 (2016) 160–169

Contents lists available at ScienceDirect

Engineering Structures

journal homepage: www.elsevier.com/locate/engstruct

Bond line models of glued wood-to-steel plate joints

Gustaf Larsson [a,*], Per Johan Gustafsson [a], Erik Serrano [a], Roberto Crocetti [b]

[a] Division of Structural Mechanics, Lund University, P.O. Box 118, SE-221 00 Lund, Sweden
[b] Division of Structural Engineering, Lund University, P.O. Box 118, SE-221 00 Lund, Sweden

ARTICLE INFO

Article history:
Received 10 September 2015
Revised 22 February 2016
Accepted 25 April 2016

Keywords:
Timber structure
Wood-to-steel plate joints
Shear plate dowel joint
Rubber foil connection
Numerical analysis
Numerical model

ABSTRACT

The competitiveness of timber as structural material in large structures is often governed by the cost of structural joints. Tests indicate that the new joint concept presented herein using glued wood-to-steel plate joints can possibly reduce the cost by matching joint strength to member strength. The design is inspired by two previously proposed designs using a single large dowel and using a rubber foil interlayer in adhesive joints. Analytical 1D and numerical 3D models of the bond line are proposed in order to further develop the concept, both in the case of a traditional adhesive joint and for the innovative rubber foil adhesive joint.

The glued wood-to-steel plate joints studied are lap joints with a load bearing capacity assumed to be governed by failure within or along the bond line. In the 1D and 3D structural models both linear elastic and non-linear fracture mechanics were applied, with the non-linear fracture mechanics model taking into account the gradual damage fracture softening in a fracture zone. For the conventional type of bond line it was found that bond line softening needs to be considered for adequate strength analysis while it was not needed for a bond line with a rubber foil.

The computational results are compared to previous full scale test results. The numerical results show good agreement and the analytical results reasonable agreement. When using a high strength adhesive, the strength of the wood along the bond line is governing joint failure. For this case, the analyses predict a 150% load bearing capacity increase by the introduction of a rubber foil as compared to a traditional design. The test results indicated an even higher increase.

1. Introduction

1.1. Background

The properties and cost of structural joints often govern the competitiveness of timber as main structural material in large structures. Ideally, a joint should be able to withstand the same forces as the main members, something which however seldom is the case due to joint detailing (leading to e.g. stress concentrations and large stresses perpendicular to the bond line).

Glued wood-to-steel joints can be designed to obtain promising properties. The high stiffness of conventional adhesives does however result in a limited active load transfer area for lap joints. As stress concentrations arise, the material strength of the adherents is reached prematurely for a small section and fracture is initiated. In order to significantly reduce the stress concentrations thus generating a more uniform stress distribution, Gustafsson [1] proposed adding an intermediate rubber layer, see Fig. 1.

1.2. The shear plate dowel connection

The shear plate dowel connection is an applied example of a glued wood-to-steel joint. It is a new design concept developed to increase connection strength while maintaining easy assembly thanks to the use of a single large diameter dowel. Fig. 2 shows the connection which is based on the concept of the "Single Large Diameter Dowel Connection" (SLDDC) design proposed by Crocetti et al. [2]. The use of externally glued steel plates minimizes the impact on the wood, for which a pure shear action is accomplished by using a larger hole in the glulam than in the steel plate. The connection type has been tested by Yang et al. [3], with and without a rubber interlayer.

Abbreviations: SLDDC, Single Large Diameter Dowel Connection; LEFM, linear elastic fracture mechanics; NLFM, non-linear fracture mechanics; EELA, equivalent elastic layer approach.

* Corresponding author.
E-mail addresses: gustaf.larsson@construction.lth.se (G. Larsson), per-johan.gustafsson@construction.lth.se (P.J. Gustafsson), erik.serrano@construction.lth.se (E. Serrano), roberto.crocetti@kstr.lth.se (R. Crocetti).

http://dx.doi.org/10.1016/j.engstruct.2016.04.053
0141-0296/

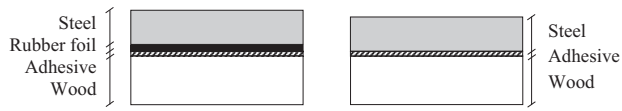

Fig. 1. Rubber foil adhesive joint (left) in comparison to conventional adhesive joint (right).

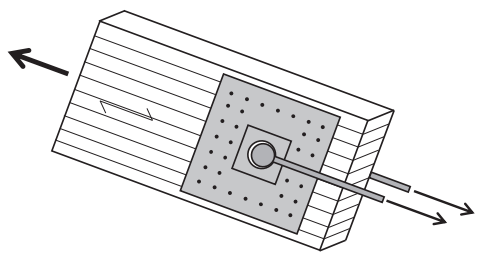

Fig. 2. Glued shear plate dowel connection.

As the steel plates of the connection reduce the risk of both splitting and shear plug failure of the loaded member end, the dowel to element end distance can be reduced from the minimum of 7d suggested by Eurocode 5 [4] thus enabling more compact connections. The connection was originally intended as a truss joint but can also be used in other applications, e.g. as hinges at arch springing points or tension ties. By combining several dowels moment stiff connections are also made possible. The rubber foil bond line can typically be used whenever a higher static or shock load bearing capacity of a glued joint is needed.

1.3. Previous work

The type of glued wood-to-steel plate joint studied herein is a new design concept and it does seem that it has not been studied in terms of detailed strength analyses previously. However, Yang et al. [3] and Gustafsson [1] have conducted tests on the connection type whereas the SLDDC has been tested in full scale tests by Kobel [5] with joints of the same type as those described by Crocetti et al. [2].

For simple lap joint geometries, such as glued wood-to-steel plate joints, the Volkersen theory [6] may be used to obtain an analytical solution by assuming pure shear action, c.f. Section 3. Adhesive bonds with more complex geometries are commonly solved using stress analysis or linear elastic fracture mechanics (LEFM) [7]. Stress or strain discontinuities occur when using continuum mechanics in design situations were adjacent materials have different stiffnesses, for which edge elements also are mesh dependent. Thus it is not trivial how to perform e.g. finite element analysis of such model. On the one hand, as the existence of a singular stress field is one of the assumptions in LEFM, such approach should in principle be appropriate. On the other hand, LEFM is only valid when the fracture process region is small compared to other dimensions of the structure, which is again seldom the case. The limitation of a small fracture process region can however be overcome using non-linear fracture mechanics (NLFM), e.g. softening plasticity [8], damage mechanics [9] or plasticity-damage models [10].

NLFM is computationally comprehensive, and thus several so-called extended LEFM models have been developed in order to reduce the number of limitations in LEFM without using stepwise or iterative numerical calculations. In this study, the extended LEFM model called the equivalent elastic layer approach (EELA) as proposed by Gustafsson [11] is used. It can been used for strength analyses of glued joints and for solid materials for which the location of the fracture plane is known in advance. The approach has been used in 2D applications by Gustafsson and Serrano [12], Coureau et al. [13] and extensively by Jensen in e.g. [14,15], but extended to 3D analysis in this paper.

1.4. Failure modes

Glued wood-to-steel plate joints can fail in the wood, in the steel or in the bond line. Here, the term bond line includes the adhesive, possible rubber foil, a thin wood layer along the glue and the material interfaces. Test results presented in [1,3] indicate, both for joints with and without a rubber foil, typically a dominant mode of shear failure in the bond line; either in the wood/adhesive interface or in the wood close to the bond line. If properly manufactured, wood failure close to bond line should be the governing failure mode. In the test series of the shear plate dowel connection [3] also shear plug failure occurred in the wood part of the joint. Reportedly the plug failure was a secondary failure occurring after bond line failure.

1.5. Present study

The present paper relates to one analytical and various numerical models for glued wood-to-steel plate joints as limited in strength by fracture in the bond line. Both joints with and without a rubber foil are studied. Using Volkersen theory [6], an analytical 1D shear stress distribution is derived. Furthermore, numerical linear and non-linear 3D analyses are conducted in order to investigate the influence of the interaction between shear and peel stresses in the bond line and also to investigate the choice of fracture model. The choice of material parameter values corresponds to failure in wood close to the bond line.

The aim of the present paper is to present an efficient and rational computational bond line strength analysis model and to indicate which factors may be of interest to include in a possible design model.

1.6. Limitations

The following main limitations apply to the models:

- Quasi-static analysis of short term strength.
- Only failure in the wood close to the bond line is considered.
- Linear elastic material model of wood (orthotropic) and steel (isotropic).

2. Calculation methods

In the calculation methods studied, steel and wood adherends are throughout modelled as isotropic and orthotropic linear elastic materials, respectively. Failure is assumed to develop in the bond line and not in the adherends. The adherends are in the 1D analysis assumed to act as bars which can be stretched in their longitudinal

direction, thus bending is not included. In the 3D analysis the adherends are modelled by 3D solid finite elements.

The bond line, with its different material layers and material interfaces as described above, is modelled as a single homogeneous layer. This layer is in the 1D analysis assumed to act as a shear–slip interface with a linear relation between the shear stress τ and the shear slip δ. In this study, two different choices regarding this linear relation, i.e. the shear stiffness of the interface, are investigated: (a) a stiffness representing the actual elastic bond line shear stiffness or (b) a stiffness chosen in order to represent correctly the strength and fracture energy of the bond line (in the sense that at the instant when the bond line strength is reached, the elastic energy stored equals the fracture energy of the bond line) [11]. These two alternatives give similar shear stiffness value for a bond line with a rubber foil. However, for a conventionally glued bond line there is commonly a very large difference between the two stiffness values, typically about one or two orders of magnitude. This is because the elastic strain capacity commonly is very small compared to the strains during plastic deformation and fracture. If the purpose of the modelling is joint strength analysis, then the shear stiffness should be chosen such that bond line strength and fracture energy are correctly represented, for details see Sections 3 and 4.

In the 3D analyses, the homogeneous layer that models the bond line is assigned a non-zero thickness equal to its physical thickness. The state of stress in the layer is defined by three stress components. Taking the 1-direction as the bond surface normal, the normal stress σ_{11} and the shear stresses τ_{12} and τ_{13} define these bond layer stress components. The corresponding strain components are denoted $\varepsilon_{11}, \gamma_{12}$ and γ_{13}. These strains are formally forced to be constant across the thickness of the layer and accordingly, the corresponding relative displacements across the bond line thickness are $\delta_{11} = t\varepsilon_{11}, \delta_{12} = t\gamma_{12}$ and $\delta_{13} = t\gamma_{13}$, where t is the bond layer thickness. Influence of in-plane stresses σ_{22}, σ_{33} and τ_{23} is not considered and these stresses are in the calculations assumed equal to zero.

In the 3D finite element analyses, the bond layer is modelled by the use of cohesive elements. The mechanical response of these elements is defined by traction-separation laws, i.e. relations between stresses $(\sigma_{11}, \tau_{12}, \tau_{13})$ and the relative displacements $(\delta_{11}, \delta_{12}, \delta_{13})$. The traction separation laws can be linear or non-linear and coupled or uncoupled. Non-linear relations for the bond layer are defined in terms of a damage model that enable analysis taking into account gradual fracture softening as described in Section 4.1. The properties are in the case of a linear relation obtained from the strength and the fracture energy parameters of the bond line under consideration. A special feature for bond lines with a rubber layer is that the effective normal stiffness is affected by edge distance. For an inner point of the bond layer, the in-plane normal strain is close to zero entailing high normal stiffness due to Poisson's ratio of rubber being close to 0.5, c.f. Section 4.2.

3. 1D analytical method

An analytical expression for the shear stress distribution of the centrically loaded shear plate dowel connection based on the Volkersen theory [6] is presented. The failure load is then derived by identifying the maximum stress and introducing a stress based failure criterion. The failure criterion accounts for the fracture energy according to the equivalent elastic layer approach.

3.1. Shear stress distribution according to Volkersen theory

Glued wood-to-steel plate joints are characterised by shear action, for which a non-uniform shear stress distribution is obtained due to the large overlap length. Volkersen [6] presents a second order homogeneous ordinary linear differential equation for the shear stress according to Eq. (1).

$$\tau_3'' - \omega\tau_3 = 0 \quad \text{where} \quad \omega^2 = \frac{G_3 b_3}{t_3}\left(\frac{1}{A_1E_1} + \frac{1}{A_2E_2}\right) \tag{1}$$

Indices 1 and 2 indicate the adherents while index 3 indicates the adhesive layer, c.f. Fig. 3.

The adhesive lap joint under consideration is schematically shown in Fig. 3. All elements are assumed to behave linear elastically, the adherents act as centrically loaded bars and the adhesive layer acts only in shear with constant shear strain across the thickness. Bending is not included.

Eq. (1) is solved individually for the two parts A and B shown in Fig. 3b. The mid length normal forces $N_1(L/2)$ and $N_2(L/2)$ at the load application point are determined using shear stress continuity and force equilibrium according to Eq. (2).

$$\begin{cases} \tau_3^A(L/2) = \tau_3^B(L/2) \\ P = N_1(L/2) + N_2(L/2) \end{cases} \tag{2}$$

By the presented boundary conditions in Fig. 3 and Eq. (2), the shear force distribution on a centrically loaded lap joint is found to be:

$$\begin{aligned} \tau_3(x) &= \begin{cases} \tau_3^A & for \quad 0 \leqslant x < L/2 \\ \tau_3^B & for \quad L/2 \leqslant x \leqslant L \end{cases} \\ \tau_3^A &= \frac{PG_3}{t_3\omega E_1A_1}\left[\left(\frac{1}{\tanh(\beta)} + \frac{\alpha - \operatorname{sech}(\beta)}{2\sinh(\beta)}\right)\cosh(\omega x) - \sinh(\omega x)\right] \\ \tau_3^B &= \frac{PG_3}{t_3\omega E_1A_1}\left[\left(\frac{\cosh(2\beta)}{2\sinh(\beta)}(\alpha + \operatorname{sech}(\beta))\right)\cosh(\omega x)\right. \\ &\quad \left. -\cosh(\beta)(\alpha + \operatorname{sech}(\beta))\sinh(\omega x)\right] \end{aligned} \tag{3}$$

where

$$\omega L = L\sqrt{\frac{G_3 b_3(1+\alpha)}{t_3E_1A_1}} \quad \alpha = \frac{E_1A_1}{E_2A_2} < 1 \quad \beta = \frac{\omega L}{2} \tag{4}$$

Fig. 11 shows the analytical variation of the shear plate dowel connection with rubber.

3.2. Choice of bond line stiffness

Slender lap joints which fail in an elastic brittle failure can be analysed using Volkersen theory. However, the non-elastic strain capacity is typically very significant for adhesive joint strength and should therefore be considered e.g. by the equivalent elastic layer approach (EELA) [11], see Fig. 4. Depending on what type of analysis is conducted, a choice of bond line stiffness thus can be made.

EELA presents a characteristic linear relation of the bond line obtained by respecting the bond line strength and fracture energy. By using a fictitious stiffness, the fracture-softening capabilities of the bond line can be included in the constitutive relations. For mode II fracture this is achieved by replacing the bond line shear stiffness with an equivalent stiffness defined according to Eq. (5).

$$\frac{G_3}{t_3} = \frac{f_v^2}{2G_f} \tag{5}$$

where

G_3: Shear modulus of bond line; f_v: Bond line shear strength.
t_3: Bond line thickness; G_f: Fracture energy of bond line.

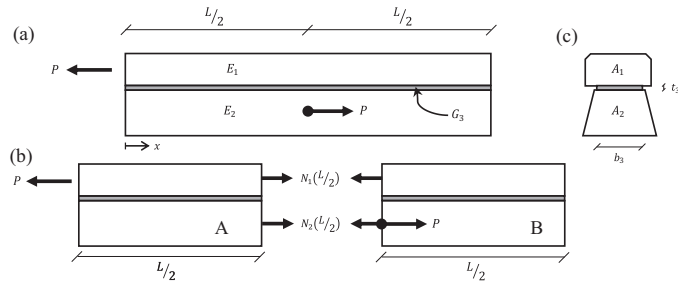

Fig. 3. Nomenclature of the theoretical analysis using Volkersen theory. Young's modulus E_i and shear stiffness of the bond line as G_3. The geometry is divided into part A and B at load application point.

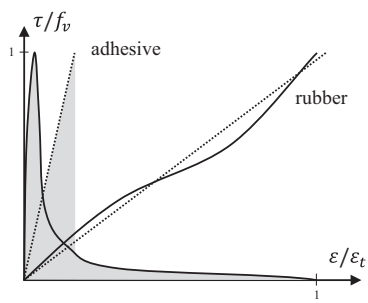

Fig. 4. A schematic comparison between normalized fracture-softening behaviour and EELA for common adhesives (two left curves) and rubber (right). Note that EELA correctly represents material strength and fracture energy, as indicated by shaded areas.

See also Fig. 4. As the shear modulus is replaced by a fictitious value, the initial elastic stiffness of the bond line is in general not represented correctly. However, as rubber behaves similar to the model in hand, the approach can for rubber foil bond lines be considered accurate also regarding deformations. For fracture in mode I, a linear elastic normal stress versus normal slip curve is defined analogously, thus enabling full 3D modelling capabilities.

Stresses are given by means of linear elastic stress analysis. Due to the special choice of properties of the elastic layer, either $\tau_{max} = f_v$ or $G = G_f$ can be used as a failure criterion. In case of mixed mode loading some mixed mode failure criterion should be used.

3.3. Failure load

A generalized Volkersen theory is obtained by applying EELA together with the Volkersen stress analysis. A failure load is then calculated by applying a stress based failure criterion: $\tau_{max} = f_v$. Maximum stress occurs at $\tau(x = 0)$ which yields the failure load according to Eq. (6).

$$P_f = f_v b_3 \frac{(1+\alpha)L}{\omega_g L} \frac{\sinh(\omega_g L)}{\alpha \cosh\left(\frac{\omega_g L}{2}\right) + \cosh(\omega_g L)} \tag{6}$$

For Volkersen theory, $\omega_g = \omega$ as defined in Eq. (4) while for the generalized Volkersen theory the normalized joint length ω_g is defined in Eq. (7).

$$\omega_g L = L\sqrt{\frac{f_v^2 b_3 (1+\alpha)}{2 G_f E_1 A_1}} \tag{7}$$

The Volkersen theory and the generalized Volkersen theory will yield the same results if rubber is present as discussed in Section 2. Shear fracture in the wood in vicinity of the bond line is the expected failure mode, thus f_v is determined by wood material strength.

As bending is not included in the Volkersen model, the presence of peel stresses due to loading eccentricity is neglected. The model should in general thus not be used for prediction of the load carrying capacity of the studied connection. However, reinforcement can be introduced in order to reduce such stresses, e.g. by means of screws. Provided that the shear stiffness of the reinforcement is either negligible or taken into account, the model should give a realistic estimation of the capacity and Eq. (6) could be used to develop a simple design criterion.

4. 3D numerical stress and strength analyses methods

Possible interaction between shear and peel stress in the joint is evaluated by means of finite element modelling in a commercial general purpose software. The simulations have been performed in 3D using a model consisting of wood, steel and a bond line. The bond line is represented by a cohesive layer with a single element in the thickness direction. The bond line thus represents the adhesive or, alternatively, the adhesive and the rubber foil if applied. The bond line also represents the material interfaces. The specimens will henceforth be called S-R and S-nR for the rubber and non-rubber specimen respectively.

4.1. S-nR – Joint without rubber layer

In order to evaluate the applicability of EELA in 3D, comparisons were made with non-linear fracture mechanics analyses where linear and bilinear fracture softening behaviours were used, see Fig. 5. The bilinear softening behaviour is a good approximation for several types of common adhesives [16], but also linear softening was studied in order to investigate whether the softening shape would influence the failure load. As EELA does not account for the true shape of the softening curve, different results of the linear and bilinear non-linear analyses would imply that EELA is not suitable for the joint type.

As depicted in Fig. 5, all three fracture models consider both the bond line strengths and its fracture energies, but by different means. When fracture softening is used, a single scalar damage

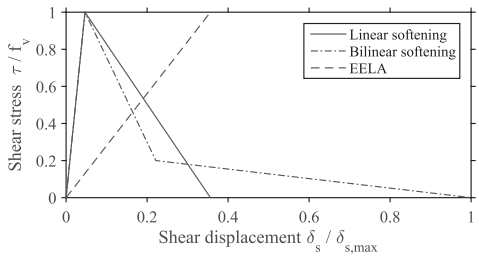

Fig. 5. Normalized stress–displacement plot illustrating the three numerical models used for the numerical analysis of the S-nR specimen. Note that material strength and fracture energy is the same for all models.

variable D is initiated after material failure which represents the material stiffness degradation. For linear softening, damage is defined as

$$D = \frac{\delta_m^f(\delta_m^{max} - \delta_m^0)}{\delta_m^{max}(\delta_m^f - \delta_m^0)} \tag{8}$$

where $\delta_m^f = 2G^c/T_{eff}^0$ with T_{eff}^0 being the effective traction at damage initiation. The maximum value of the effective displacement attained during the loading history is referred as δ_m^{max}, which can be determined using the fracture energy G^c. During analysis, D is determined for the different modes respectively but the minimum is used for all.

For the case of bilinear softening curves for normal and shear modes, see Fig. 5, damage was back-calculated from experimental data [17] and then used as tabular input to the software. Mixed mode is defined in terms of tractions and is expressed by

$$\begin{aligned} \phi_1 &= \frac{2}{\pi}\text{atan}\frac{\tau}{\langle t_n \rangle} \\ \phi_2 &= \frac{2}{\pi}\text{atan}\frac{t_t}{t_s} \end{aligned} \tag{9}$$

where $\tau = \sqrt{t_s^2 + t_t^2}$ is the vector sum of the two shear components. Using this nomenclature, $\phi_1 = 0$ corresponds to mode I, $\phi_2 = 0$ to mode II in the first shear direction and $\phi_2 = 1$ to mode II in the second shear direction.

4.2. S-R – Joint with rubber layer

When rubber foil is applied, its flexible behaviour will dominate the deformations and the bond line is thus represented by rubber properties. In comparison to adhesives, the bond line has for this case close to zero fracture-softening capability.

In dominant shear action rubber can be modelled as being linear elastic with fairly good accuracy, c.f. Fig. 4 and [18]. The incompressible behaviour of rubber will, however, to a large extent affect the normal stiffness. Given an isotropic linear elastic material in plane strain, one can theoretically identify the normal stiffness k_n as a function of Poisson's ratio v, modulus of elasticity E, and layer thickness t, for an edge point and inner point of the rubber layer respectively, see Fig. 7 and Eq. (10).

$$k_{n,edge} = \frac{E}{t(1-\nu^2)} \quad k_{n,inner} = \frac{E(1-\nu)}{t(1+\nu)(1-2\nu)} \tag{10}$$

As the rubber properties are to be modelled using cohesive elements, the size of a transition region close to the free edge of the rubber was investigated using linear finite element analysis. A plane strain tensile test of a wide specimen made of a rubberlike linear elastic material perfectly bonded to stiff plates was analysed, see Figs. 6 and 7.

The equivalent normal stiffness of the rubber shows a variation along the width due to the pronounced Poisson's effect, which is obvious from inspection of Fig. 6 showing the normal stress distribution for a state of uniform normal strain of the rubber layer. It is further clear from Fig. 7 that the inner stiffness is well represented by the theoretical results. However, stress concentrations arise at the ends due to the sudden change in stiffness. Further investigations reveal a mesh size dependence of the peak stress value at the ends of the specimen but also that extrapolating the stress curve from values coincide with the theoretical values of Eq. (10). These findings make it plausible to exclude the concentration as a numerical artefact, and at the same time the findings provide a mean of disregarding this very local phenomenon. A transition length is defined as the distance from the edge to the point where 99% of the plateau value is reached. Linear simulations of a rubber-like material indicate an influence of Poisson's ratio and bond line thickness on this transition length. For rubber (low stiffness and Poisson's ratio close to 0.5) this is approximated by Eq. (11).

$$l_{transition} = 9t \tag{11}$$

The transition length has a positive effect in the applied analyses of the connection as the position of maximum peel stress does not coincide with the position where maximum shear stress is found, the latter typically being located at the bond line edge.

Similar simulations were conducted to verify the shear stress distribution. As the theory predicts, analyses indicate zero shear stress at the specimen ends and an effective shear stiffness being equal to the shear modulus, i.e. $G = E/2(1+v)$. The transition length and variation of equivalent shear stiffness is negligible and thus considered constant along the bond line.

For the joint design in hand, this linear modelling approach has been verified by comparing the obtained stress distribution to the one obtained from non-linear, third order analyses using both neo-Hookean [19] and Yeoh [20] material models. As seen in Section 5.4, reasonable agreement with conducted tests is also obtained.

The strength of the bond line is found using a stress based failure criterion, for which a Norris criterion [21] is deemed suitable for the 2D bond line. Compressive normal stress will not cause failure and is thus not included in the criterion, see Eq. (12).

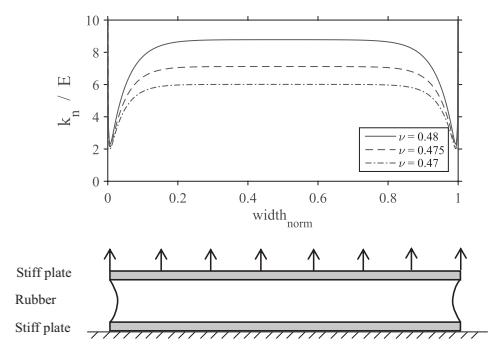

Fig. 6. Stiffness variation determined by numerical tension simulation of a rubberlike material. The specimen width is 30 times the rubber layer thickness. The rubber layer is modelled using an isotropic linear elastic material with $E = 3.6$ MPa.

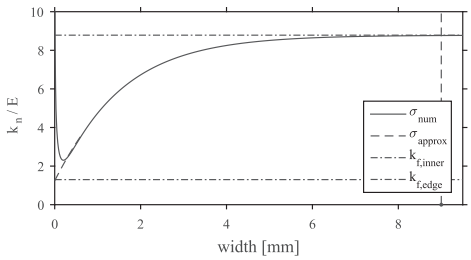

Fig. 7. Normal stress distribution plotted over the transition length. By excluding the stress concentration at the end, data fitting validates the theoretical edge stiffness. The transition length according to Eq. (11) indicated by the vertical dashed line.

$$\left(\frac{\sigma_{11}}{f_{t90}}\right)^2 + \left(\frac{\tau_{12}}{f_v}\right)^2 + \left(\frac{\tau_{13}}{f_{v90}}\right)^2 - 1 = 0 \tag{12}$$

Index t indicates tension, index v indicates shear and index 90 is used for the perpendicular to grain direction. Stress directions are defined in Section 2.

5. Calculation results and comparison to tests

5.1. Test series

The calculation results will be compared to tests conducted by Yang et al. [3]. The shear plate dowel connections was subjected to quasi-static displacement controlled tensile test according to Fig. 8. Each specimen had a length of 2 m with identical connections in each end. Three nominally equal specimens were tested in each series, i.e. 6 tested joints in total. However, the non-failing joint is disregarded in this work. The size of the steel plates was 400×400 mm^2 with a thickness of 8 mm. The plates were 13 mm thick in the area close to the dowel in order to avoid yielding and possible buckling. It should be noted that the plates were not only glued, but also 34 screws (70×6 mm) were inserted to keep the plates in position during curing. Two similar test series were conducted with the only difference being the presence of a rubber layer.

The glulam used was of strength class GL30c while the steel was of grade Q345B with a nominal yield stress of 345 MPa. The rubber was a mix of natural rubber and SBR (styrene-butadiene) with a hardness of 62° Shore A, which is approximately equivalent to a shear modulus 1.2 MPa [18]. The tensile strength of the rubber is 22.4 MPa while its shear strength is 9.4 MPa. The failure elongation in tension is 595% [3] and the rubber layer had a thickness of 1.0–1.2 mm. The rubber was vulcanized to the steel plate which ensures a steel–rubber interface strength similar to the rubber itself. A 2-component polyurethane (Purbond CR421, glue + hardener) was used to adhere the rubber to the glulam while epoxy (SHB) was used to adhere the steel directly to the glulam for the connections without any rubber layer.

The displacement of the steel plate relative the side of the beam was recorded, see Fig. 8. The failure load P_f and average shear stress at failure τ_f of the specimens are found in Table 1.

The test results suggest a considerable strength increase in the connection by introducing a rubber foil. Failure examination of the S-nR specimen does however indicate premature failure at the steel–adhesive interface rather than in the wood, c.f. [3]. Furthermore, a mistake in the test set-up design of the first S-R specimen

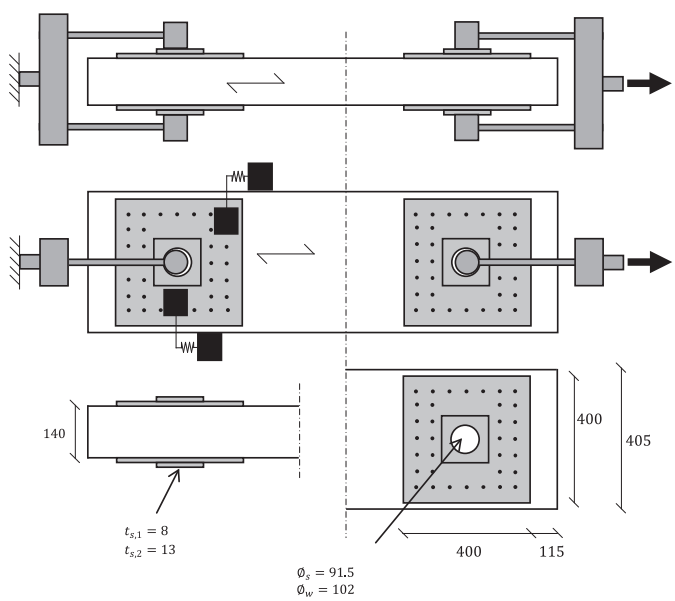

Fig. 8. Geometry and test setup used by Yang et al. [3]. Subscript s for steel, w for wood. All dimensions are in mm and the typical arrangement of displacement gauges is shown in the lower part of the middle figure.

Table 1
Failure loads and mean shear stress at failure of laboratory test series with (S-R) and without rubber (S-nR).

S-nR	P_f (kN)	$\overline{\tau_f}$ (MPa)	S-R	P_f (kN)	$\overline{\tau_f}$ (MPa)
I	281	0.93	I	843	2.78
II	209	0.69	II	1076	3.54
III	165	0.54	III	1052	3.46
AVG	218	0.7	AVG	990	3.3

Table 2
Adopted elastic material parameters for wood [7]. Parameters are given in MPa and (–).

Young's modulus (MPa)		Shear modulus (MPa)		Poisson's ratio	
E_L	14,000	G_{TR}	60	υ_{TR}	0.3
E_T	500	G_{TL}	700	υ_{TL}	0.02
E_R	800	G_{RL}	600	υ_{RL}	0.02

Table 3
Bond line parameters. Units: MPa and J/m^2.

	σ_{perp}	τ_0	τ_{90}
S-nR	$E = 3000$	$G = 1000$	$G = 1000$
	$G_{f,I} = 470$	$G_{f,II} = 740$	$G_{f,II} = 300$
	$f_{t90} = 4.9$	$f_v = 4.4$	$f_{v90} = 1.6$
S-R	$E = 3.6$	$G = 1.2$	$G = 1.2$
	$f_{t90} = 4.9$	$f_v = 4.4$	$f_{v90} = 1.6$
	c.f. Eqs. (10) and (11)		

resulted in bending of the glulam which lowered its capacity. This bending was prevented in the later S-R tests.

5.2. Numerical analysis parameters

A linear elastic rectilinear orthotropic material model was chosen for the wood using the elastic parameters given in Table 2, no identification experiments were conducted. The steel plate is modelled as a linear elastic isotropic material with Young's modulus $E = 210$ GPa and a Poisson's ratio, $\nu = 0.3$.

The bond line is modelled according to Section 4, thus dependent on the presence of rubber. As the prominent failure mode is wood shear failure close to the bond line, wood properties are used for strengths and fracture energies. The values shown in Table 3 are those given by Berblom Dahl [22] and Serrano [7] respectively for clear wood specimens. The effective normal stiffness for S-R was applied to a perimeter zone according to Section 4.2 assuming a Poisson's ratio of 0.497. This value was found by comparing stress levels from simulations using a linear elastic rubber layer with those from simulations using a hyperelastic (Neo-Hookean) material model for the rubber. Bond line stiffness for the adhesive in the S-nR joints is also found in Table 3.

Table 4
Failure load comparison of full-sized S-nR test specimens. The variation of the results indicates the importance of fracture analysis on adhesive connections. The bilinear model is considered realistic, which further indicates the premature failure of the test series.

Type of analysis	Failure load (kN)	Average shear stress (MPa)
1D Analytical, linear	92	0.30
3D Numerical, linear	128	0.42
Test	**218**	**0.72**
3D Numerical, NLFM Bilinear softening	**562**	**1.85**
3D Numerical, NLFM Linear softening	795	2.62
3D Numerical, EELA	803	2.64
1D Analytical, EELA	863	2.84

For simplicity, the simulations were run in load control. By doing so there was no need to model the dowel itself, nor its interaction with the steel plate which would call for detailed contact modelling. Instead a non-uniform pressure load was prescribed on the hole edges to simulate pin pressure. The simulations were run without introducing artificial stabilization (viscous damping) and using the built-in automatic incrementation features of the software. The minimum step length was expressed as ratio of total load and was set to $5 \cdot 10^{-3}$. Double symmetry was used and the load was applied horizontally to the right, see Figs. 8 and 9.

The element mesh commonly used is shown in Fig. 9. First order solid elements with full integration over 8 nodes were used for the glulam and steel while cohesive elements were used for the bond line with one element in the thickness direction. With the presented modelling approach stress concentrations at the edges are substantially reduced thus enabling the use of a simple stress failure criterion.

5.3. Results for S-nR – Joint without rubber layer

The predicted failure load of the S-nR specimen varies greatly depending on the calculation method used, see Table 4. The test results are also presented for which the premature failure should be kept in mind, c.f. Section 5.1. As the stiffness of the adhesive is considerably larger than for the screws, the latter are excluded from the analysis as they only have a minor influence on the joint strength. In comparison to the linear 1D analysis according to Eq. (3), the joint geometry causes a more uniform shear stress distribution in the linear 3D, and thus yields a higher failure load even though the 3D analysis considers stress interaction. Due to the high adhesive stiffness, the linear 3D analysis is sensitive to discretization in comparison to fracture softening analysis.

EELA shows good resemblance between analytical 1D and numerical 3D results, but also with the linear fracture softening model. The bilinear model does however imply that the failure loads found by EELA are unreasonably high, which indicates a frac-

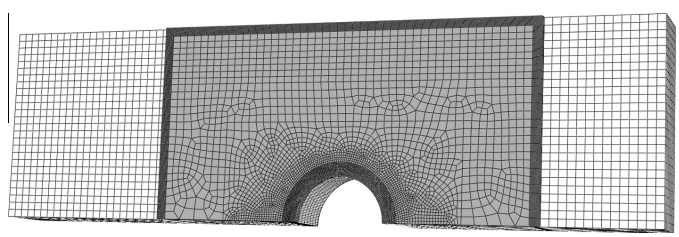

Fig. 9. Typical FE-mesh used in the analyses (double symmetry used). Approximately 80,000 elements in total. Wood elements shown in white, steel plate in grey.

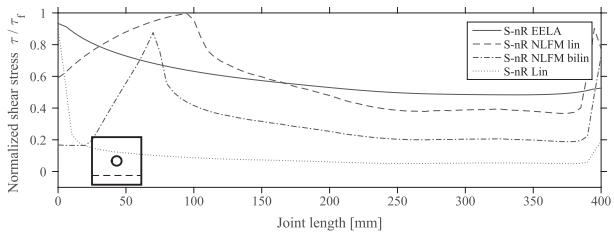

Fig. 10. Shear stress distribution comparison between presented models in Section 2 at failure load. The distribution is along a line at 60 mm distance from the plate edge, see lower left corner. Conventional linear stress analysis 'S-nR Lin' underestimates the capacity significantly. The load is directed right.

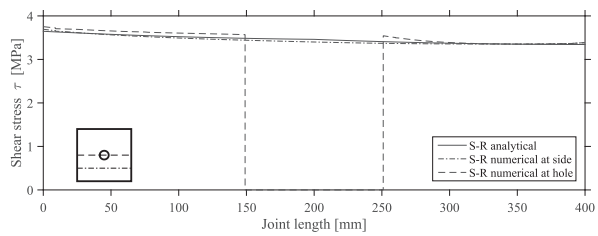

Fig. 11. Shear stress distribution of the S-R specimen; 1D analytical and 3D numerical EELA for a total connection load of 1050 kN directed right. The numerical stress paths are taken in the middle (hole) and at 60 mm distance from the plate edge (side), see lower left corner.

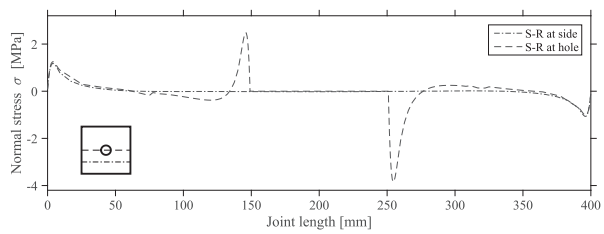

Fig. 12. Normal stress distribution by numerical EELA analysis of the S-R specimen. Total load is 1050 kN directed right. The peel stress (positive) peak at $x \approx 150$ mm governs the failure region.

ture softening behaviour dependency of the failure load. This indication makes the use of EELA not suitable for the connection in hand as it disregards the shape of the softening curve as well as assumes that all fracture energy can be activated during the propagating failure. Since no detailed knowledge about the exact shape of the softening curve is available for the bond line studied, no further analyses of the joint without rubber foil were performed. As a comparison, the shear stress distribution at failure is illustrated in Fig. 10. The bilinear model verifies the premature failure in the test series discussed in Section 5.1.

5.4. Results for S-R – Joint with rubber layer

In comparison to the S-nR specimen, a self-similar stress distribution throughout the load application is obtained for the S-R specimen due to the linear analysis. A good resemblance between the analytical 1D expressions and the numerical 3D models is found for which a close to uniform distribution is obtained, shown in Fig. 11.

The higher load capacity in combination with a slightly larger eccentricity due to increased bond line thickness results in higher normal stresses in the S-R specimen in comparison to the S-nR. The numerical results are shown in Fig. 12.

The combined state of stress is evaluated using the Norris stress criterion according to Section 4.2, and applying a single point maximum stress failure criterion. A comparison of the load bearing capacity of the connection is presented in Table 5. For the geometry at hand, the linear numerical analysis shows a reasonable agreement with the test results, especially if the first test result is disregarded, c.f. Section 5.1. The analysis further indicates that including peel stress reduces the failure load by 20% as compared

Table 5
Failure load comparison of the S-R specimen.

Type of analysis	Failure load (kN)	Average shear stress (MPa)
Test	990	3.26
3D Numerical	1050	3.46
1D Analytical	1270	4.18

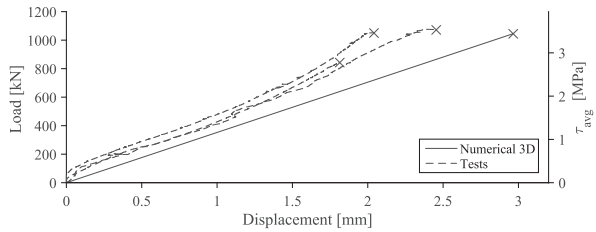

Fig. 13. Load–slip comparison of the rubber plate connection between tests and numerical analysis.

to the analytical 1D-solution and also predicts the failure region to be close to the hole instead of being located at the outer perimeter of the steel plate.

In order to evaluate the linear elastic representation of rubber, a load–slip comparison to test data is of interest, see Fig. 13. The deformation measure used for the numerical results in this plot is chosen so as to represent the measurement points used in the tests. It can be concluded that the numerical analysis underestimates the joint stiffness, which is possibly due to the large amount of screws used but not modelled.

6. Discussion

A large increase in load bearing capacity of the shear plate connection by using a rubber foil between the steel plate and the wood was recorded in the tests, partly due to premature failure discussed in Section 5.1. If the steel–adhesive interface can be made sufficiently strong and failure in the wood close to the bond line is made the governing factor, the numerical results for the S-nR specimen reported herein predicts a failure strength increase of 150% when the rubber foil is applied. In addition, the *elastic* behaviour of the relatively soft rubber foil also suggests a considerably higher capacity in cyclic loading since the response is reversible up to load levels very close to the failure load.

The shear stress distribution is close to uniform for a 1 mm rubber foil thickness, hence no significant strength increase is possible by using a thicker foil. However, a thicker foil would most probably increase the joint's impact resistance and, of course, reduce joint stiffness. Such characteristics can be of interest in shock loading situations or when mechanical fasteners are needed to interact with a glued bond line.

A full analysis of a rubber layer requires a non-linear material model, non-linear geometry (due to high straining) and a considerable amount of elements in the thickness direction in order to accurately capture the deformation pattern. By using the suggested method of analysis with cohesive elements, a considerably faster analysis run time is attained.

Peel stresses in the bond line can be reduced by fastening the plate also with screws. The same screws can also be used to obtain curing pressure for the adhesive. The failure load comparison presented in Table 5 suggests a good resemblance between the numerical 3D analysis and the test results. However, the numerical model does not include the screws shown in Fig. 8 which should increase the load carrying capacity of the joint as the rubber enables screw-adhesive interaction [1]. The numerical analysis indicates a failure region just behind the hole, thus it can be of interest to insert screws also there. Note that the failure region differs between the presented models, from the outer perimeter of the bond line behind the load in the Volkersen analysis to the hole perimeter behind the load in the numerical analysis. This shift is due to the inclusion of peel stresses in the FE-analyses and the use of the Norris failure criterion based on the multi-axial stress state.

Even though strength analyses of the rubber foil adhesive joints are promising, additional efforts are needed in order to account for long term effects, dynamic loading and fire safety before structural application.

7. Conclusions

- An analytical expression of the 1D shear stress distribution, based on Volkersen theory, was developed for centrically loaded glued lap joints. The analysis indicates that the generalized Volkersen theory can be used to determine the load bearing capacity of the joint with reasonable agreement when an intermediate layer with a rubber foil is applied. The predicted load is higher than can be expected due to the neglected bending.
- Numerical bond line models of glued wood-to-steel plate joints are presented for which a bilinear fracture softening model is suggested for traditional wood-to-steel plate adhesive joints and a linear elastic model is suggested if an intermediate rubber foil layer is used.
- If only failure of wood close to the bond line is considered, the suggested models indicate a 150% increase of the load bearing capacity by introducing a rubber foil. The increase is lower than experimental experience, indicating difficulties in properly bonding the steel plate to wood. Compared to a traditional adhesive bond, the numerical results indicate that the failure load is reached without early damage initiation and evolution in the bond line when a rubber foil is used.

Acknowledgements

The financial support provided by *Formas* through grant 2012-879 is gratefully acknowledged. The authors would also like to thank associate professor Huifeng Yang and others at Nanjing Tech University for a pleasant stay and for providing information on the experimental work.

Appendix A. Supplementary material

Supplementary data associated with this article can be found, in the online version, at http://dx.doi.org/10.1016/j.engstruct.2016.04.053.

References

[1] Gustafsson PJ. Tests of full size rubber foil adhesive joints. Lund University; 2007.
[2] Crocetti R, Axelson M, Sartori T. Strengthening of large diameter single dowel joints. SP Technical Research Institute of Sweden; 2010.

[3] Yang H, Crocetti R, Larsson G, Gustafsson P-J. Experimental study on innovative connections for large span timber truss structures. In: IASS working groups 12 + 18 International Colloquium 2015, Tokyo, Japan; 2015.
[4] Swedish Standards Institute. SS-EN 1995-1-1:2004: Eurocode 5: design of timber structures. Stockholm, Sweden: SSI; 2009.
[5] Kobel P. Modelling of strengthened connections for large span truss structures. Master thesis. Lund University; 2011.
[6] Volkersen O. Die Nietkraftverteilung in zugbeanspruchten Nietverbindungen mit. Luftfahrtvorschung 1938;15:41–7.
[7] E. Serrano. Adhesive joints in timber engineering, modelling and testing of fracture properties. PhD thesis. Lund; 2000.
[8] Ottosen NS, Olsson K-G. Hardening/softening plastic analysis of adhesive joint. J Eng Mech 1988;114(1):97–116.
[9] Krajcinovic D. Damage mechanics. Mech Mater 1989;8:117–97.
[10] Edlund U. Mechanical analysis of adhesive joints: models and computational methods. PhD thesis. Linköping, Sweden; 1992.
[11] PJ Gustafsson. Analysis of generalized Volkersen joints in terms of non-linear fracture mechanics. In: Proc of European mechanics colloquium 227 "Mechanical behavior of adhesive joints"; 1987. p. 323–38.
[12] Gustafsson PJ, Serrano E. Glued truss joints analysed by fracture mechanics. In: 5th World conference on timber engineering, Montreux, Switzerland; 1998.
[13] Coureau J-L, Gustafsson PJ, Persson K. Elastic layer model for application to crack propagation problems in timber engineering. Wood Sci Technol 2006;40:275–90.
[14] Jensen JL. Quasi-non-linear fracture mechanics analysis of the double cantilever beam specimen. J Wood Sci 2005;51:566–71.
[15] Jensen JL, Gustafsson PJ. Shear strength of beam splice joints with glued-in rods. J Wood Sci 2004;50:123–9.
[16] Wernersson H, Gustafsson PJ. The complete stress–slip curve of wood–adhesives in pure shear. Mech Behav Adhes Joints 1987:139–50.
[17] Wernersson H. Wood adhesive bonds – fracture softening properties in shear and in tension. PhD thesis. Lund: Lund University; 1990.
[18] Austrell P-E. Modelling of elasticity and damping for filled elastomers. PhD thesis. Lund: Lund University; 1997.
[19] Treloar LRG. The physics of rubber elasticity. 3rd ed. Oxford: Clarendon Press; 1975.
[20] Yeoh OH. Some forms of the strain energy function for rubber. Rubber Chem Technol 1993;66:754–71.
[21] Norris CB. Strength of orthotropic materials subjected to combined stresses. Report no. 1816. Madison: U.S. Department of Agriculture; 1962.
[22] Berblom Dahl K. Mechanical properties of clear wood from Norway spruce. PhD thesis. Trondheim, Norway: Norwegian University of Science and Technology; 2009. ISBN 978-82-471-1911-2.

Paper D

WCTE 2016
World Conference on Timber Engineering
August 22-25, 2016 | Vienna, Austria

ANALYSIS OF THE SHEAR PLATE DOWEL JOINT AND PARAMETER STUDIES

Gustaf Larsson[1], Per Johan Gustafsson[2], Erik Serrano[3], Roberto Crocetti[4]

ABSTRACT: The shear plate dowel joint is a single large dowel joint with rubber-glued steel plates. The design has shown promising results in terms of strength in experimental work. The paper presents results from theoretical models that have been developed to enable further studies of the joint. The failure load obtained through a numerical 3D analysis is in good agreement with test results. Parameter studies and design alterations are presented, which concludes that the joint design is efficient and that the shear slip stiffness can be designed to match commonly used fasteners.

KEYWORDS: Shear plate dowel joint, rubber foil adhesive joint, single dowel, numerical model, timber, connection, joint

1 INTRODUCTION

The properties and cost of structural joints often govern the competitiveness of timber as main structural material in large structures. Mechanical fasteners such as dowels, screws and nails are typically used as they provide strength and ductility to the timber joint. However, in order to avoid splitting, proper distances are required to member edges as well as between different fasteners as described in the European design code Eurocode [1]. These distances entail an increase of member dimensions, which subsequently reduces the utilisation factor of the member in span and thus causes excessive material use.

Several types of timber reinforcements have been studied in order to enhance the brittle properties of wood. Early research focused on global element reinforcements [2] [3] of which textiles were proposed suitable also as local reinforcement in e.g. joints [4]. Several studies have since been aimed specifically at minimizing the required distances between mechanical fasteners and end distance by e.g. self-tapping screws [5] and fibre textile [6] [7]. The shear plate dowel joint (SPDJ) distinguishes itself from previous joint proposals by combining high strength with efficient on and off site production, while maintaining a short end distance. The design also enables easy joint-to-member strength matching.

1.1 THE SHEAR PLATE DOWEL JOINT

The favourable properties of the SPDJ design is achieved by combining the strength of a flexible lap joint with the simplicity of a single dowel design.

A limiting factor in design of lap joints is shear stress concentrations at the joint ends, which grow significantly for large lap lengths. These concentrations reduce the active load transfer region of the joint and thus limit the total load bearing capacity. This premature failure is further deprived due to the high stiffness of commonly used structural adhesives.

In order to minimize the stress concentrations by softening the bond line, Gustafsson [8] suggested adding an intermediate rubber layer as see Figure 1. A close to uniform shear stress distribution over the lap joint length is found even for thin rubber layers, dramatically increasing the elastic load bearing capacity. The stiffness of a rubber foil adhesive joint is typically comparable to, if not stiffer than, bolted joints [8].

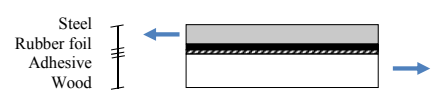

Figure 1: *Pull-pull adhesive lap joint with intermediate rubber layer*

[1] Gustaf Larsson, Lund University, Sweden, gustaf.larsson@construction.lth.se, P.O. Box 118, SE-221 00 Lund, Sweden
[2] Per Johan Gustafsson, Lund University, Sweden, per-johan.gustafsson@construction.lth.se
[3] Erik Serrano, Lund University, Sweden, erik.serrano@construction.lth.se
[4] Roberto Crocetti, Lund University, Sweden, roberto.crocetti@kstr.lth.se

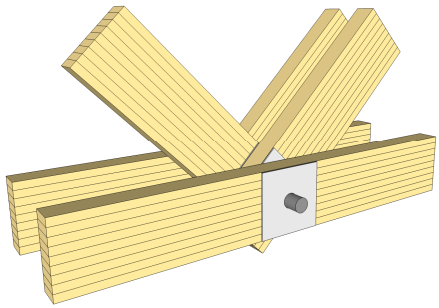

Figure 2: *The shear plate dowel joint used in a truss node*

A high degree of prefabrication and easy on site assembly can be achieved by a using a single dowel joint design, see Figure 2. However, a single dowel would be very prone to splitting failure and is thus in need of a large end distance, if no type of reinforcement is used.

Several types of reinforcements have been tested for large diameter dowels, such as self-tapping screws [9] [10] and fibre textile [11], but none of these techniques efficiently reduce the possibility of shear plug failure. However, by combining the concepts of a single large dowel and the rubber foil adhesive joint, the premature shear plug failure is avoided.

The rubber foil adhesive technique is used to externally glue large metal plates with vulcanized rubber to the timber member, see Figure 2. Shear action between timber and rubber is then assured by using a larger hole diameter in the timber than in the steel plates. As the rubber foil enables the use of the bonded area, the member strength can simply be matched by an appropriate choice of plate size. Screws can be used to apply curing pressure, minimize steel plate bending due to eccentricity, and increase joint bearing capacity as the rubber foil can be designed to match the slip of the screws.

The SPDJ was first tested in [8], but later in full scale by Yang et al. [12] along with comparative tests without a rubber foil. For a steel plate size of 400x400 mm^2 and dowel diameter of 91 mm, the average failure load was found being 218 kN without rubber foil, compared to 990 kN with rubber foil. The dominant failure mode was shear failure in the bond line, but indications of wood failure also exist [8] [12]. Even though a premature failure in the steel-adhesive interface was found for the specimens without rubber, the benefit of the rubber layer on load bearing capacity is clear.

1.2 PRESENT STUDY

The purpose of this paper is to establish validated and efficient strength analysis procedures of the SPDJ as limited in strength by fracture in the bond line or the timber member. Here, the term bond line includes the adhesive, rubber foil, a thin wood layer along the glue and the material interfaces.

Analytical 1D expressions and a numerical 3D approach are presented to determine the failure load of the joint. The 1D analysis is based upon the Volkersen theory [13], which considers the shear stress distribution, while the numerical 3D approach is needed to also consider peel stress interaction. The analytical expressions can be used to develop design procedures of the joint.

2 1D ANALYTICAL ANALYSIS

The SPDJ is characterised by lap shear action between the steel plate and timber element. A non-uniform shear stress distribution is obtained for large overlap lengths due to the various stiffnesses of the joint materials. Based on studies on large riveted overlap connections in steel, Volkersen [13] presented a differential equation for the shear distribution as Equation (1).

$$\tau_3'' - \omega\tau_3 = 0$$
$$\omega^2 = \frac{G_3 b_3}{t_3}\left(\frac{1}{A_1E_1} + \frac{1}{A_2E_2}\right) \tag{1}$$

Indices 1 and 2 indicate the adherents while 3 indicates the adhesive layer, see further Figure 3. In the Volkersen theory, the adherends are assumed to act as centrically loaded bars and the adhesive layer can only transfer shear stress, which is constant over the thickness. Bending is thus not included and all materials are modelled as linear elastic.
Using stress continuity and force equilibrium over the centric load application point, the analytical shear force distribution for the SPDJ is governed by (2).

$$\tau_3(x) = \begin{cases} \tau_3^A & for \quad 0 \le x < {}^{L}/_{2} \\ \tau_3^B & for \quad {}^{L}/_{2} \le x \le L \end{cases}$$

$$\tau_3^A = \frac{PG_3}{t_3\omega E_1A_1}\left[\left(\frac{1}{\tanh(\beta)} + \frac{\alpha - \operatorname{sech}(\beta)}{2\sinh(\beta)}\right)\cosh(\omega x) - \sinh(\omega x)\right] \tag{2}$$

$$\tau_3^B = \frac{PG_3}{t_3\omega E_1A_1}\left[\left(\frac{\cosh(2\beta)}{2\sinh(\beta)}\left(\alpha + \operatorname{sech}(\beta)\right)\right)\cosh(\omega x) - \cosh(\beta)\left(\alpha + \operatorname{sech}(\beta)\right)\sinh(\omega x)\right]$$

in which

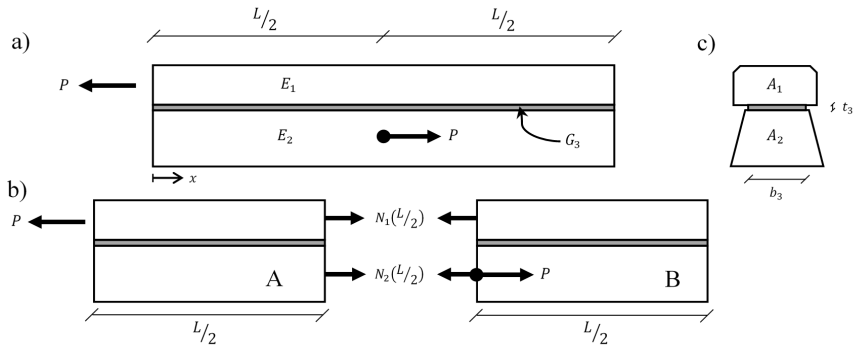

Figure 3. *Nomenclature of the theoretical analysis using Volkersen theory. Young's modulus is denoted E_i for wood and steel respectively, and shear stiffness of the bond line is denoted G_3. The geometry is divided into part A and B at the load application point.*

$$\omega L = L\sqrt{\frac{G_3 b_3(1+\alpha)}{t_3 E_1 A_1}}$$

$$\alpha = \frac{E_1 A_1}{E_2 A_2} < 1 \qquad (3)$$

$$\beta = \frac{\omega L}{2}$$

This analytical shear stress distribution is shown in Figure 7.

For a given a shear strength f_v, the maximum load bearing capacity, P_f, is limited by the shear stress behind the applied load at $x = 0$ in Equation (2). Thus, the failure load can be expressed as

$$P_f = f_v b_3 \frac{(1+\alpha)L}{\omega L} \frac{\sinh(\omega L)}{\alpha \cosh\left(\frac{\omega L}{2}\right) + \cosh(\omega L)} \qquad (4)$$

Among the simplifications made in the Volkersen theory, disregarding bending is of special concern for the SPDJ design. Due to the eccentricity between the system lines of the steel plate and timber member, bending will occur and thus it is expected than Equation (4) will overestimate the load carrying capacity of the joint.

However, the bond line peel stresses can be reduced if adequate reinforcement is introduced, e.g. by means of screws. The model could then probably be used to obtain a realistic estimation of the capacity, provided also that the shear stiffness of the screws are either negligible or taken into account.

3 3D NUMERICAL ANALYSIS

3.1 GENERAL

Numerical 3D analysis can be used in order to consider the stress interaction between shear and peel stresses in the bond line. For this, the general-purpose finite element software ABAQUS was used. The simulations were performed in 3D using a model consisting of wood, steel and a bond line.

3.2 STEEL AND WOOD MATERIAL MODELS

Wood is modelled using a linear elastic material formulation. Orthotropic parameters are used in both rectilinear and polar manner, see Table 1 and Figure 4. Failure in the wood member is evaluated by a Tsai-Wu failure criterion [14], in which the strength interaction coefficients are set to zero. Strength parameters are found in Table 2.

The steel is modelled as an isotropic linear elastic material using Young's modulus of 210 GPa and Poisson's ratio of 0.3.

Table 1: *Elastic material properties for wood* **[15]**. *Units are given in MPa and [-].*

Young's modulus		Shear modulus		Poisson's ratio	
E_L	13700	G_{TR}	60	υ_{TR}	0.3
E_T	500	G_{TL}	700	υ_{TL}	0.02
E_R	800	G_{RL}	600	υ_{RL}	0.02

Table 2: *Wood strength parameters in MPa* **[16]**.

	Tensile	*Compression*		
f_L	63	29	f_{TL}	4.4
f_R	4.9	3.6	f_{RL}	6.1
f_T	2.8	3.8	f_{RT}	1.6

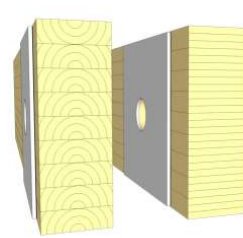

Figure 4: *Polar and rectilinear material model used in wood stress analysis.*

3.3 BOND LINE MODEL

The bond line represents the rubber and the adjacent interfaces between rubber-wood and rubber-steel. An efficient bond line model is of interest and thus a linear analysis with a minimum amount of elements is favoured even though a non-linear elastic behaviour is characteristic for rubber. However, shear action can be modelled with a linear behaviour with a reasonable accuracy, and as it is the main action of the joint, a reasonable agreement is found with non-linear material models.

Special consideration is needed in order to model the incompressibility of rubber as the Poisson's ratio approaches 0.5, which highly affects the normal stiffness of the bond line. Based upon a linear elastic material formulation, one can identify a difference in normal stiffness between edge and inner points of the material due to strain boundary conditions. The stiffness is a function of Young's modulus E, Poisson's ratio ν and the rubber thickness t according to Equation (5).

$$k_{n,edge} = \frac{E}{t(1-\nu^2)}$$
$$k_{n,inner} = \frac{E(1-\nu)}{t(1+\nu)(1-2\nu)} \quad (5)$$

A transition region with an increasing normal stiffness from $k_{n,edge}$ to $k_{n,inner}$ is thus expected. The region is defined as the distance from the edge to a point at which a stiffness of 99% of $k_{n,inner}$ is found, which was investigated using linear finite element analysis. There, a rubberlike linear elastic material was perfectly bonded to stiff plates and subjected to tensile forces in plain strain conditions. The normal stiffness variation is plotted over the specimen width in Figure 5, which indicates that the inner stiffness is well represented by the theoretical results. Parameter studies indicate a linear relation between the transition length and the rubber thickness according to Equation (6) for Poisson's ratio close to $\nu = 0.5$.

$$l_{transition} = 9t \quad (6)$$

However, stress peaks arise at the ends due to sudden stiffness change. These peaks are mesh dependent, but data extrapolation suggests that the theoretical edge stiffness is accurate. These findings make it plausible to exclude the edge stress concentration as a numerical artefact, and at the same time provide a mean of disregarding this local phenomenon.

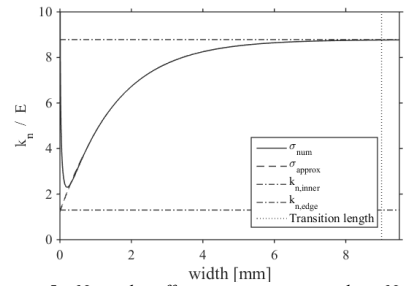

Figure 5: *Normal stiffness variation on edge. Numerical stiffness σ_{num} compared to theoretical values k_n from Equation (5) with the approximated distribution in dashed curve. The transition length, as given in Equation (6), is indicated as a vertical line.*

Conducted test series [12] indicated that wood failure close to the bond line was the governing failure mode, and thus wood strength parameters were used in a Norris strength criterion [17]. It was found that good model characteristics were achieved using a single cohesive element in the thickness direction, for which the normal stiffness variation as described above was applied. The material properties of the bond line are found in Table 3, representing the elastic properties of rubber for normal (σ_{perp}), principal shear (τ_0) and transverse shear direction (τ_{90}) [18] while using wood strength characteristics [16]. The stiffness was then determined using Eq (5), in which Poisson's ratio was set to 0.497.

Table 3: *Material properties for the cohesive model of the bond line. Units are given in MPa.*

σ_{perp}		τ_0		τ_{90}	
E	3.6	G	1.2	G_{90}	1.2
$f_{t,90}$	4.9	f_v	4.4	$f_{v,90}$	1.6

4 MODEL EVALUATION

4.1 EXPERIMENTAL WORK

In order to validate the presented models, comparison is made to conducted test series by Yang et al. [12]. The presented material properties are chosen to represent the used materials, while the test setup and geometry is given in Figure 6.

Two identical SPDJ were prepared in each end of a 2 m long glulam element. The 400x400 mm^2 steel plates were thicker around the hole to prevent local buckling. The steel plates were fastened by 34 screws during curing. Three nominally equal specimens were included in the test series, with a resulting average failure load of 990 kN [12].

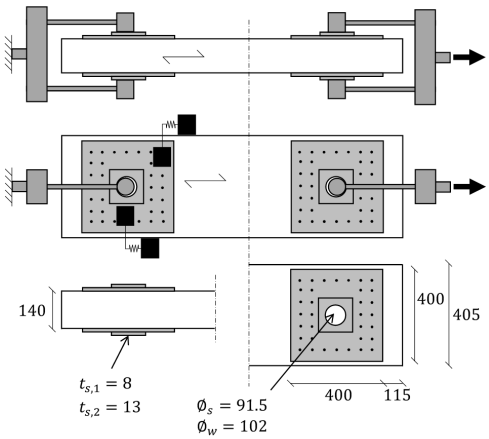

Figure 6: *Test setup and geometry used by Yang et al.* **[12]**, *with displacement gauges indicated by black solids. Dimensions are given in millimetres.*

4.2 BOND LINE STRESS DISTRIBUTION

The bond line shear stress distribution is given by both the analytical 1D and the numerical 3D model. The distributions show good agreement as shown in Figure 7, which also reveals the close to uniform stress distribution needed for good load carrying capacity of the joint.

The normal stresses in the bond line are only evaluated in the numerical 3D analysis, and the results are found in Figure 8. Stress peaks occur on the hole perimeter due to the load application eccentricity, but a bending of the entire steel plate can also be seen. The lower bond line normal stiffness at the edges, discussed in Section 3.3, results in reduced normal stresses at the ends.

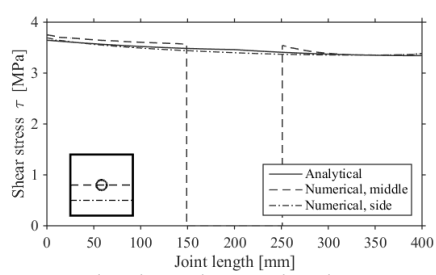

Figure 7: *Analytical 1D and numerical 3D shear stress distribution at a joint load of 1050 kN directed right. The numerical middle and side path are indicated by left legend.*

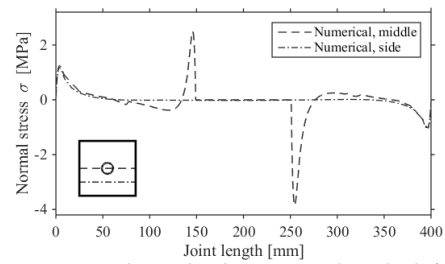

Figure 8: *Normal stress distribution at a total joint load of 1050 kN directed right (c.f. Figure 6).*

The critical peel stresses are found in Figure 8 as positive normal stresses. By introducing the peel stress component in the failure analysis, the failure region is moved from the edge behind the load (maximum shear stress) to the hole perimeter (maximum peel stress).

4.3 STRENGTH AND STIFFNESS

Table 4 provides a failure load comparison of the presented 1D- and 3D calculation methods, as well as the average failure load from tests [12]. As expected, the analytically determined failure load according to Eq (4) is found to be higher by disregarding peel-shear stress interaction. Deviating 6% from experimental values, the 3D numerical analysis shows reasonable agreement. Yang [12] describes a test setup error, which resulted in a low failure strength of the first specimen (see also Figure 9). If excluded from the average, the 3D analysis deviates 4% from test results, independent of polar or rectilinear wood model was used.

The stress state evaluation of the 3D model was conducted according to a Norris failure criterion, which concludes that bond line failure is reduced by 20% by regarding peel stresses. By such, the bond line failure region is also changed from the outer perimeter of the plate to the vicinity of the hole.

Table 4: *Bond line failure load and corresponding average shear stress according Eq (4) and FEM.*

Type of analysis	Failure load	Avg shear stress
Test [12]	990 kN	3.26 MPa
3D Numerical	1020 kN	3.35 MPa
1D Analytical	1270 kN	4.18 MPa

The numerical model also enables stiffness comparison between model and tests, which is found in Figure 9. The typical S-shaped curve of the non-linear elastic behaviour of rubber is seen in the test results, while it is assumed linear in the bond line model. It can further be seen that the numerical model indicates a softer joint than the test series, which is possibly due to the large amount of screws used but not modelled.

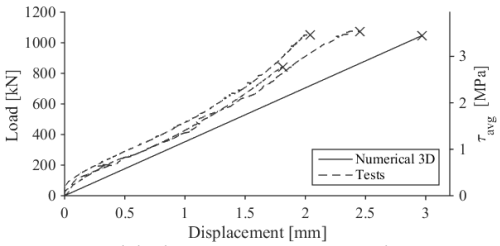

Figure 9: *Load-displacement curve comparison between tests and numerical 3D model. Average shear stress is found on the right y-axis.*

4.4 WOOD STRESS ANALYSIS

Using the presented bond line model, a good strength agreement was found with tests. However, as indications of timber failure were found in the tests [12] the stress situation in the timber member was also investigated, see Table 5.

The linear stress analysis indicates large tensile stresses parallel to grain in the upper and lower hole perimeter. Evaluating the stress tensor at this point by a Tsai-Wu failure criterion [14] indicates a failure already at a load level of 660 kN, which is 35% lower than the test results indicate. However, this concentration is possibly a crack initiation point, which could explain the combined bond line and shear plug failure seen in the tests. Previously assumed as a secondary failure, these findings make it plausible that the shear plug occurred simultaneously, if not prior, to the bond line failure.

The failure load is further decreased using polar coordinates for the wood representation (Figure 4). The Tsai-Wu criterion indicates failure at 560 kN, with a new failure region at the outer bond line perimeter in front of the applied load.

In comparison to the estimated bond line failure according to Norris, the Tsai-Wu criterion of the wood identifies more localized peak values for both the rectilinear and polar material models. This local behaviour lowers the capacity of the joint by acting as possible fracture initiation points. Even so, by comparing the numerical results to the tests indicates that the bond line failure is the ultimate failure.

Table 5: *Bond line failure load from numerical 3D analyses.*

Type of analysis	Failure load
Test [12]	990 kN
Bond line	1020 kN
Rectilinear wood	660 kN
Polar wood	560 kN

5 SPDJ DESIGN EVALUATION

5.1 RUBBER PARAMETER ANALYSIS

A large variety of rubber materials can be found on the market today, typically used as seals or to reduce vibrations. As such, the resistance to chemicals, effective temperature range and the hardness are the relevant design aspects. However, high shear strain capacity, high shear strength and low creep are needed for the implementation of the SPDJ. A thin rubber layer is also favourable, along with a suitable shear stiffness.

The shear stiffness and the rubber thickness are intimately related as they affect the bond line flexibility. The flexibility is needed to allow different elongation of the adherends and thus increase the joint strength. However, normal stresses have a negative impact on the joint, as seen in Section 4.3, which are increased for thicker rubber layers.

In Figure 10, the joint failure strength is shown as a function of rubber hardness for different thicknesses. The hardness is given in shear modulus as well as the industry standard degrees Shore A, which is non-linear in comparison to the shear modulus [18]. It is of little surprise that the load capacity increases for a decreasing hardness, assuming the wood failure is governing. However, as shown in Figure 11 the joint slip also increases for decreased hardness, which is often undesirable. A good balance must thus be found between joint slip and load carrying capacity, which is dependent on the application and possible interaction with other types of fasteners. Note that the strength capacity is, however, predominantly determined by the size of the plate.

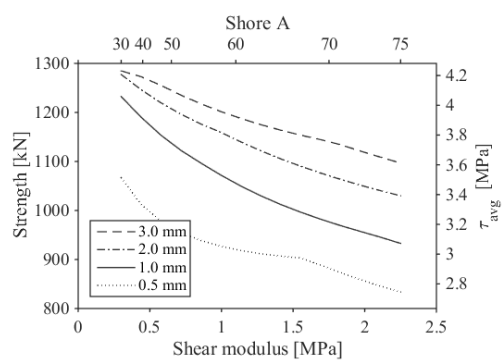

Figure 10: *Failure strength of the SPDJ reference design for increasing stiffness using different rubber layer thicknesses. Stiffness is given in Pascal (lower x-axis) and Shore A (upper x-axis).*

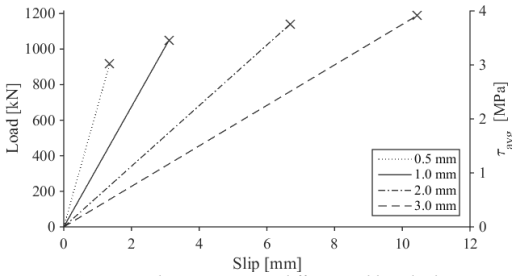

Figure 11: *Linear slip curves using different rubber thicknesses with a shear modulus* $G = 1.1\ MPa$.

5.2 ALTERNATIVE DESIGNS

Two alternative designs were analysed in order to potentially reduce the stress concentrations in the wood presented in Section 4.4. Both designs in Figure 12 reduce the bonded area in vicinity of the hole, with the aim of minimizing stress transfer around the hole.

In the first design, elliptical cut-outs are removed from the steel plate (elliptical design), while an area in the middle is left unbonded in the second (strip design). The steel plates are, in both cases, made longer in order to have the same effective area as the reference square design. The failure loads are compared to the original design in

Table 6. It is evident that, for capacity reasons alone, a given bond area is better used in the strip design than the other tested.

Peel stress concentration arose at the hole perimeter in the original design as was presented in Figure 8. Similar concentrations are found for the elliptical design, but are eliminated in the strip design due to the lack of bonded area at the hole perimeter. The only peel stresses acting on the strip design are at the ends due to global plate bending, similar to what was also found for the original design. However, due to the longer plate in the strip design, the peel stresses are lower even though a stress concentration arises at the inner corner.

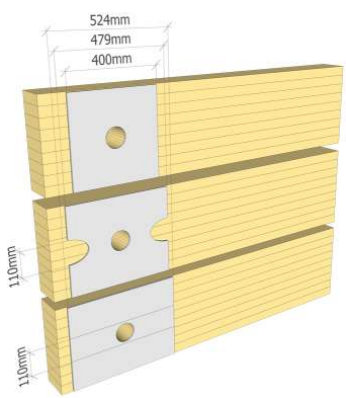

Figure 12: *Alternative designs investigated to possibly minimize stress concentrations around the hole.*

The intermediate rubber layer distributes the shear stress close to uniform for the three overlap areas. However, as also the Volkersen theory identifies, the distribution is more non-uniform for longer overlap areas. The peak shear stress in the strip design now coincides with the considerably lower peak peel stress, resulting in a bond line failure of 1100 kN.

The strip design is again promising when looking at the wood. Removing the bond line stress concentrations around the hole also lowers the corresponding stresses in the wood. The tensile stress parallel to grain is reduced by approximately 25% while the shear stress concentration is removed entirely.

All the designs are similar in terms of joint slip, but the strip design is the better choice in terms of strength at the cost of a larger joint. The strength increase is not necessarily worth the increased size, showing that the original square plate design is indeed efficient.

Table 6: *Failure load comparison of different geometries. Rectilinear wood model was used.*

Geometry	Bond line failure load	Wood failure load
Original	1020 kN	660 kN
Reduced elliptical	950 kN	660 kN
Reduced strip	1100 kN	990 kN

Ductility is also of interest in timber joints, especially in areas with seismic activity. The work presented here has had the aim of finding the ultimate strength of the SPDJ design, which has resulted in the characteristic brittle wood failure. However, ductility can be achieved by careful designing of the steel parts to enable yielding and/or buckling within the joint. Either the plate can be made thin to obtain a deformation zone in the unbonded region of the hole, or the steel dowel can be designed to deform in the contact zone. The latter has been studied by e.g. Pavković et al. [11], and is considered the best alternative.

6 CONCLUSIONS

The presented research has shown that the SPDJ can efficiently withstand large forces using a simple design with a high degree of prefabrication. Failure modes commonly found for dowel connections are prevented, and the joint strength can with ease be designed to match member strength.

Calculation models have been presented in order to allow numerical investigations, while an analytical equation preferably can be used to suggest a design code procedure. By disregarding stress interaction, the analytical failure load is found being approximately 30% too high, while the numerical model shows a reasonable agreement.

Analysis of alternative designs indicate that the original square plate design is not only simple to manufacture, but also an efficient shape. However, the ratio between load bearing capacity and bonded area can be increased if the presented strip design is used.

The rubber foil adhesive joint can typically be used whenever a strong adhesive bond line is required. The SPDJ is one interesting application that the technique enables, but many more are possible. Ongoing studies aim to determine fundamental properties of the rubber foil adhesive joint, such as strength characteristics and long-term behaviour.

ACKNOWLEDGEMENT

We gratefully acknowledge the financial support provided by the Swedish research council *Formas* through grant 2012-879.

REFERENCES

[1] European Committee for Standardization (CEN), EN 1995-1-1:2004: Eurocode 5: Design of Timber structures, Brussels, Belgium, 2004.

[2] B. Bohannon, "Prestressed laminated wood beams," Forest products lab, Madison, Wisconsin, 1964.

[3] K. B. Borgin, G. F. Loedolff and G. R. Saunders, "Laminated wood beams reinforced with steel strips," *Structural Divison,* vol. 94, no. 7, pp. 1681-1706, 1968.

[4] R. E. Rowlands, R. P. Van Deweghe, T. L. Laufenberg and G. P. Kreuger, "Fiber-reinforced wood composites," *Wood abd Fiver Science,* vol. 18, no. 1, pp. 39-57, 1986.

[5] H. Min-juan and L. Hui-fen, "Comparison of glulam post-to-beam connections reinforced by two different dowel-type fasteners," *Construction and Building Materials,* vol. 99, pp. 99-108, 2015.

[6] D. F. Windorski, L. A. Soltis and R. J. Ross, "Feasibility of fiberglass-reinforced bolted wood connections," Forest Products Laboratory, Madison, Wisconsin, 1997.

[7] P. Haller, T. Birk, P. Offermann and H. Cebulla, "Fully fashioned biaxial weft knitted and stitch bonded textile reinforcements for wood connections," *Composites: Part B ,* vol. 37, pp. 278-285, 2006.

[8] P. J. Gustafsson, "Tests of Full Size Rubber Foil Adhesive Joints," Lund University, 2007.

[9] R. Crocetti, M. Axelson and T. Sartori, "Strengthening of large diameter single dowel joints," SP Technical Research Institute of Sweden, 2010.

[10] P. Kobel, "Modelling of Strengthened Connections for Large Span Truss Structures," Master Thesis, Lund University, 2011.

[11] K. Pavkovic, V. Rajcic and M. Haiman, "Large diameter fastener in locally reinforced and non-reinforced timber loaded perpendicular to grain," *Engineering Structures,* vol. 74, pp. 256-265, 2014.

[12] H. Yang, R. Crocetti, G. Larsson and P.-J. Gustafsson, "Experimental study on innovative connections for large span timber truss structures," in *IASS working groups 12 + 18 International Colloquium 2015*, Tokyo, Japan, 2015.

[13] O. Volkersen, "Die Nietkraftverteilung in zugbeanspruchten Nietverbindungen mit konstanten Laschenquerschnitten," *Luftfahrtvorschung,* vol. 15, pp. 41-47, 1938.

[14] S. Tsai and E. Wu, "A general theory of the strength of anisotropic materials," *Journal of Composite Materials,* vol. 5, pp. 58-80, 1971.

[15] E. Serrano, Adhesive Joints in Timber Engineering, modelling and testing of fracture properties, Lund, 2000.

[16] K. Berblom Dahl, Mechanical properties of clear wood from Norway spruce, ISBN 978-82-471-1911-2 ed., Trondheim, Norway: Norwegian University of Science and Technology, 2009.

[17] C. B. Norris, Stength of orthotropic materials subjected to combined stresses, Madison: U.S. Department of Agriculture, 1962.

[18] P.-E. Austrell, "Modelling of elasticity and damping for filled elastomers," Lund University, Lund, 1997.